

REPORT 1091

EFFECT OF ASPECT RATIO ON THE LOW-SPEED LATERAL CONTROL CHARACTERISTICS OF UNTAPERED LOW-ASPECT-RATIO WINGS EQUIPPED WITH FLAP AND WITH RETRACTABLE AILERONS ¹

By JACK FISCHEL, RODGER L. NÆSETH, JOHN R. HAGERMAN, and WILLIAM M. O'HARE

SUMMARY

A low-speed wind-tunnel investigation was made to determine the lateral control characteristics of a series of untapered low-aspect-ratio wings. Sealed flap ailerons of various spans and spanwise locations were investigated on unswept wings of aspect ratios 1.13, 2.13, 4.13, and 6.13; and various projections of 0.60-semispan retractable ailerons were investigated on the unswept wings of aspect ratios 1.13, 2.13, and 4.13 and on a 45° sweptback wing. The retractable ailerons investigated on the unswept wings spanned the outboard stations of each wing; whereas the plain and stepped retractable ailerons investigated on the sweptback wing were located at various spanwise stations.

The variation of experimental flap aileron effectiveness with wing aspect ratio was not accurately predicted for all spans of flap ailerons by any one of the three theoretical methods with which a comparison was made. Flap aileron effectiveness increased as aileron span or wing aspect ratio was increased. The rolling effectiveness of 0.50-semispan outboard flap ailerons decreased with increasing aspect ratio, except for the low lift-coefficient range, where the aspect-ratio-2.13 wing gave somewhat higher values of rolling effectiveness than the aspect-ratio-1.13 wing produced.

At equal aileron projections, the rolling effectiveness of the retractable ailerons increased with increase in aspect ratio of the unswept wings and decreased with wing sweepback; however, the rolling velocities of the wings tested are estimated to be approximately equal for a given wing area at the maximum aileron projection investigated.

The aileron effectiveness of plain retractable ailerons on the sweptback wing generally increased when spanwise location of the aileron was moved inboard; whereas, the effectiveness of stepped retractable ailerons on the same wing generally increased at low and moderate angles of attack when this spanwise location was moved outboard.

Design charts based on experimental results are presented for estimating the flap aileron effectiveness for low-aspect-ratio, untapered, unswept wings.

INTRODUCTION

Low-aspect-ratio wings are being incorporated in current high-speed aircraft and missile designs because their use delays the onset of or reduces adverse compressibility effects (reference 1). One of the problems encountered in such

designs is the provision of adequate lateral control. The National Advisory Committee for Aeronautics is currently investigating the applicability of various types of lateral-control devices to wings having plan forms suitable for flight at high-subsonic or transonic speeds. In addition to flap ailerons, a promising lateral-control device, the retractable aileron or spoiler, is being investigated. Previous spoiler-aileron investigations made with unswept and swept wings of moderate and high aspect ratio (references 2 to 8 and unpublished data) indicate some of the beneficial effects that are obtained with spoiler ailerons, such as: increase in rolling moment with increase in Mach number, increase in rolling effectiveness with increase in lift-flap deflection, generally favorable yawing moments, practicable use of full-span flaps with spoiler ailerons, and smaller wing twisting moments than flap ailerons and hence higher reversal speeds with spoiler ailerons (reference 9). In addition, spoiler ailerons provide low stick forces; and, in the investigation of reference 3, no appreciable effects on the hinge-moment characteristics were observed with changes in Mach number for the spoiler aileron.

A series of untapered low-aspect-ratio wings was investigated at low speed to determine the effect of aspect ratio on the lateral control characteristics of the wings. Four unswept wings (aspect ratios 1.13, 2.13, 4.13, and 6.13) were equipped with 0.25-chord sealed flap ailerons of various spans and spanwise locations. Three of the same wings (aspect ratios 1.13, 2.13, and 4.13) were tested with 0.60-semispan spoiler ailerons of the retractable type at the 0.70-wing-chord station and, in addition, an untapered 45° sweptback wing of aspect ratio 2.09 was tested with 0.60-semispan plain and stepped retractable ailerons at the 0.70-wing-chord station. The effects of retractable-aileron spanwise location and aileron actuating arms on the lateral control characteristics of the sweptback wing were also determined for both the plain- and stepped-retractable-aileron configurations.

The lateral control characteristics as well as basic aerodynamic characteristics and lateral-stability parameters of the wings are presented.

COEFFICIENTS AND SYMBOLS

The data are referred to the stability axes (fig. 1), which are a system of axes with the origin at the center of moments (0.25 M.A.C. (figs. 2 to 4)). The Z-axis is in the plane of

¹Supersedes NACA TN 2347, "Effect of Aspect Ratio and Sweepback on the Low-Speed Lateral Control Characteristics of Untapered Low-Aspect-Ratio Wings Equipped with Retractable Ailerons" by Jack Fischel and John R. Hagerman, 1951, and NACA TN 2343, "Effect of Aspect Ratio on the Low-Speed Lateral Control Characteristics of Unswept Untapered Low-Aspect-Ratio Wings" by Rodger L. Naeseth and William M. O'Hare, 1951.

symmetry and perpendicular to the relative wind, the X -axis is in the plane of symmetry and perpendicular to the Z -axis, and the Y -axis is perpendicular to the plane of symmetry.

The coefficients and symbols used are defined as follows:

- C_L lift coefficient ($Lift/qS$)
- C_D drag coefficient ($Drag/qS$)
- C_Y lateral-force coefficient (Y/qS)
- C_m pitching-moment coefficient (M/qSc)
- C_l rolling-moment coefficient (L/qSb)
- C_n yawing-moment coefficient (N/qSb)
- Y lateral force, pounds
- M pitching moment about Y -axis, foot-pounds
- L rolling moment due to control about X -axis, foot-pounds
- N yawing moment due to control about Z -axis, foot-pounds

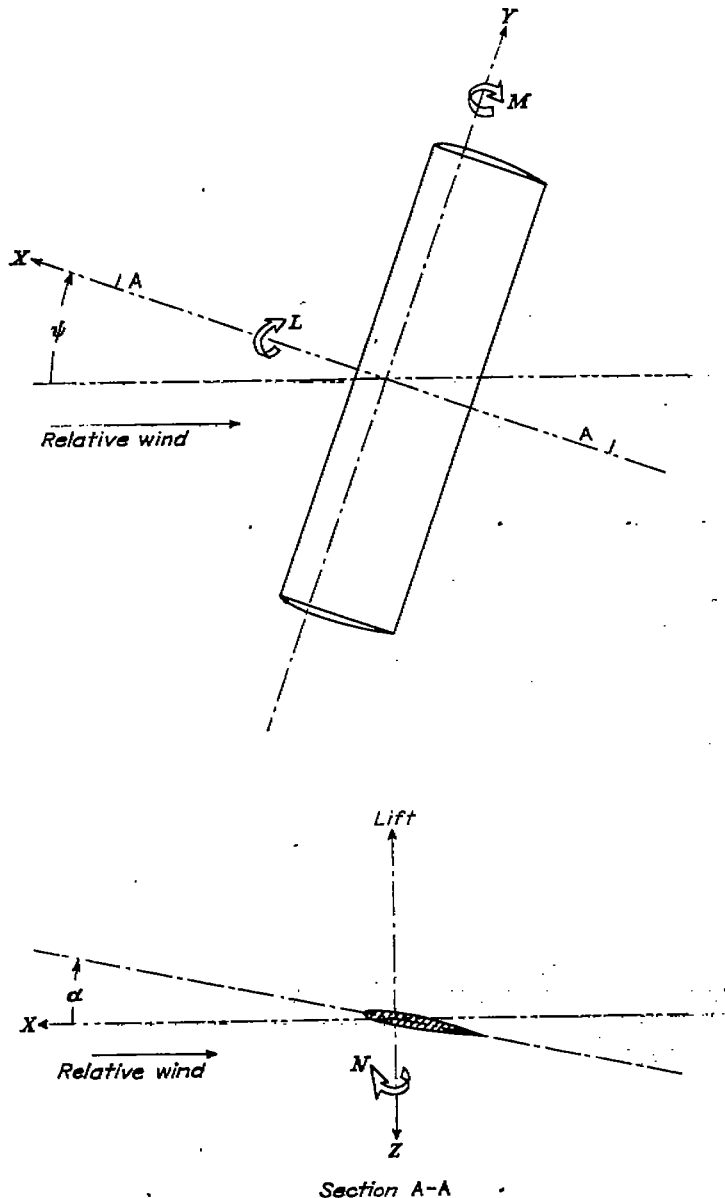


FIGURE 1.—System of stability axes. Positive values of forces, moments, and angles are indicated by arrows.

- S wing area (table I), square feet
- q free-stream dynamic pressure, pounds per square foot ($\frac{1}{2} \rho V^2$)
- A aspect ratio (table I) (b^2/S)
- ρ mass density of air, slugs per cubic foot
- c local wing chord, measured parallel to plane of symmetry, feet
- \bar{c} wing mean aerodynamic chord (table I), feet ($\frac{2}{S} \int_0^{b/2} c^2 dy$)
- c_a local aileron chord, feet
- $C_{\dot{\alpha}}$ damping-in-roll coefficient, that is, rate of change of rolling-moment coefficient with wing-tip helix angle ($\partial C_l / \partial \frac{pb}{2V}$)
- $pb/2V$ wing-tip helix angle, radians
- b wing span, measured parallel to Y -axis (table I), feet
- b_a aileron span, measured parallel to Y -axis, feet
- y lateral distance from plane of symmetry, measured parallel to Y -axis, feet
- y_0 lateral distance from plane of symmetry to outboard end of aileron, measured parallel to Y -axis, feet
- y_i lateral distance from plane of symmetry to inboard end of aileron, measured parallel to Y -axis, feet
- p rolling velocity, radians per second
- V free-stream velocity, feet per second
- α angle of attack of wing-chord plane, degrees
- ψ angle of yaw (angle between relative wind and plane of symmetry), measured in XY -plane, degrees
- Λ angle of sweepback, degrees
- δ_a aileron deflection relative to wing-chord plane, measured in a plane perpendicular to aileron hinge axis and positive when trailing edge is down, degrees
- $C_l/\Delta\alpha$ rolling-moment coefficient produced by 1° difference in angle of attack of various right and left parts of a complete wing
- α_s flap-effectiveness parameter, that is, effective change in wing angle of attack caused by unit angular change in control-surface deflection
- $(L/D)_{max}$ maximum ratio of lift to drag

TABLE I.—GEOMETRIC CHARACTERISTICS OF UNTAPERED LOW-ASPECT-RATIO WING MODELS

[NACA 64A010 airfoil section normal to the wing leading edge]

Aspect ratio	Sweep (deg)	Span (ft)	Root chord (ft)	M.A.C. (ft)	Area (sq ft)	Distance from z/4 to wing leading edge (ft)
6.13	0	6.100	1.000	0.987	6.087	0.250
4.13	0	5.021	1.224	1.221	6.097	.306
2.13	0	3.638	1.732	1.714	6.199	.432
1.13	0	2.693	2.443	2.409	6.394	.611
2.09	45	3.686	1.732	1.718	6.154	1.279

$$C_{L_{\alpha}} = \left(\frac{\partial C_L}{\partial \alpha} \right)_{\delta_a=0} \text{ measured near } \alpha=0^\circ$$

$$C_{l_{\delta_a}} = \left(\frac{\partial C_l}{\partial \delta_a} \right)_{\alpha=0} \text{ measured near } \delta_a=0^\circ$$

$$C_{l_{\psi}} = \frac{\partial C_l}{\partial \psi}$$

$$C_{r_{\psi}} = \frac{\partial C_r}{\partial \psi}$$

$$C_{Y_{\psi}} = \frac{\partial C_Y}{\partial \psi}$$

Subscripts:

max maximum

A any aspect ratio unless value of *A* is given as in

$$\left(\frac{C_l}{\Delta \alpha} \right)_{A=6}$$

Rolling-moment and yawing-moment coefficients represent the aerodynamic moments on a complete wing produced by deflection of the flap aileron or projection of the retractable aileron on only the right semispan of the wing.

MODEL AND APPARATUS

Each complete-wing model was mounted horizontally on a single strut support in the Langley 300 MPH 7- by 10-foot

tunnel, and all forces and moments acting on the model were measured by means of the tunnel balance system.

The geometric characteristics of the untapered complete-wing models investigated are itemized in table I, and sketches of the models are given in figures 2 to 4. The wing models had NACA 64A010 airfoil sections, and the wing tips were formed by rotating the airfoil sections to produce bodies of revolution. The models were constructed of a laminated mahogany and steel core enclosed in a covering composed of 1/8-inch sheet aluminum glued between sheets of 1/8-inch fir.

Plain ailerons were investigated on the unswept wings of aspect ratios 6.13, 4.13, 2.13, and 1.13. The right semispan of each wing was equipped with a 0.25*c* aluminum flap divided into four parts. The deflection of each flap segment was adjusted by means of hinge clamps. The hinge-line gap and all chordwise gaps between flap segments of equal deflection were sealed for all tests. Because the wings of aspect ratios 6.13 and 4.13 were thin, bodies of revolution (fig. 2) were used as fairings to enclose the strut pivot and thereby to permit more accurate determination of strut tare effects.

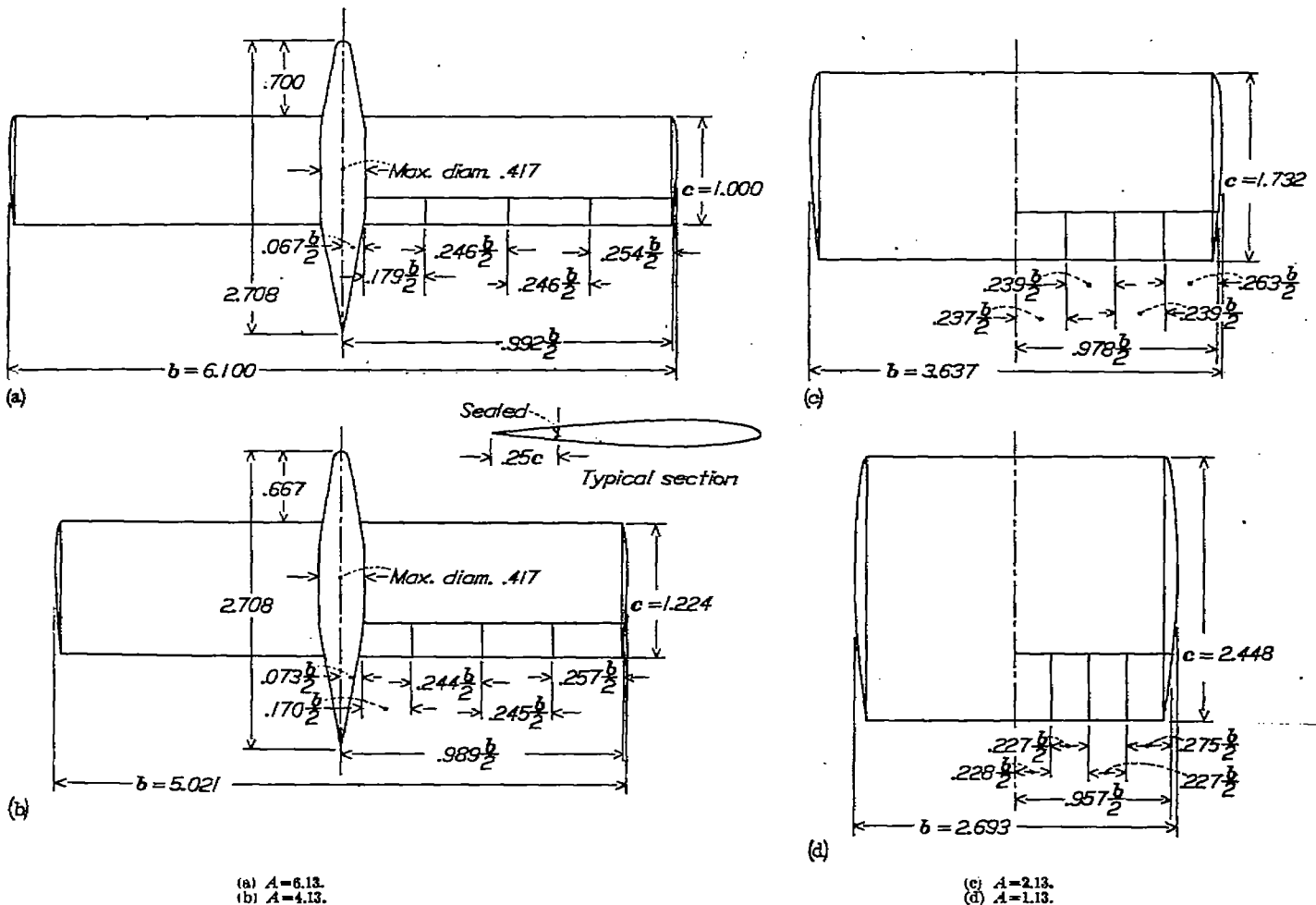


FIGURE 2.—Geometric characteristics of the unswept untapered wings investigated with flap ailerons. All dimensions are in feet.

Retractable ailerons were investigated on the unswept wings of aspect ratios 4.13, 2.13, 1.13 and on a 45° swept-back wing of aspect ratio 2.09. One of the two configurations of retractable ailerons investigated consisted of plain, $0.60 \frac{b}{2}$, continuous-span, retractable ailerons attached to the upper surface of the right wing along the $0.70c$ line of each wing model (figs. 3 and 4). The other configuration consisted of six individual retractable-aileron segments, each having a span of $0.10 \frac{b}{2}$ and a total aileron span of $0.60 \frac{b}{2}$, attached to the upper surface of the right wing of the 45° sweptback-wing model in a stepped fashion with the span of each segment normal to the plane of symmetry (fig. 4). The midpoint of each stepped-retractable-aileron segment was on the $0.70c$ line of the sweptback wing. Several ailerons, each having different projections, were used in tests of the two retractable-aileron configurations, and each aileron was prefabricated of aluminum angle and was mounted in such a manner that the front face of each aileron was normal to

the wing surface (figs. 3 and 4). On the unswept-wing models, the ailerons were mounted on the outboard portions of the wing; whereas, on the 45° sweptback-wing model, the spanwise location of the ailerons was varied during the investigation. To distinguish clearly between the two aileron configurations investigated on the sweptback wing, they are referred to herein as the "plain retractable aileron" and the "stepped retractable aileron." The body-of-revolution fairing (fig. 2) was not used on the $A=4.13$ wing for the retractable-aileron tests (fig. 3).

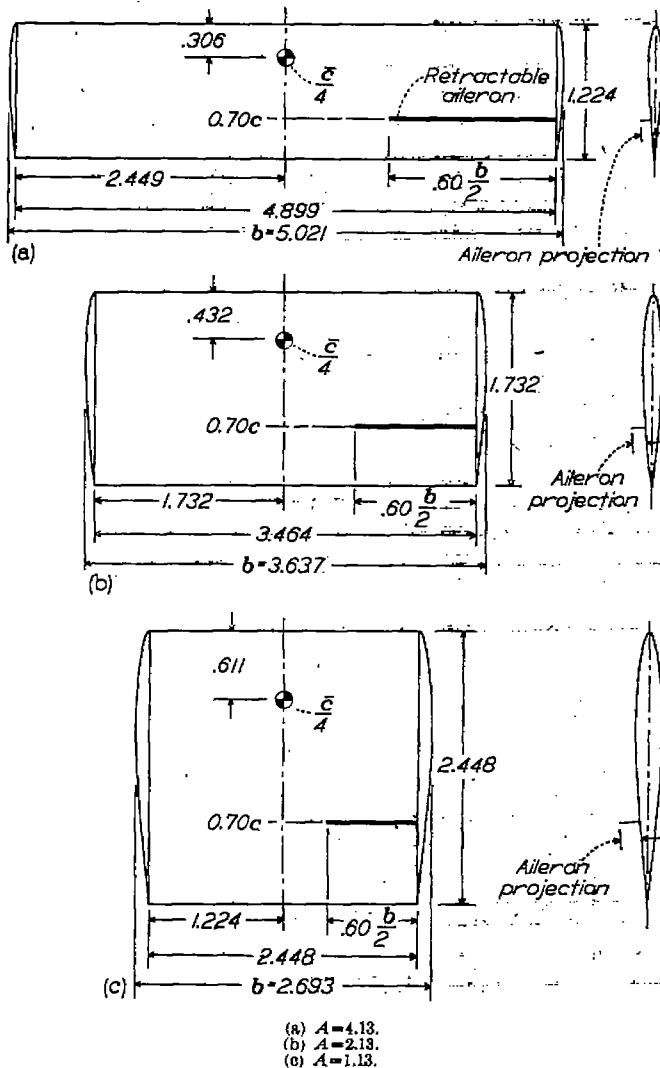


FIGURE 3.—Geometric characteristics of the unswept untapered wings investigated with retractable ailerons. (All dimensions are in feet except where noted.)

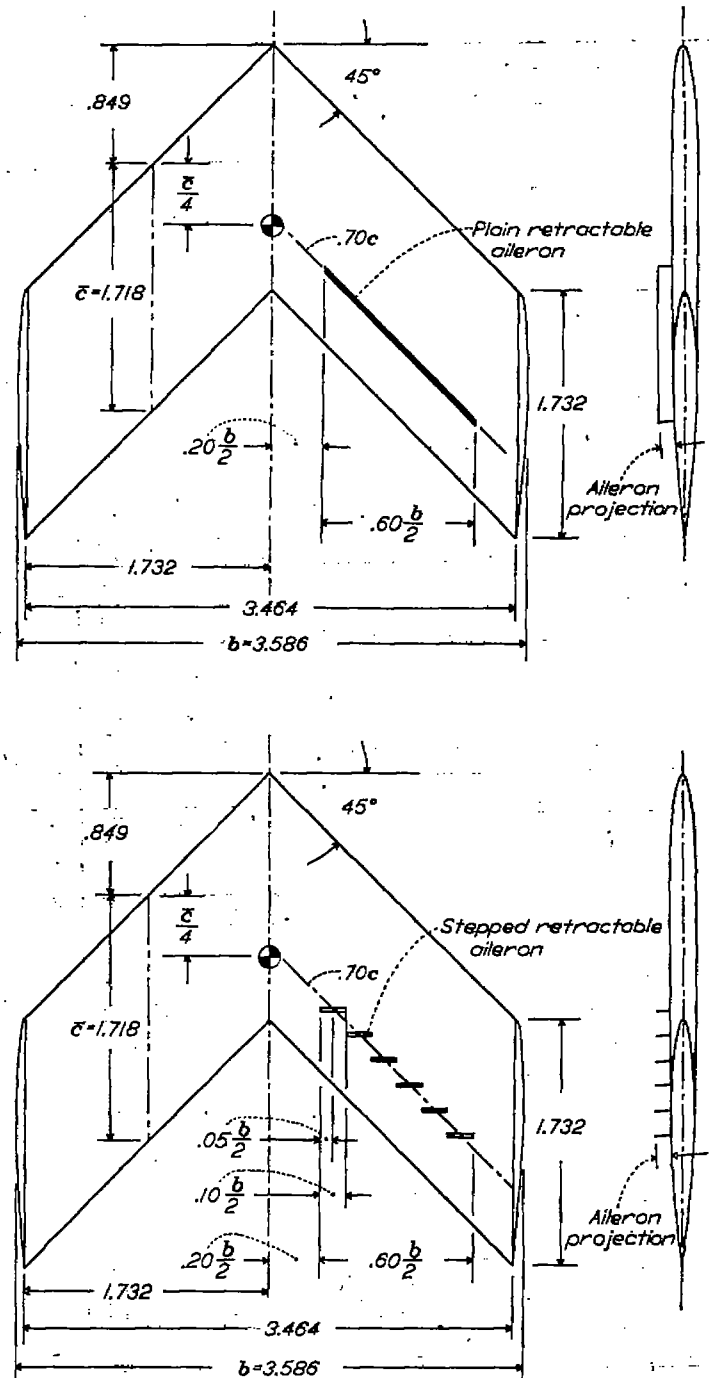


FIGURE 4.—Geometric characteristics of the 45° sweptback untapered wing investigated with plain and stepped retractable ailerons. $A=2.09$. (All dimensions are in feet except where noted.)

The simulated actuating arms tested on the sweptback-wing model in conjunction with $0.60 \frac{b}{2}$ plain and stepped retractable ailerons having projections of $-0.08c$ and various spanwise locations are shown in figure 5. The arms were constructed of thin solid triangular-shaped pieces of aluminum, each of which had a chord of 10 percent of the wing chord parallel to the plane of the actuating arm and a maximum height of $0.08c$. The actuating arms were mounted normal to the wing surface and to the front face of each aileron at spanwise intervals of $0.10 \frac{b}{2}$ for the plain retractable aileron and at the inboard and outboard ends of each stepped-retractable-aileron segment (fig. 5).

TESTS

All the tests were performed in the Langley 300 MPH 7-by 10-foot tunnel at an average dynamic pressure of approximately 99 pounds per square foot, which corresponds to a Mach number of 0.26. Reynolds numbers, based on the mean aerodynamic chord of each wing, were as follows:

Aspect ratio, A	Sweep, Λ (deg)	Mean aerodynamic chord, \bar{c} (ft)	Reynolds number	Ailerons investigated
6.13	0	0.997	1.8×10^6	Flap type.
4.13	0	1.221	2.2	Flap and retractable type.
2.13	0	1.714	3.1	Flap and retractable type.
1.13	0	2.409	4.4	Flap and retractable type.
2.09	45	1.718	3.1	Retractable type.

Data for each test were obtained through an angle-of-attack range from -6° to beyond the wing stall. Lift, drag, and pitching-moment data were obtained for each plain wing at $\psi=0^\circ$, and tests on the unswept models were made at $\psi=\pm 5^\circ$ to obtain the lateral-stability derivatives. Lateral-control data were obtained for each of the wings with the various spans of inboard and outboard flap ailerons

TABLE II.—FLAP-AILERON CONFIGURATIONS TESTED

Aspect ratio	Aileron location					
	Outboard ailerons			Inboard ailerons		
	Span	$\frac{y_1}{b/2}$	$\frac{y_2}{b/2}$	Span	$\frac{y_1}{b/2}$	$\frac{y_2}{b/2}$
6.13	0.925 $\frac{b}{2}$	0.067	0.992			
	.716	.246	.992	0.425 $\frac{b}{2}$	0.067	0.492
	.600	.492	.992	.179	.067	.246
4.13	.916	.073	.989			
	.716	.243	.989	.414	.073	.487
	.502	.487	.989	.170	.073	.243
2.13	.978	0	.978			
	.741	.237	.978	.476	0	.476
	.502	.476	.978	.237	0	.237
1.13	.957	0	.957			
	.729	.228	.957	.455	0	.455
	.502	.455	.957	.228	0	.228
2.09	.957	0	.957			
	.729	.228	.957	.455	0	.455
	.502	.455	.957	.228	0	.228

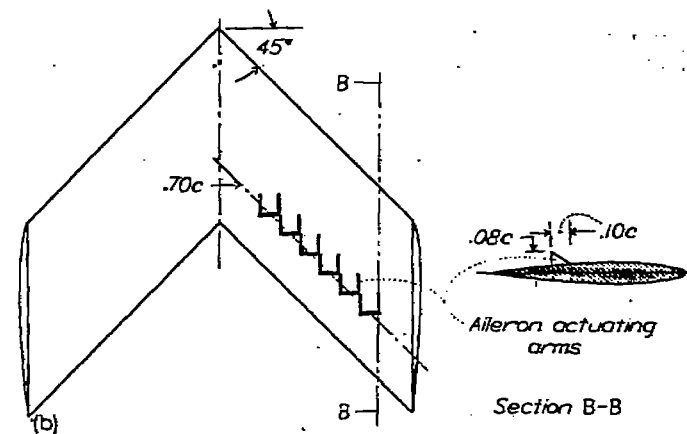
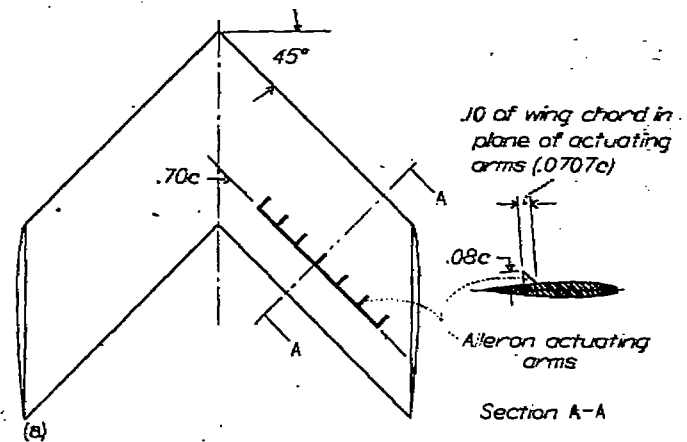
listed in table II through a deflection range of $\pm 20^\circ$, except for the $A=1.13$ wing model for which the deflection range extended to $\pm 30^\circ$. The retractable aileron configurations listed in table III were tested with projections up to $-0.08c$.

CORRECTIONS

Jet-boundary (induced upwash) corrections were applied to the angle of attack and the drag and rolling-moment coefficients according to the methods of reference 10. The data were also corrected for blockage effects by the method of reference 11 and for model-support-strut tares.

TABLE III.—RETRACTABLE-AILERON CONFIGURATIONS TESTED

Aspect ratio	Sweep	Aileron location			Type of retractable aileron
		Span	$\frac{y_1}{b/2}$	$\frac{y_2}{b/2}$	
4.13	0	0.80	0.40	1.00	Plain.
2.13	0	.80	.40	1.00	Plain.
1.13	0	.80	.40	1.00	Plain.
2.09	45	.80	0	.80	Plain with and without actuating arms and stepped with and without actuating arms.
		.80	.20	.80	
		.80	.40	1.00	



(a) Plain-retractable-aileron configuration.
 (b) Stepped-retractable-aileron configuration.

FIGURE 5.—Geometric characteristics of the plain and stepped retractable ailerons tested with aileron actuating arms on the 45° sweptback wing of aspect ratio 2.09, $b_a=0.60 \frac{b}{2}$.

DISCUSSION

WING AERODYNAMIC CHARACTERISTICS

Effect of aspect ratio.—Lift, drag, and pitching-moment characteristics of the wing models are presented in figure 6. The variation of $C_{L\alpha}$, C_{Lmax} , $(L/D)_{max}$, and aerodynamic-center location with wing aspect ratio is shown in figure 7.

The data of figure 6 show fairly regular variations of α , C_D , and C_m with C_L except for the $A=1.13$ wing. The lift curve of the $A=1.13$ wing exhibited a break between $\alpha=16^\circ$ and 18° , and a corresponding rapid drag rise and a large change in pitching-moment coefficient toward more negative values occurred in this α range. Observation of the tufts on this wing showed that this phenomenon occurred as a result of a sudden leading-edge separation which left only the tufts in the region of the wing tips definitely steady. With decrease in the angle of attack, observation of the tufts indicated that the flow reattached at about the same value of α and over an equally small increment of α . This phenomenon may be a function of the Reynolds number of the tests and may not exist at flight Reynolds numbers.

The wing lift-curve slopes increased with increasing aspect ratio (fig. 7) and the variation of $C_{L\alpha}$ with aspect ratio was accurately predicted by the method of reference 12. The variation of maximum lift coefficient and $(L/D)_{max}$ with aspect ratio is similar to that reported in reference 13 in which an investigation of low-aspect-ratio wings of Clark Y airfoil section indicated a peak value of the maximum lift coefficient at about $A=1$ and an increase in $(L/D)_{max}$ with increasing aspect ratio. The aerodynamic center of each wing model, measured at low lift coefficients, was ahead of its respective quarter chord of the mean aerodynamic chord. This distance was small for the $A=2.13$, 4.13, and 6.13 wing models but became significant for the $A=1.13$ wing model. As indicated in figure 6, above $C_L \approx 0.5$ all of the pitching-moment curves became stable.

Effect of sweep.—A comparison of the unswept wing of aspect ratio 2.13 with the 45° sweptback wing of aspect ratio 2.09 indicates that the maximum lift coefficient of the sweptback wing was larger than that of the unswept wing. The aerodynamic-center locations for the two wings were at about the same percent M.A.C. Sweeping the wing back had little effect on the value of $(L/D)_{max}$.

A theoretical value of $C_{L\alpha}$ of 0.042 computed for the swept wing by the method of reference 12 agrees very well with the experimental lift-curve slope (measured near $C_L=0^\circ$) of 0.041.

LATERAL STABILITY CHARACTERISTICS OF UNSWEPT WINGS

The variation of the lateral-stability derivatives C_{l_p} , C_{n_p} , and C_{Y_p} with lift coefficient obtained for the unswept models is given in figure 8. The effective dihedral parameter C_{l_p} increased approximately linearly with increasing C_L until the wing began to stall. Since the extent of the lift-coefficient range wherein C_{l_p} varies linearly with C_L is a function of Reynolds number (unpublished data), the experimental data are not necessarily indicative of the variation of C_{l_p} with C_L near the wing stall for flight Reynolds number.

The slopes of the curves of C_{l_p} plotted against C_L measured near $C_L=0$ increased with decreasing aspect ratio; this variation of C_{l_p} with C_L for various aspect ratios agrees qualitatively with the variation reported in reference 14.

Throughout the lift-coefficient range, the values of C_{n_p} and C_{Y_p} were small. The values of C_{n_p} were generally slightly negative and these negative values indicate positive directional stability.

LATERAL CONTROL CHARACTERISTICS OF FLAP AILERONS

Rolling-moment-coefficient and yawing-moment-coefficient data obtained through the angle-of-attack range for each of the four wings equipped with various spans of outboard and inboard flap ailerons are presented in figures 9 to 32. Cross plots of C_l against δ_a at $\alpha \approx 0^\circ$ for the aileron spans tested on the unswept wings are given in figure 33. The slopes of the curves of C_l against δ_a for outboard ailerons, measured at $\delta_a=0^\circ$ in figure 33, are presented in figure 34 as a function of $\frac{y_i}{b/2}$.

Rolling-moment characteristics.—The data for the $A=1.13$ wing (figs. 9 to 14) indicate a rapid loss in aileron effectiveness at an angle of attack considerably below the plain-wing stall but approximately the same as or slightly above that angle at which the leading-edge separation previously described occurred. Below this angle the curves of rolling moment against angle of attack indicate fairly constant rolling moments for all deflections.

The curves of rolling moment against angle of attack for the $A=2.13$ wing (figs. 15 to 20) show relatively constant rolling moments over the angle-of-attack range up to the angle of attack for plain-wing stall.

The data for the $A=4.13$ and 6.13 wings (figs. 21 to 32) indicate generally constant rolling moments up to the angle of attack for plain-wing stall for negative aileron deflections. The rolling moments produced by positive deflections, however, tended to approach zero at a lower angle of attack as the aileron deflection was increased. This effect was more pronounced for the larger-span ailerons.

In general, the $A=1.13$ wing gave fairly constant rolling moments over an increased angle-of-attack range for greater aileron deflections than did the higher-aspect-ratio wings.

The curve of C_l plotted against δ_a at $\alpha \approx 0^\circ$ for the $A=6.13$ wing shows a decrease in effectiveness at about $\delta_a=15^\circ$; whereas the curves of C_l plotted against δ_a for the wings of lower aspect ratio have generally constant slopes through the deflection ranges tested (for $A=4.13$ and 2.13, $\delta_a = \pm 20^\circ$; for $A=1.13$, $\delta_a = \pm 30^\circ$). (See fig. 33.)

The spanwise-effectiveness curves of the ailerons on the four wings (fig. 34) show that aileron effectiveness decreases as aileron span or wing aspect ratio decreases. However, because the damping in roll also decreases with decreasing aspect ratio (reference 15), the ratio of control-surface area to wing area required to maintain a constant rolling effectiveness will not show so great a variation with decreasing aspect ratio as indicated by the aileron-effectiveness data.

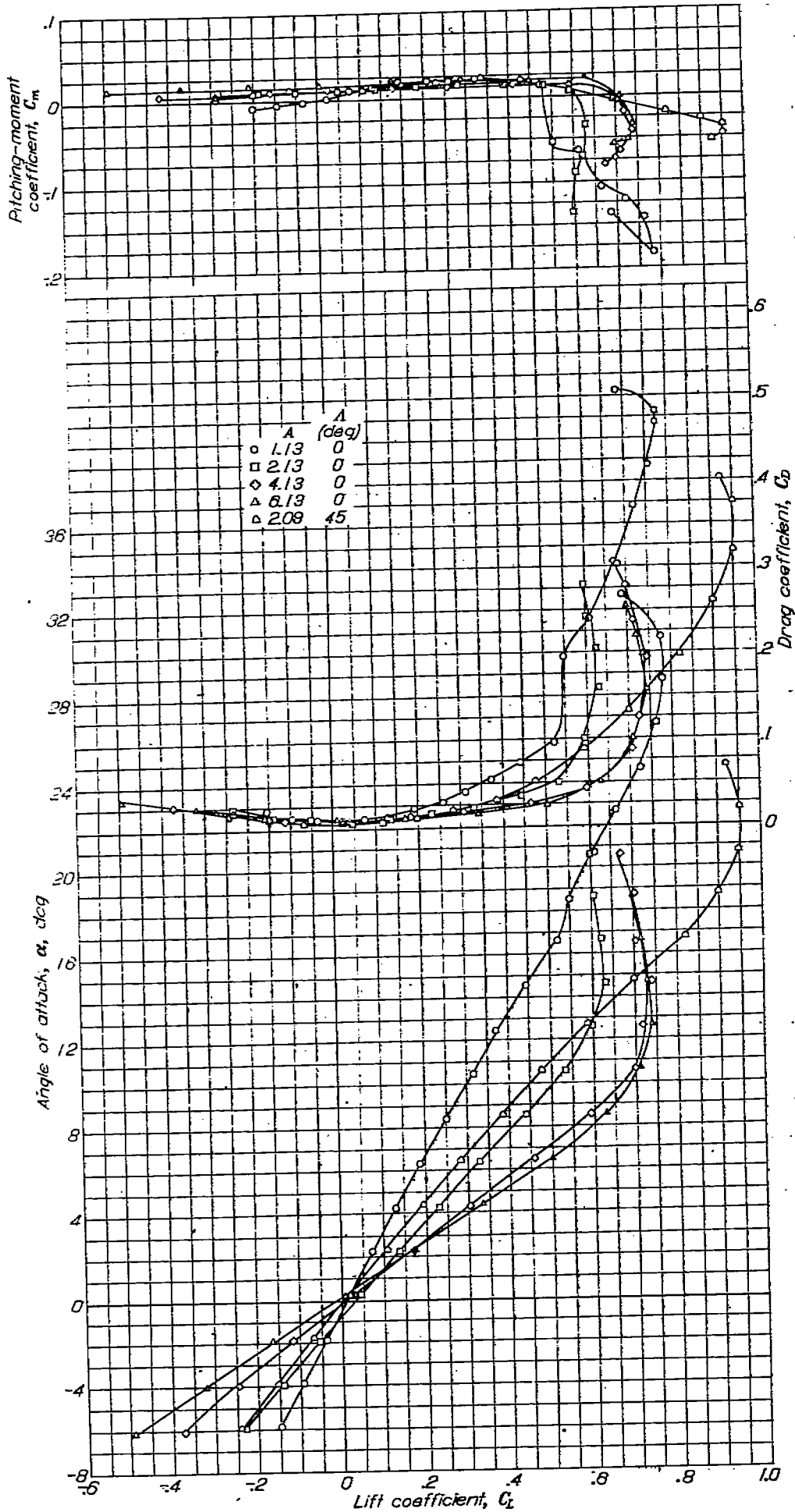


FIGURE 6.—Aerodynamic characteristics in pitch of the plate wings. $\psi = 0^\circ$.

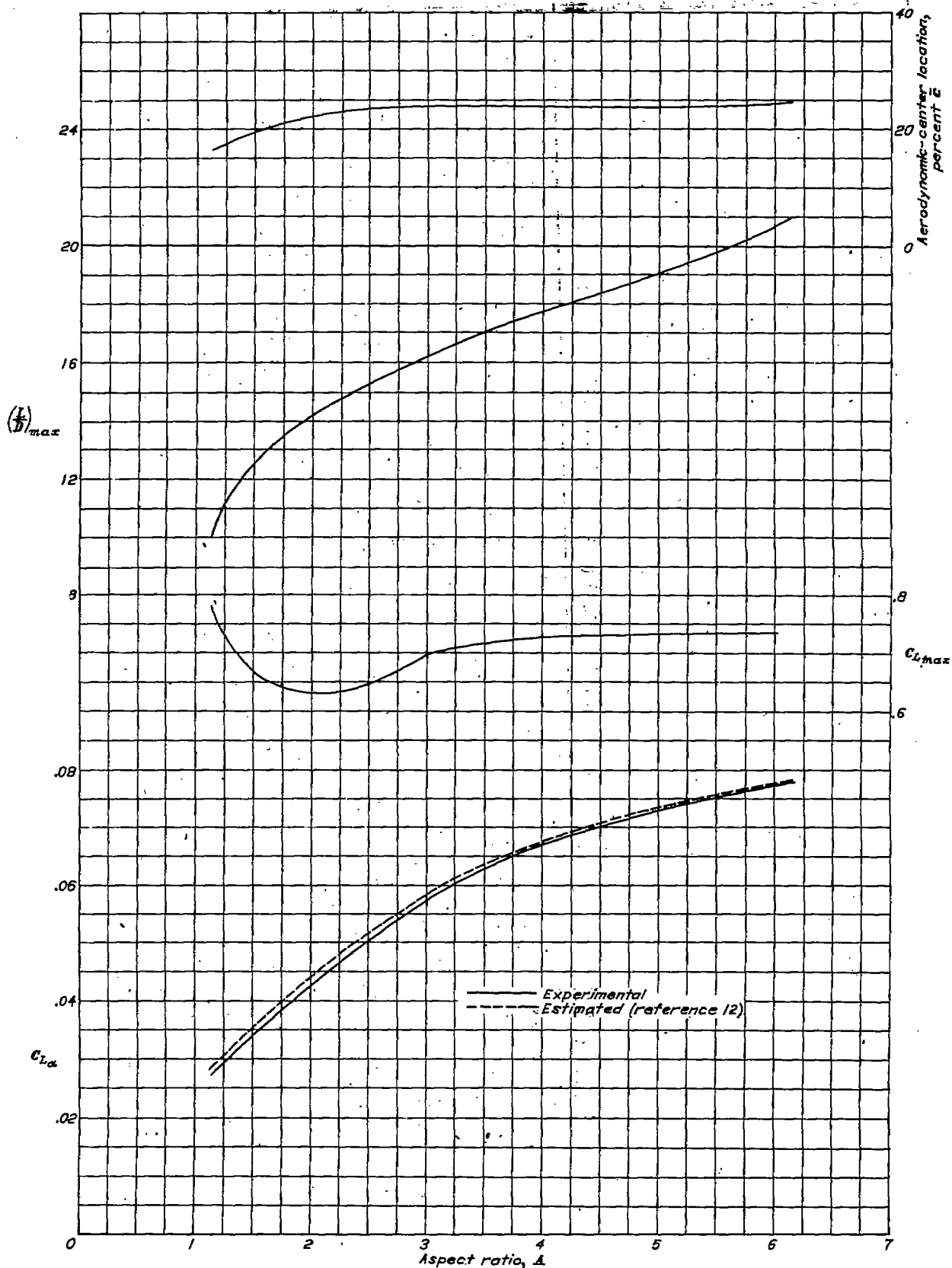
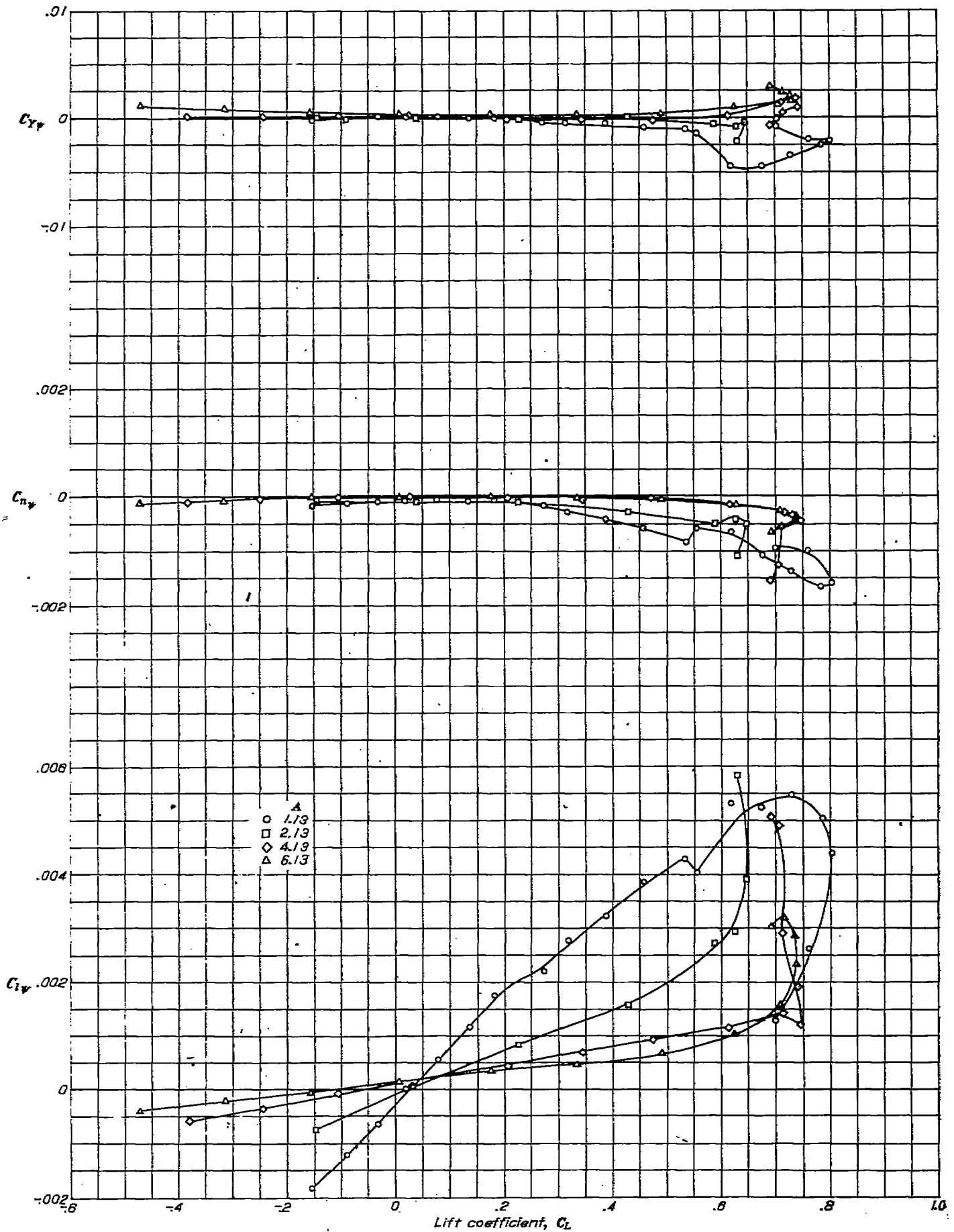


FIGURE 7.—Variation of C_{l_α} , $C_{l_{max}}$, $(L/D)_{max}$, and aerodynamic-center location with aspect ratio for unswept wings.

The rolling-moment data of figures 33 and 34 show that spanwise-effectiveness curves based on the effectiveness of outboard ailerons can be used to estimate the effectiveness of inboard ailerons (reference 16) because the value of C_{l_α} for an aileron spanning any portion of the wing is the difference between the values of C_{l_α} at the inboard end and C_{l_α} at

the outboard end of the aileron. The effectiveness of the inboard ailerons estimated in this manner agrees reasonably well with the corresponding values of C_{l_α} determined from figure 33. A comparison of the value of C_{l_α} for inboard and outboard ailerons (fig. 33 or 34) shows that outboard ailerons are more effective than inboard ailerons of the same span.

FIGURE 8.—Variation of the derivatives C_{l_p} , C_{n_p} , and C_{i_p} with lift coefficient for the unswept wings.

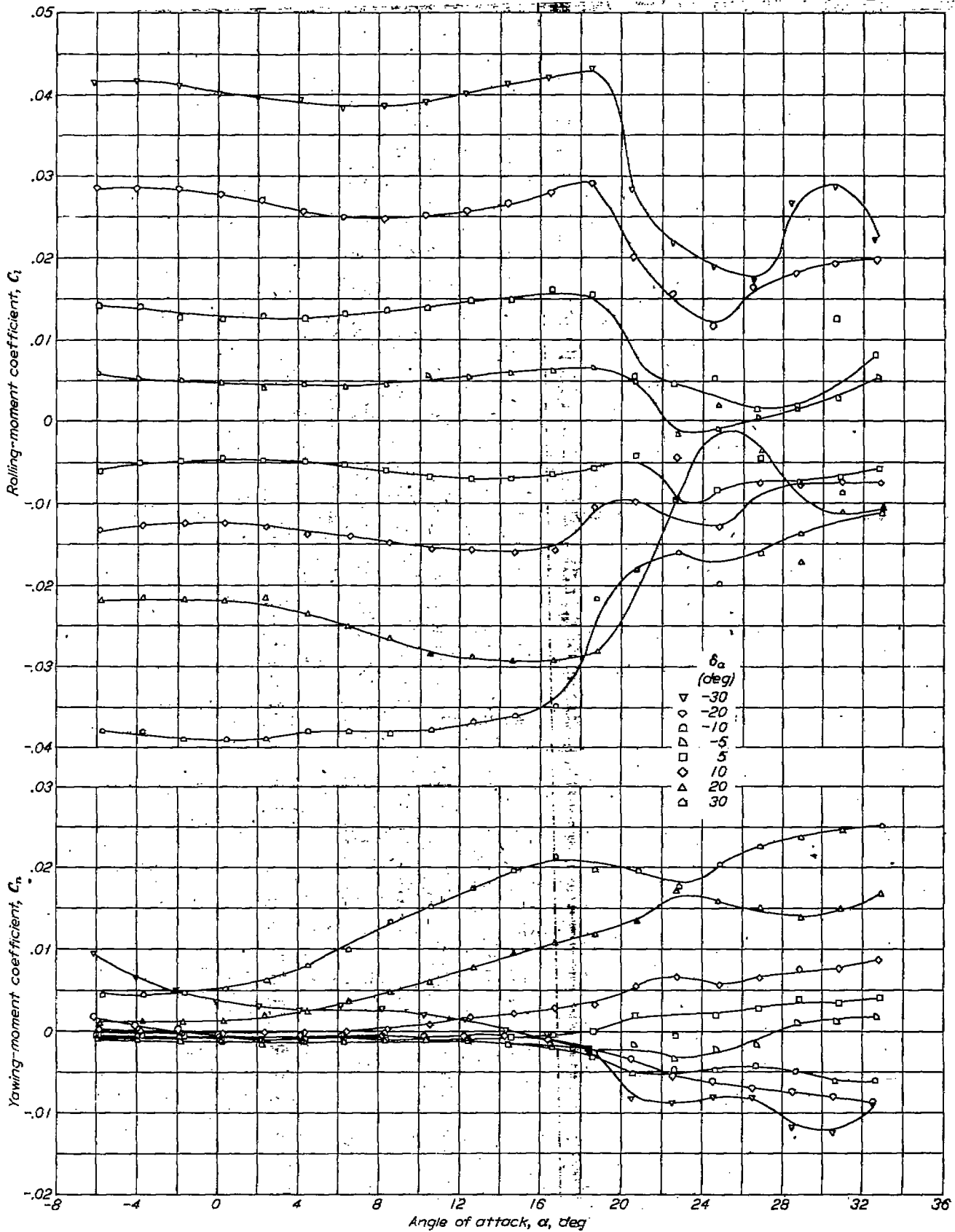


FIGURE 9.—Variation of the lateral control characteristics with angle of attack of the A-1.13 wing equipped with flap ailerons. Outboard ailerons; $\frac{b_a}{b/2} = 0.957$.

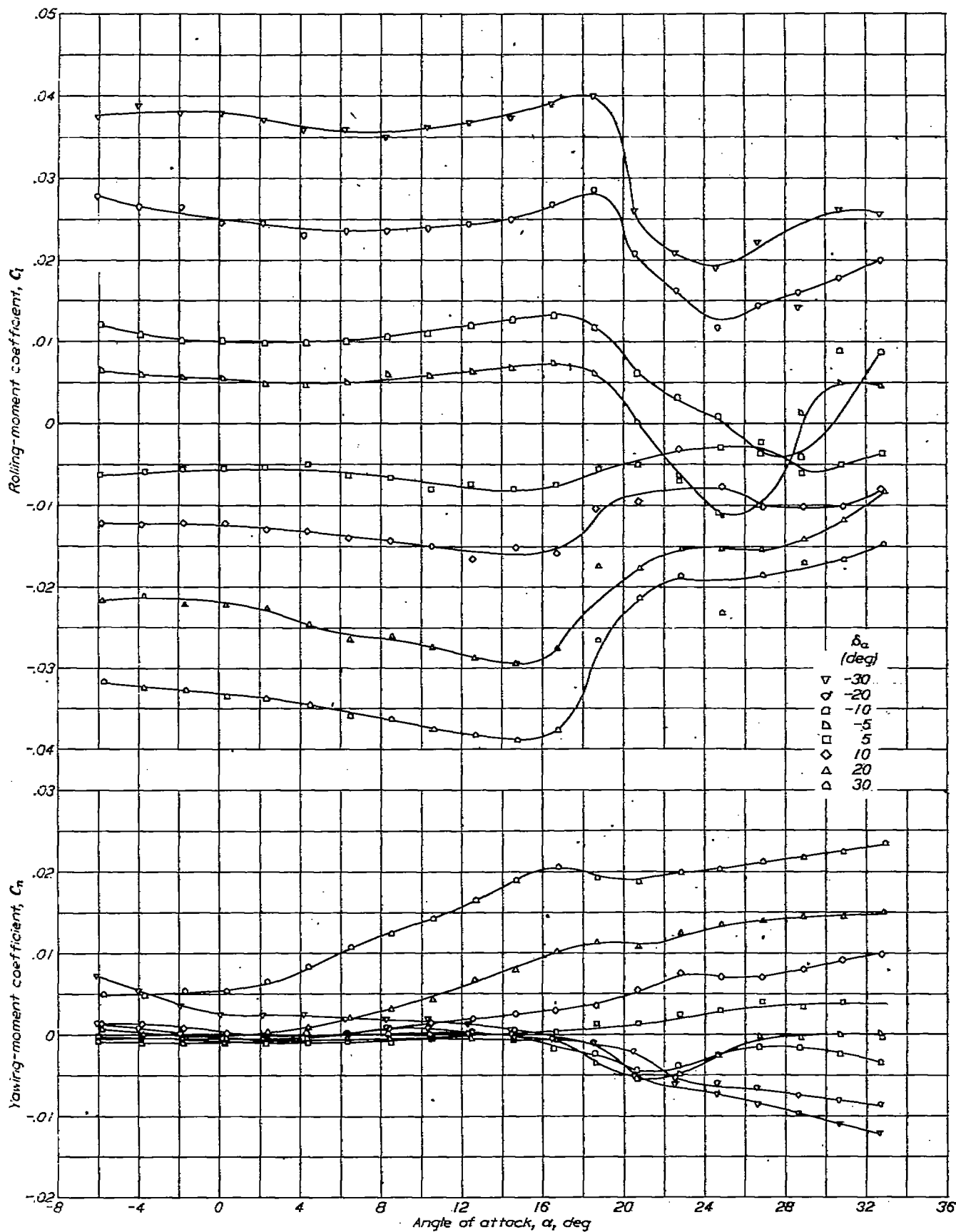


FIGURE 10.—Variation of the lateral control characteristics with angle of attack of the $A=1.13$ wing equipped with flap ailerons. Outboard ailerons; $\frac{b_e}{b/2}=0.729$.

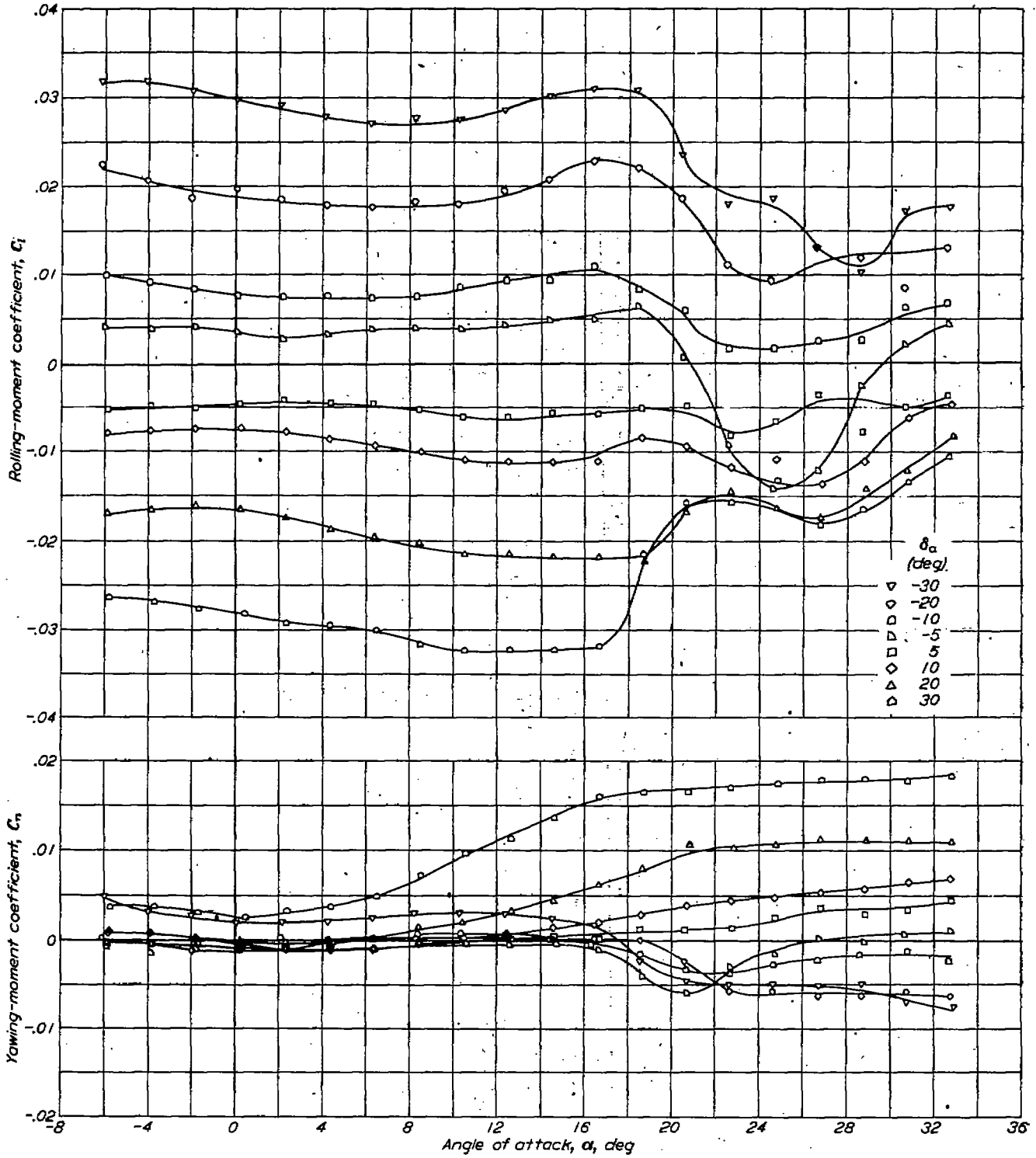


FIGURE 11.—Variation of the lateral control characteristics with angle of attack of the $A=1.13$ wing equipped with flap ailerons. Outboard ailerons; $\frac{\delta_a}{b/2}=0.502$.

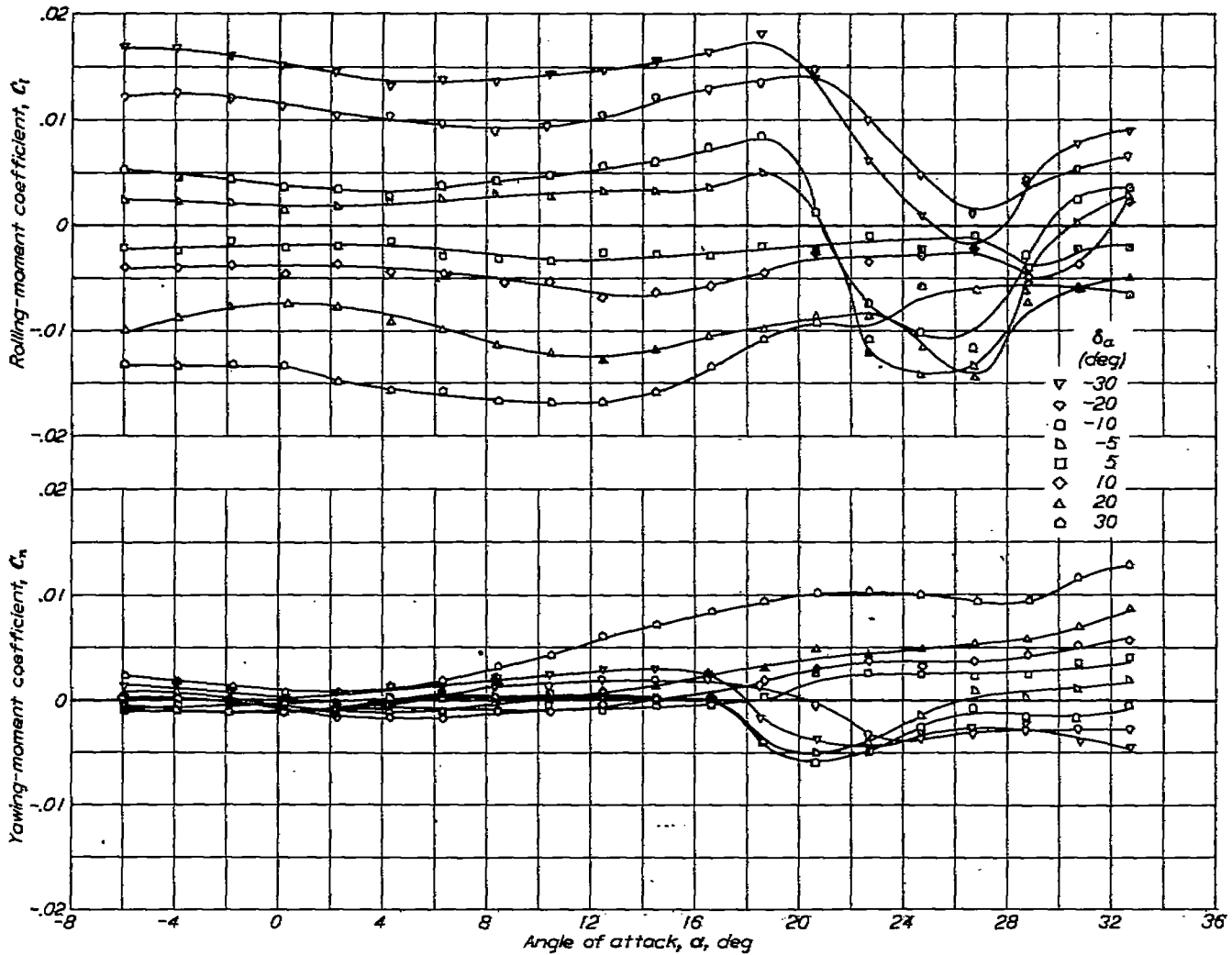


FIGURE 12.—Variation of the lateral control characteristics with angle of attack of the $A=1.13$ wing equipped with flap ailerons. Outboard ailerons; $\frac{b_a}{b} = 0.275$.

Yawing-moment characteristics.—The total yawing-moment coefficient resulting from equal up and down deflections of the ailerons was approximately zero at small angles of attack but became adverse (sign of yawing moment opposite to sign of rolling moment) as α was increased and as the aileron deflection was increased.

The negative values of the C_n/C_l ratio for each wing did not exceed -0.2 for lift coefficients equal to or less than

$0.9 C_{L_{max}}$, except for the $A=1.13$ wing for which a sharp rise in $-C_n/C_l$ is judged to reflect the abnormally high values of drag above $C_L \approx 0.55$ previously discussed. For the range of aspect ratio investigated, it appears that the problems associated with adverse yawing moments on unswept wings of moderate aspect ratio become serious well below $C_{L_{max}}$ if partial flow separation in the linear lift range is characteristic of the wings.

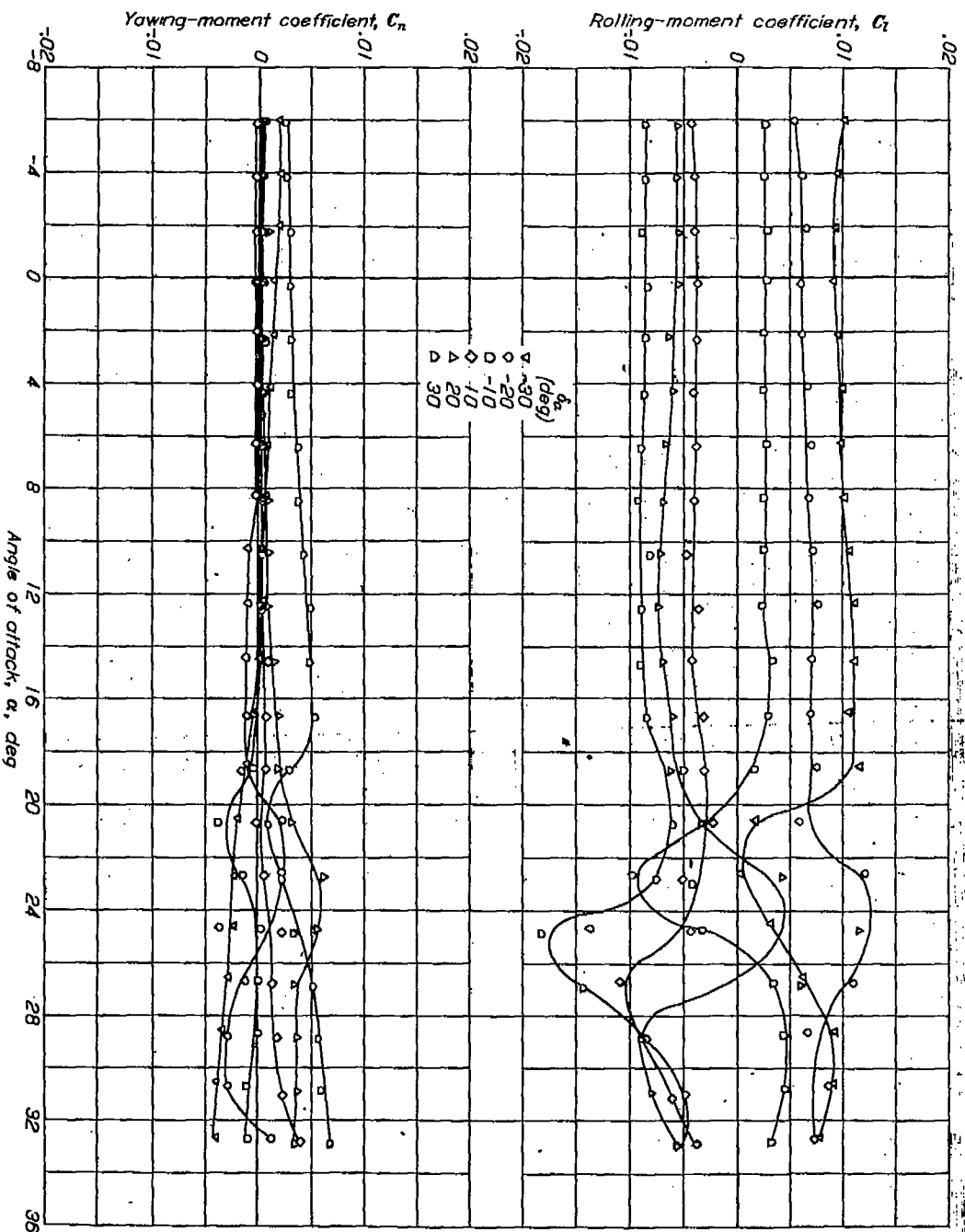


FIGURE 13.—Variation of the lateral control characteristics with angle of attack of the $\Delta=1.13$ wing equipped with flap slatons. Inboard slatons; $\frac{\delta_{flaps}}{b/2}=0.455$.

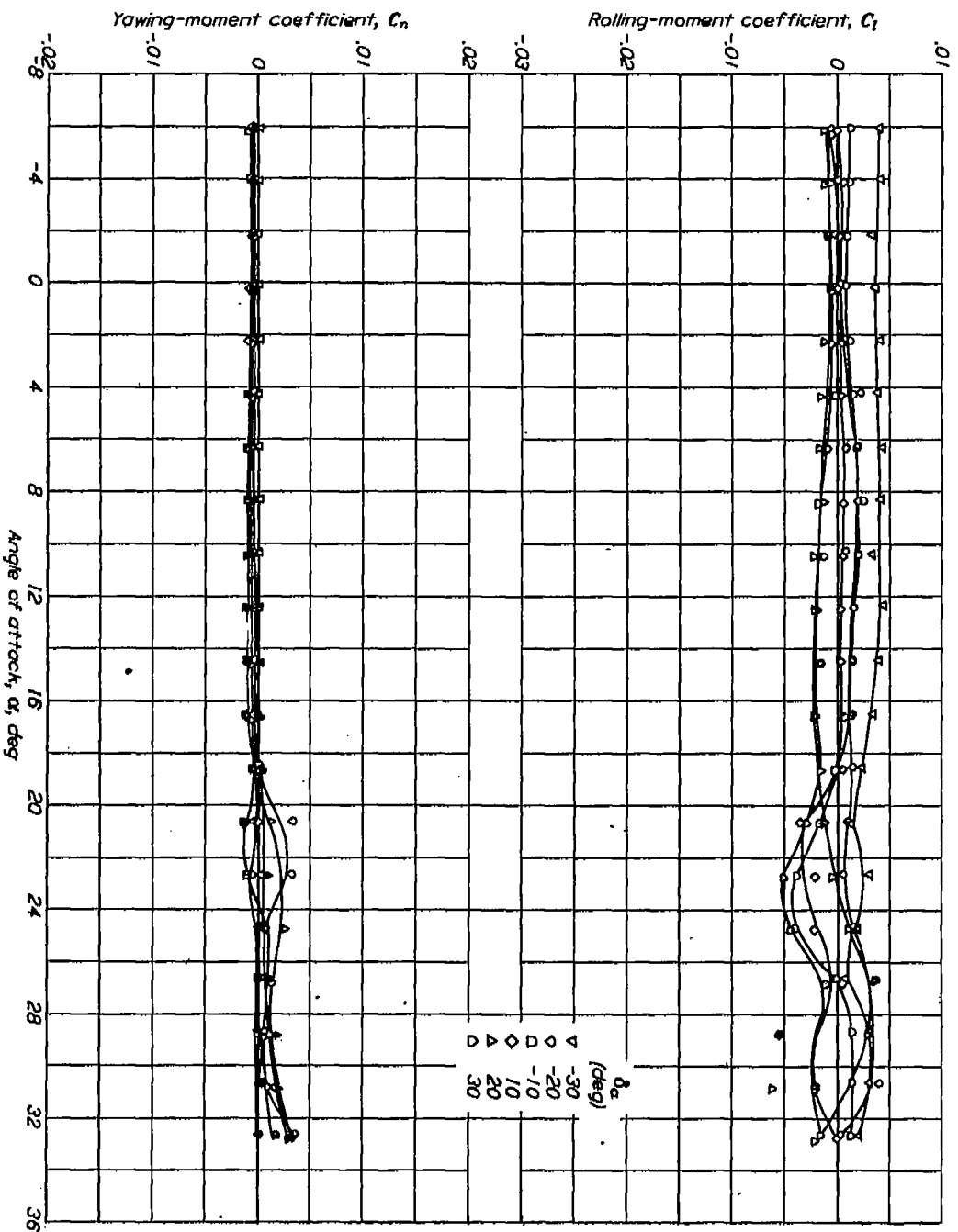


FIGURE 14.—Variation of the lateral control characteristics with angle of attack of the $A=1.13$ wing equipped with flap ailerons. Inboard ailerons; $b/\lambda=0.228$.

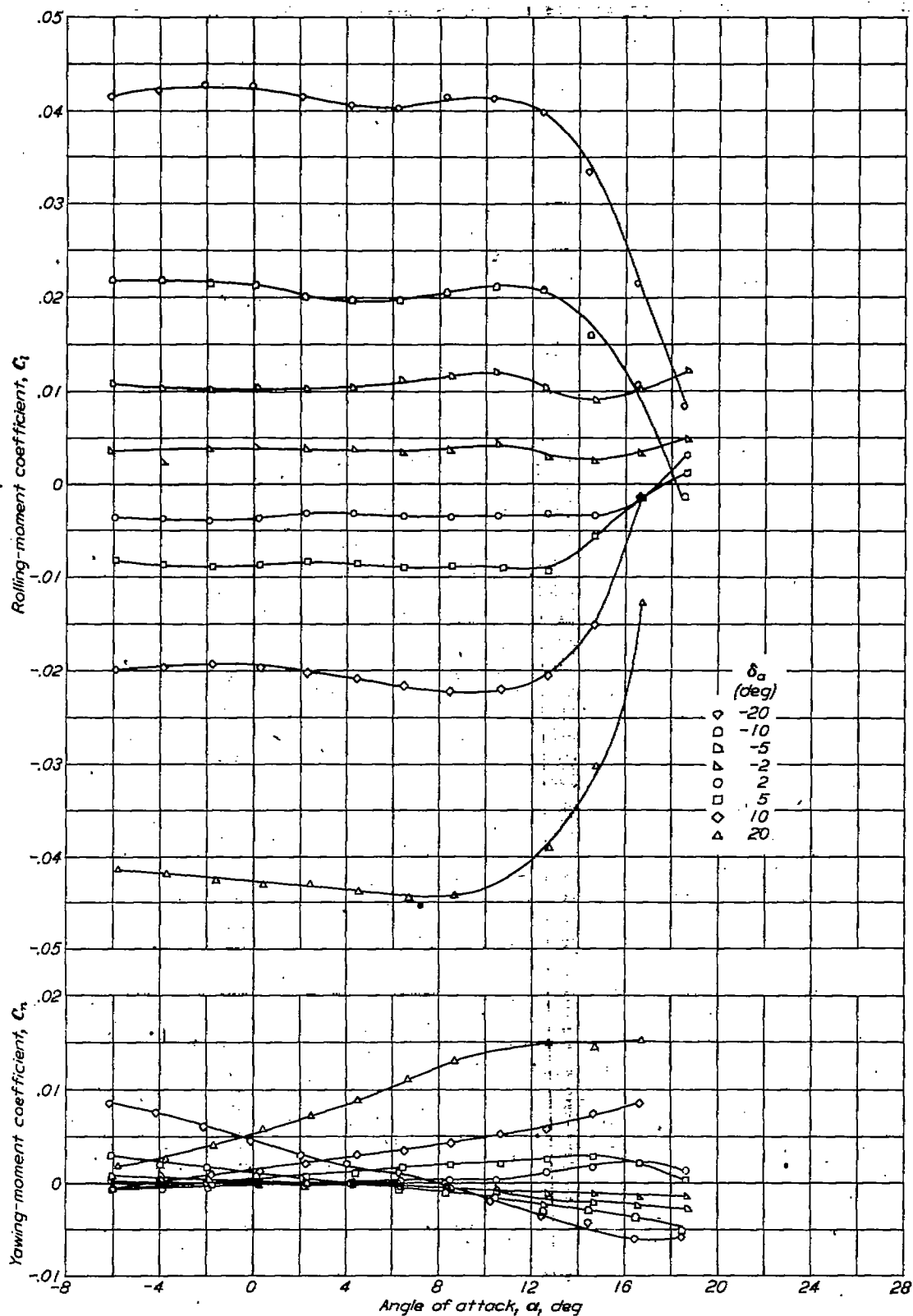


FIGURE 15.—Variation of the lateral control characteristics with angle of attack of the $A=2.13$ wing equipped with flap ailerons. Outboard ailerons; $\frac{b_o}{b} = 0.978$.

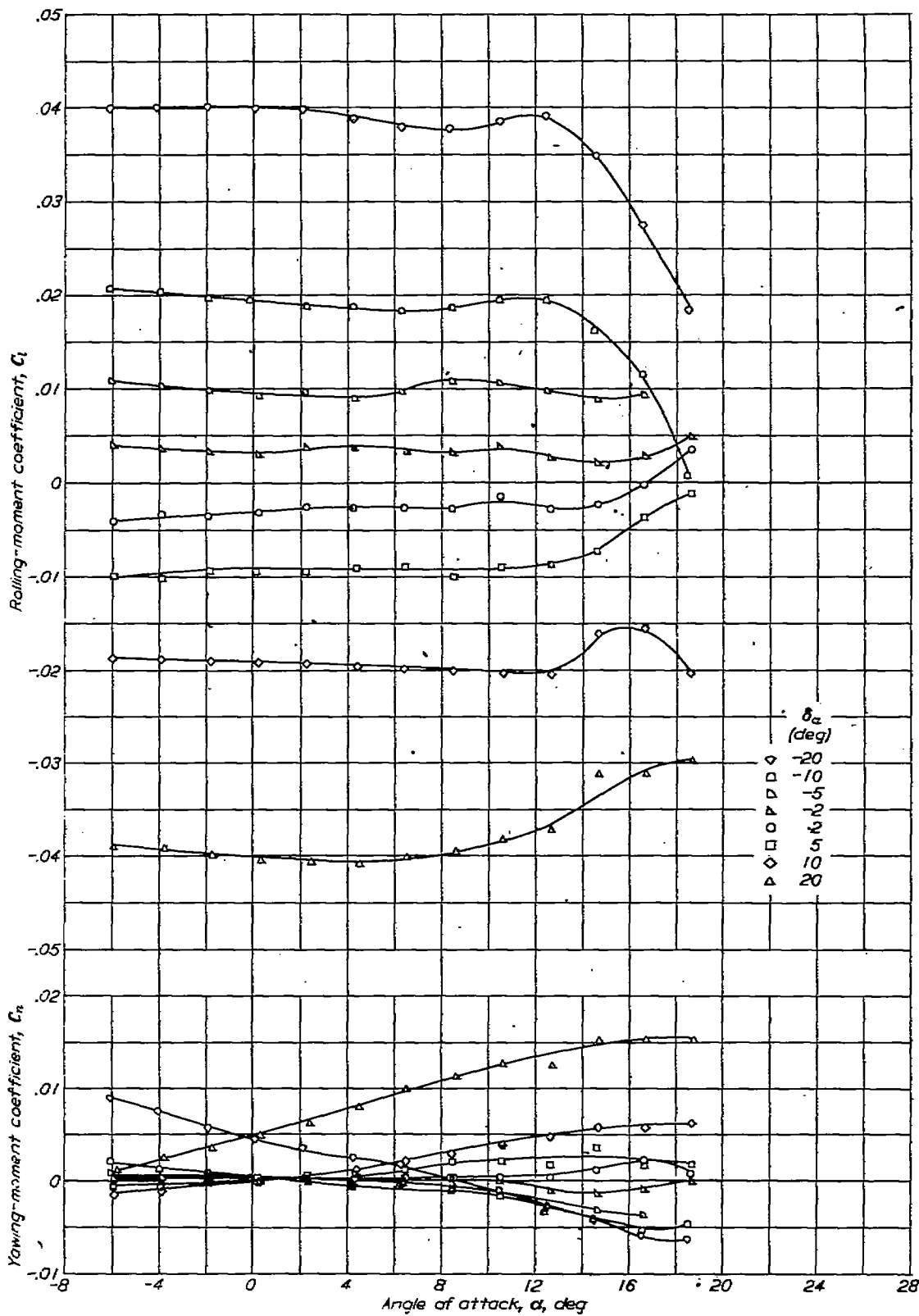


FIGURE 16.—Variation of the lateral control characteristics with angle of attack of the $A=2.13$ wing equipped with flap ailerons. Outboard ailerons; $\frac{b_w}{b} = 0.741$.

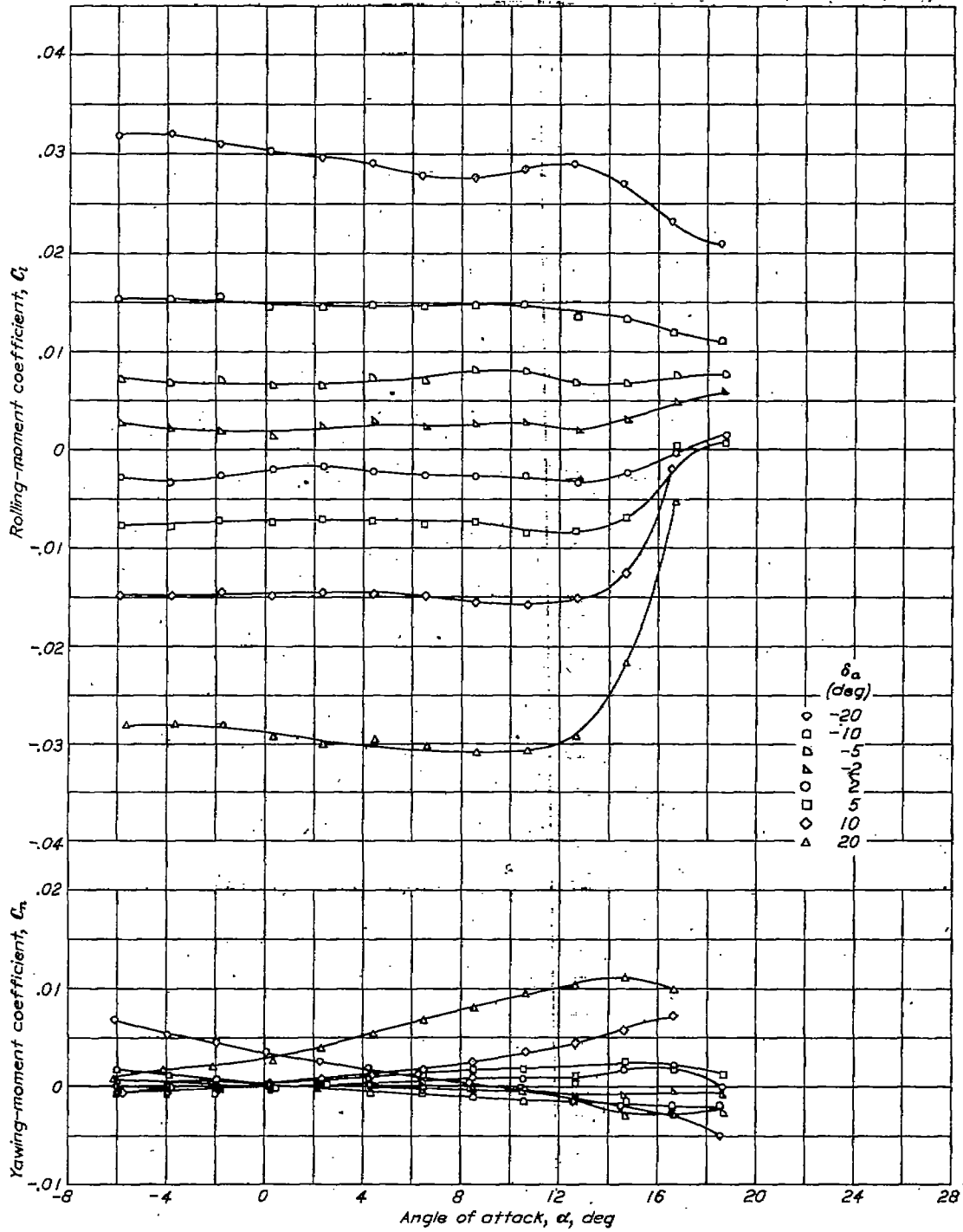


FIGURE 17.—Variation of the lateral control characteristics with angle of attack of the A-2.13 wing equipped with flap ailerons. Outboard ailerons; $\frac{b_a}{b} = 0.502$.

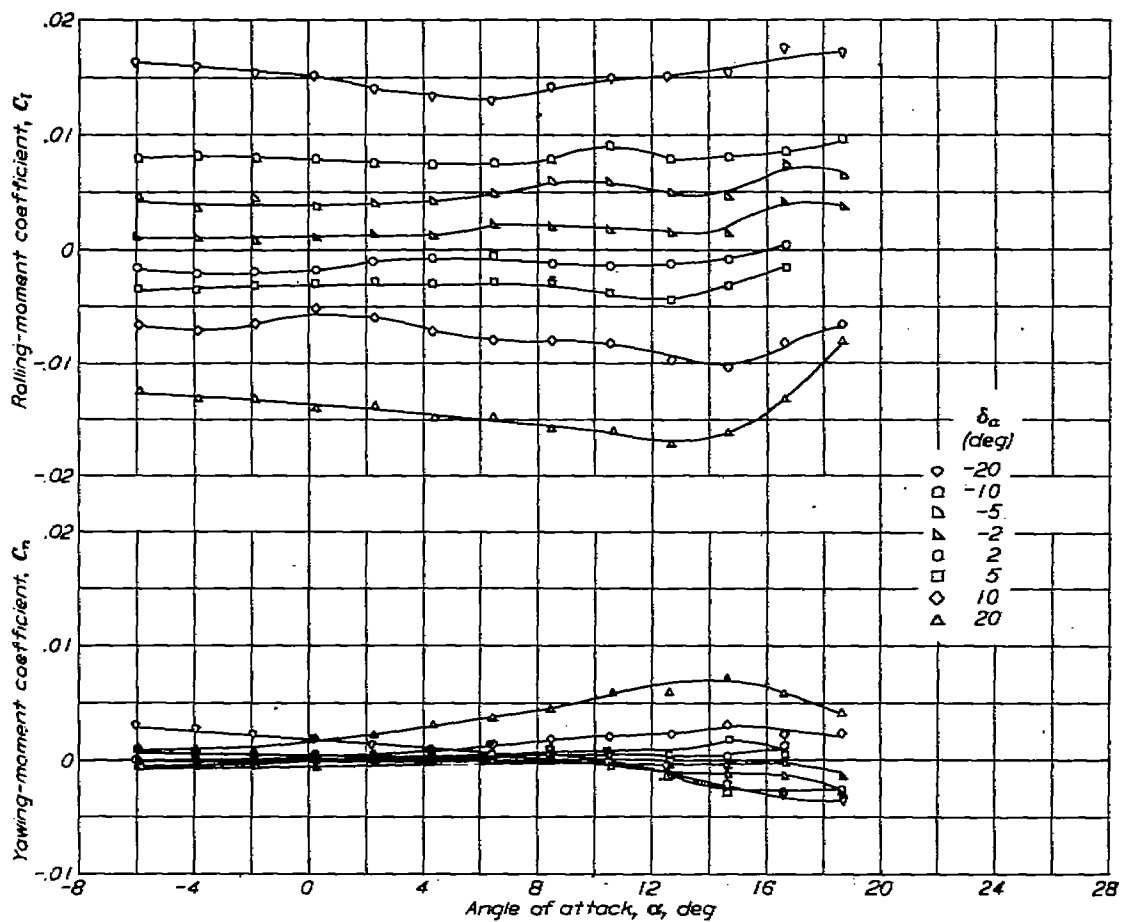


FIGURE 18.—Variation of the lateral control characteristics with angle of attack of the $A=2.13$ wing equipped with flap ailerons. Outboard ailerons; $\frac{b_a}{b/2}=0.263$.

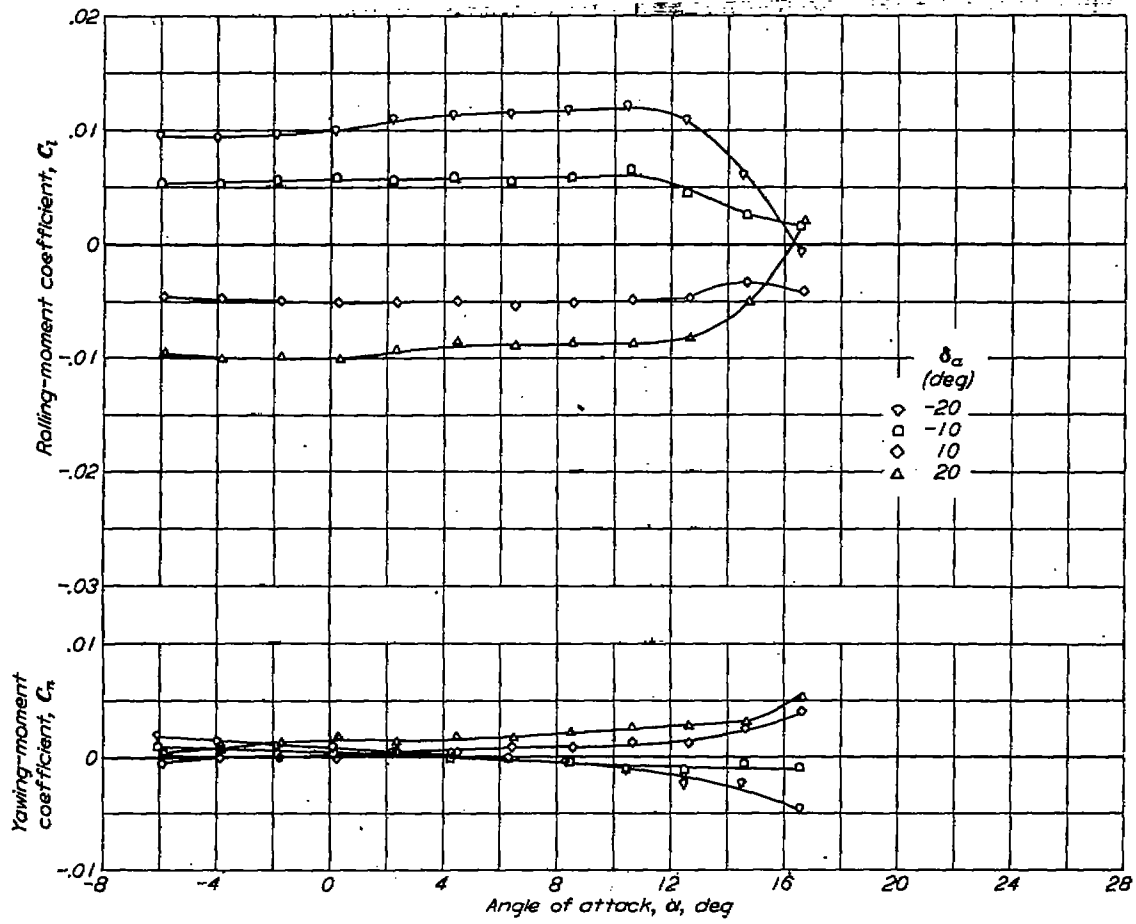


FIGURE 19.—Variation of the lateral control characteristics with angle of attack of the $A=2.13$ wing equipped with flap ailerons. Inboard ailerons; $\frac{b_a}{b^2}=0.476$.

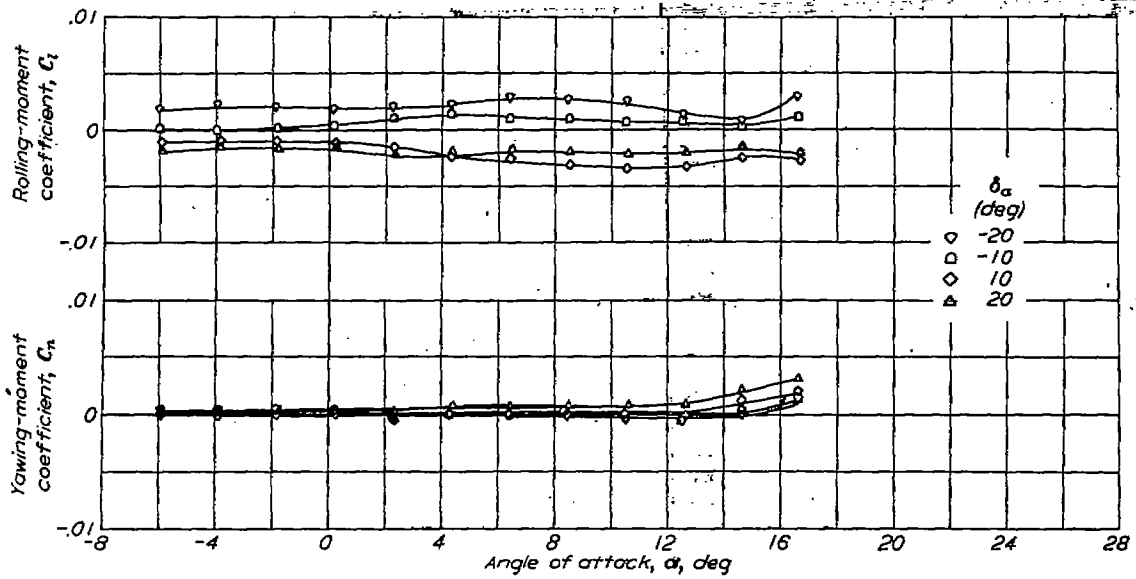


FIGURE 20.—Variation of the lateral control characteristics with angle of attack of the $A=2.13$ wing equipped with flap ailerons. Inboard ailerons; $\frac{b_a}{b^2}=0.237$.

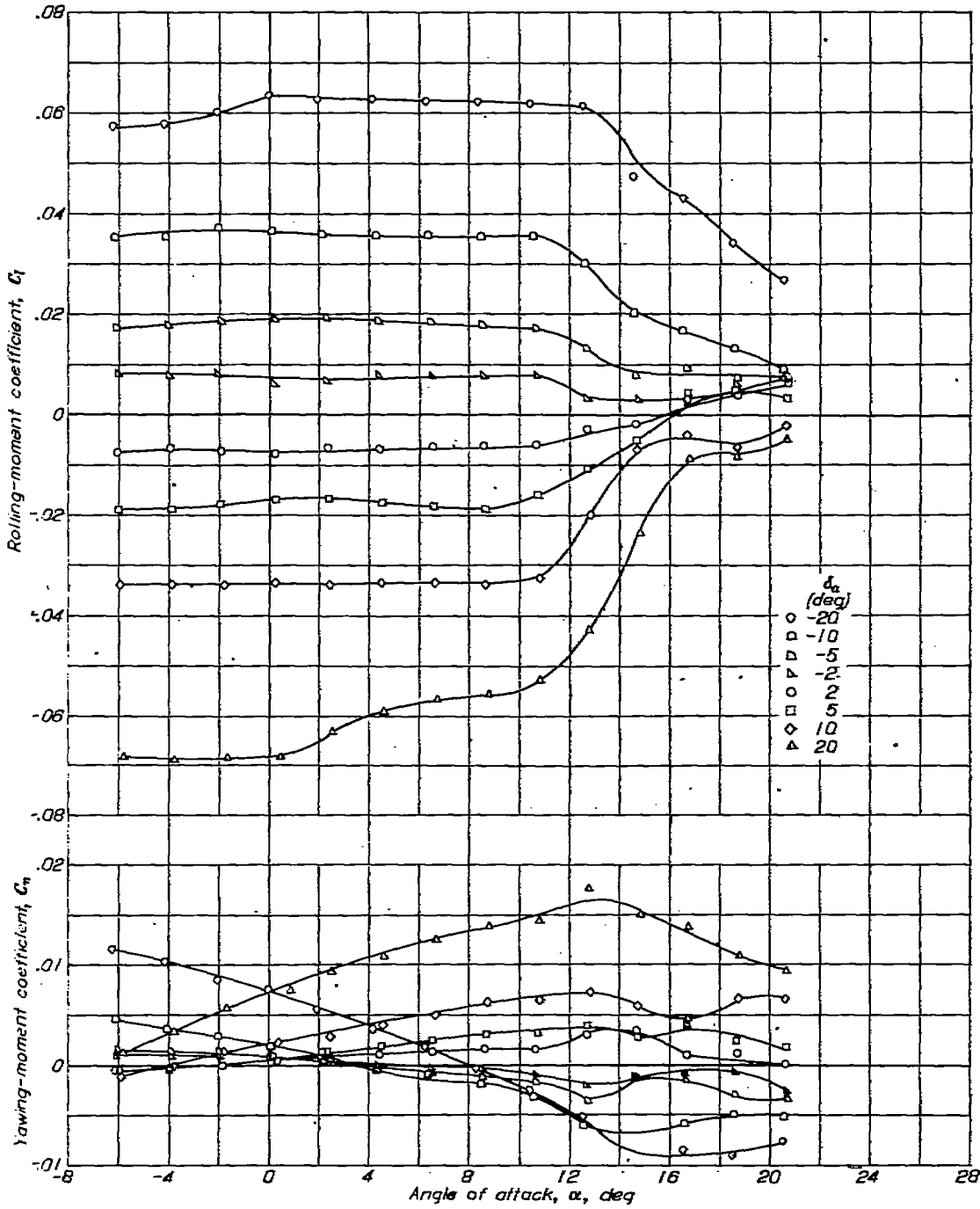


FIGURE 21.—Variation of the lateral control characteristics with angle of attack of the $A=4.13$ wing equipped with flap allerons. Outboard allerons; $\frac{b_a}{b/2}=0.916$.

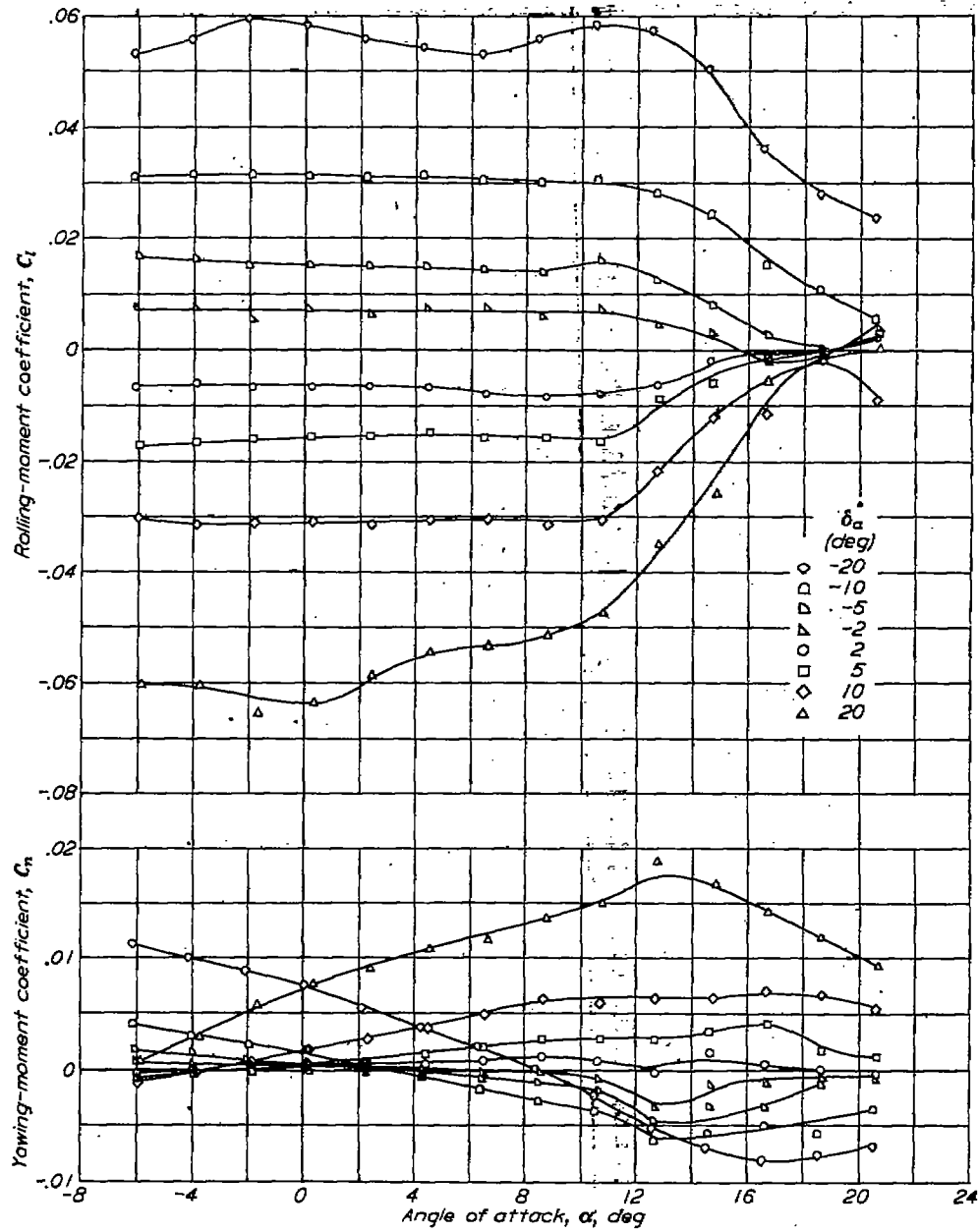


FIGURE 22.—Variation of the lateral control characteristics with angle of attack of the $A=4.13$ wing equipped with flap ailerons. Outboard ailerons; $\frac{b_a}{b/2}=0.746$.

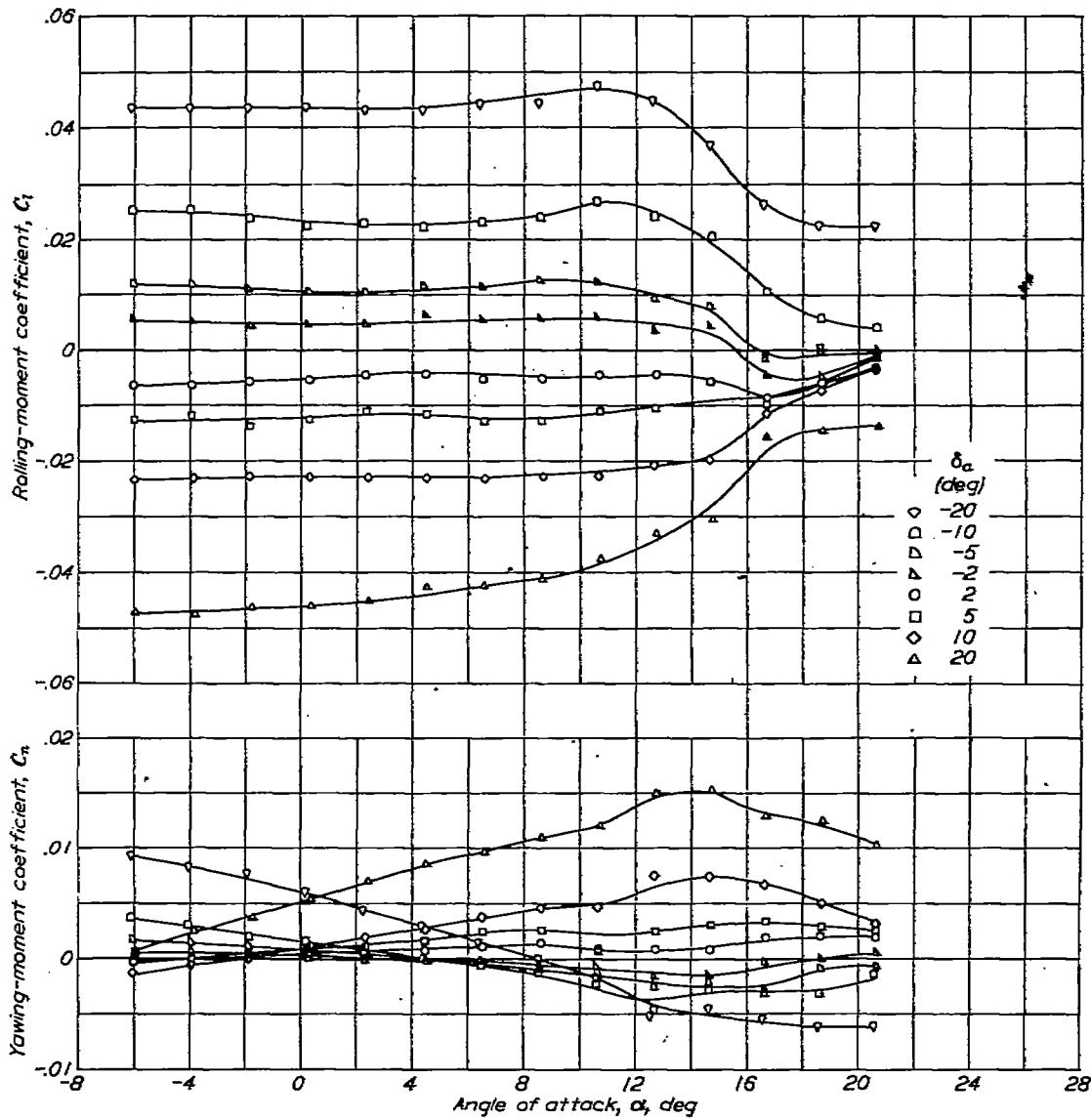


FIGURE 23.—Variation of the lateral control characteristics with angle of attack of the $A=4.13$ wing equipped with flap allerons. Outboard allerons; $\frac{\delta_a}{b/2} = 0.502$.

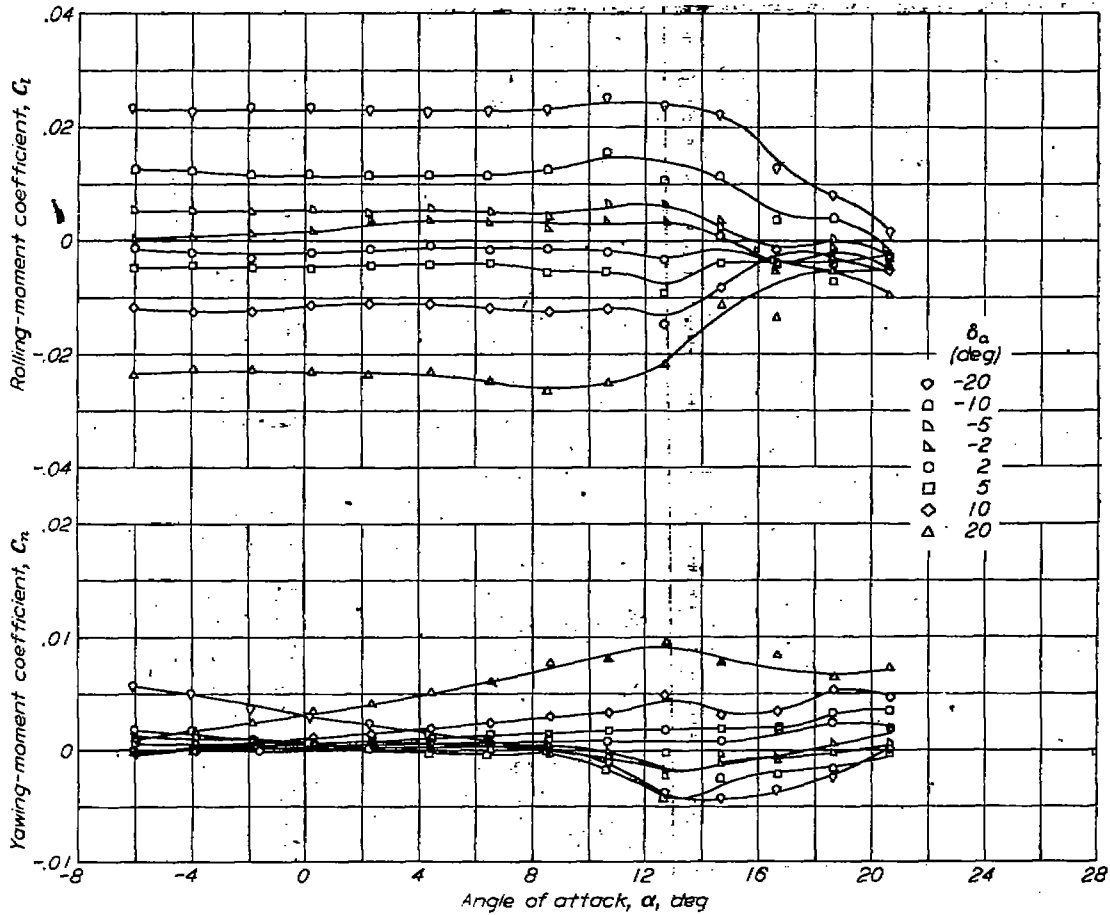


FIGURE 24.—Variation of the lateral control characteristics with angle of attack of the A-4.13 wing equipped with flap allerons. Outboard allerons; $\frac{b_a}{b/2} = 0.287$

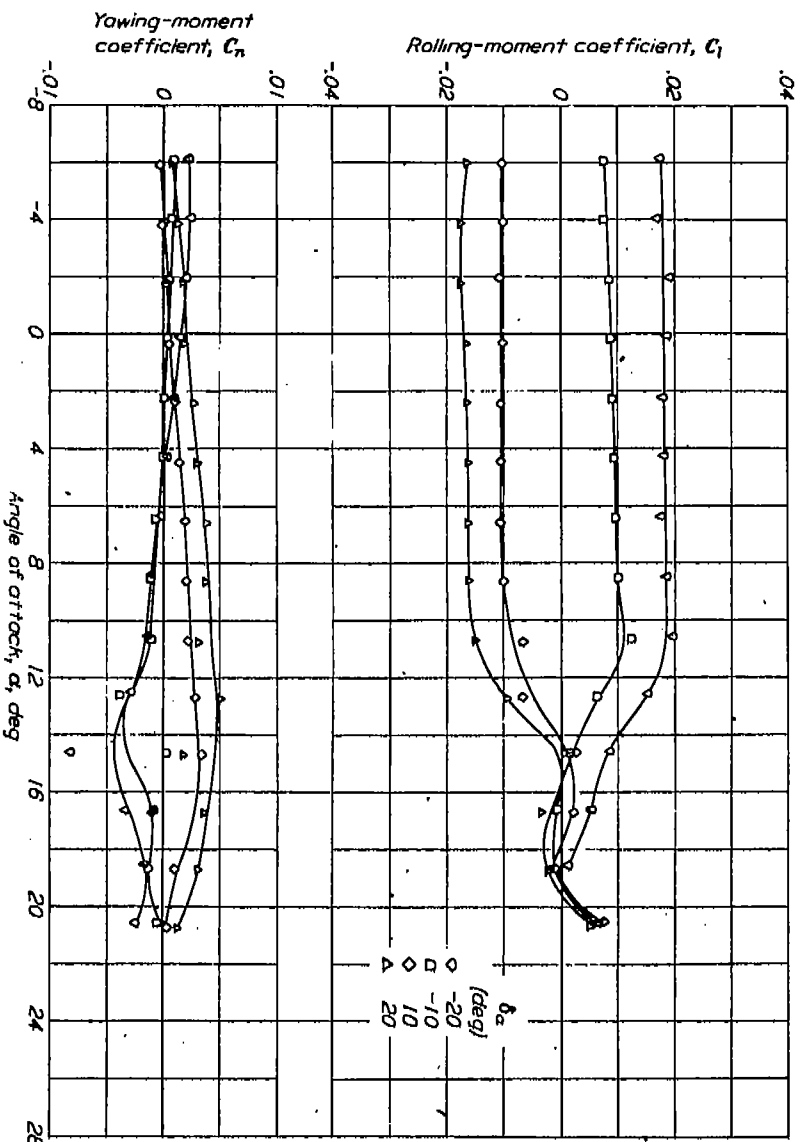


FIGURE 25.—Variation of the lateral control characteristics with angle of attack of the $A=4.13$ wing equipped with flap ailerons. Inboard ailerons; $b/c = 0.414$

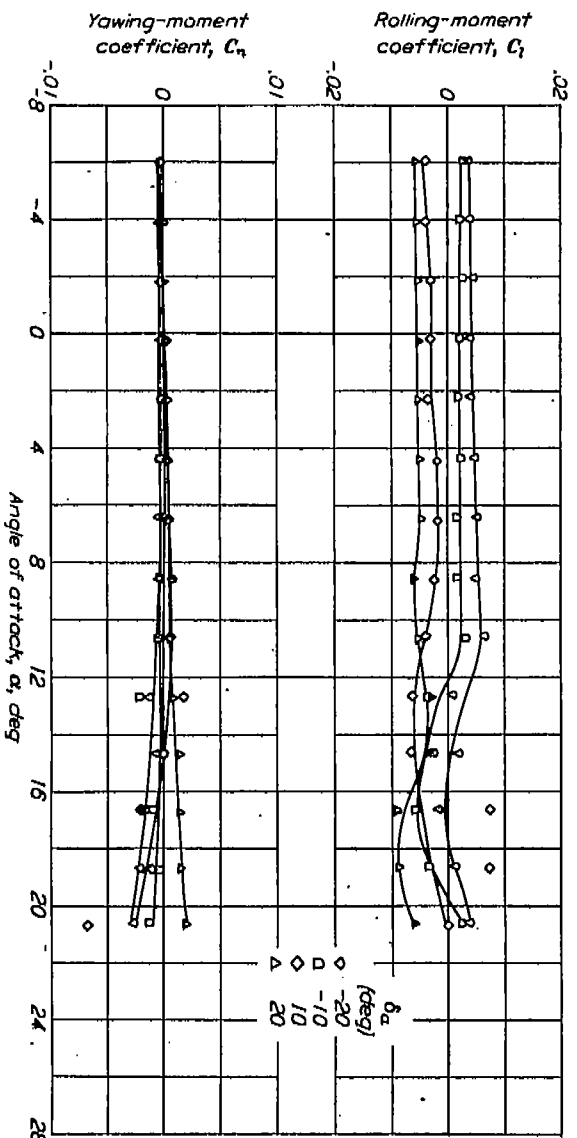


FIGURE 26.—Variation of the lateral control characteristics with angle of attack of the $A=4.13$ wing equipped with flap ailerons. Inboard ailerons; $b/c = 0.4170$.

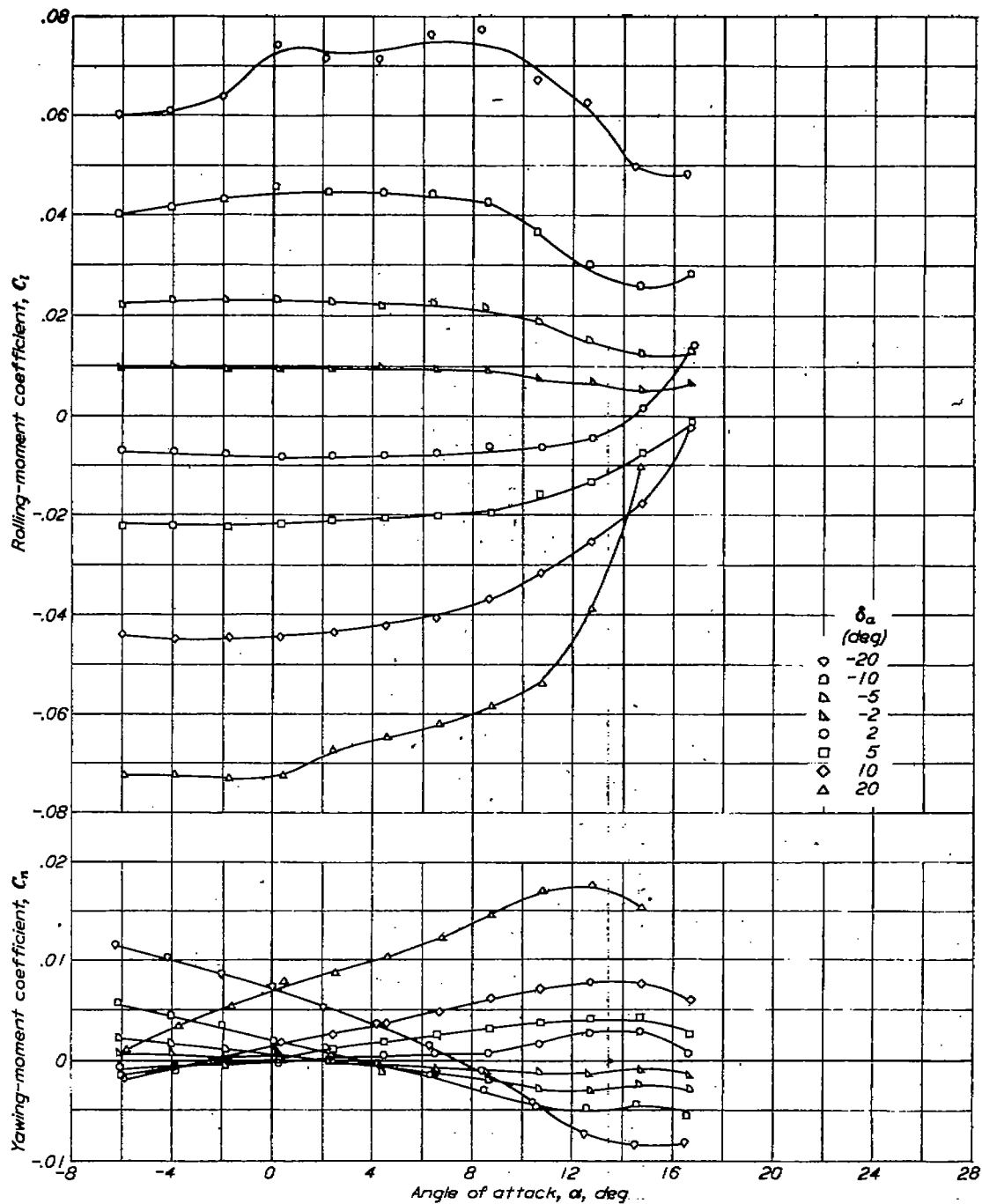


FIGURE 27.—Variation of the lateral control characteristics with angle of attack of the $A=6.13$ wing equipped with flap ailerons. Outboard ailerons; $\frac{b_a}{b/2}=0.925$.

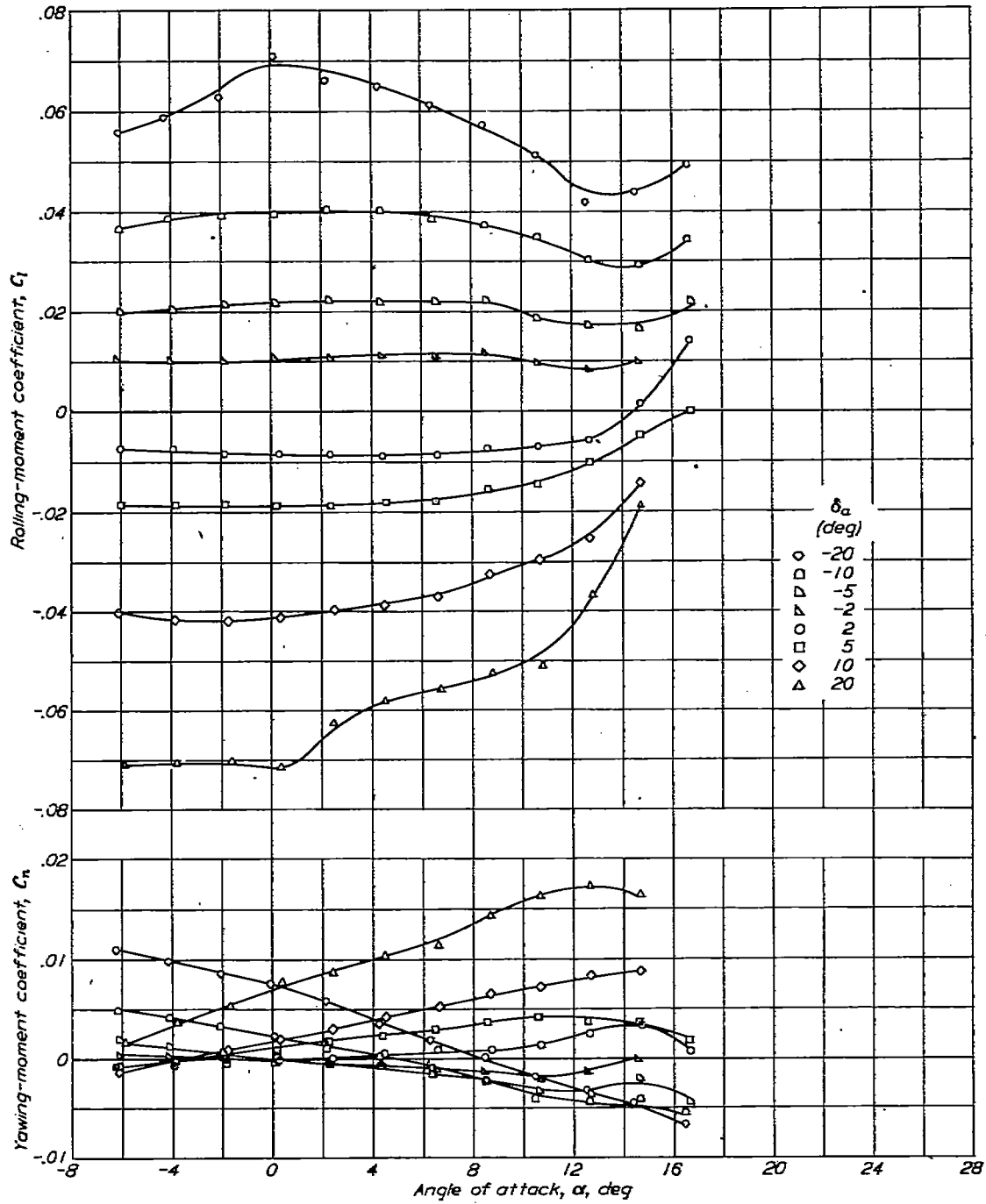


FIGURE 28.—Variation of the lateral control characteristics with angle of attack of the $A=6.18$ wing equipped with flap allerons. Outboard allerons: $\frac{b_a}{b} = 0.746$.

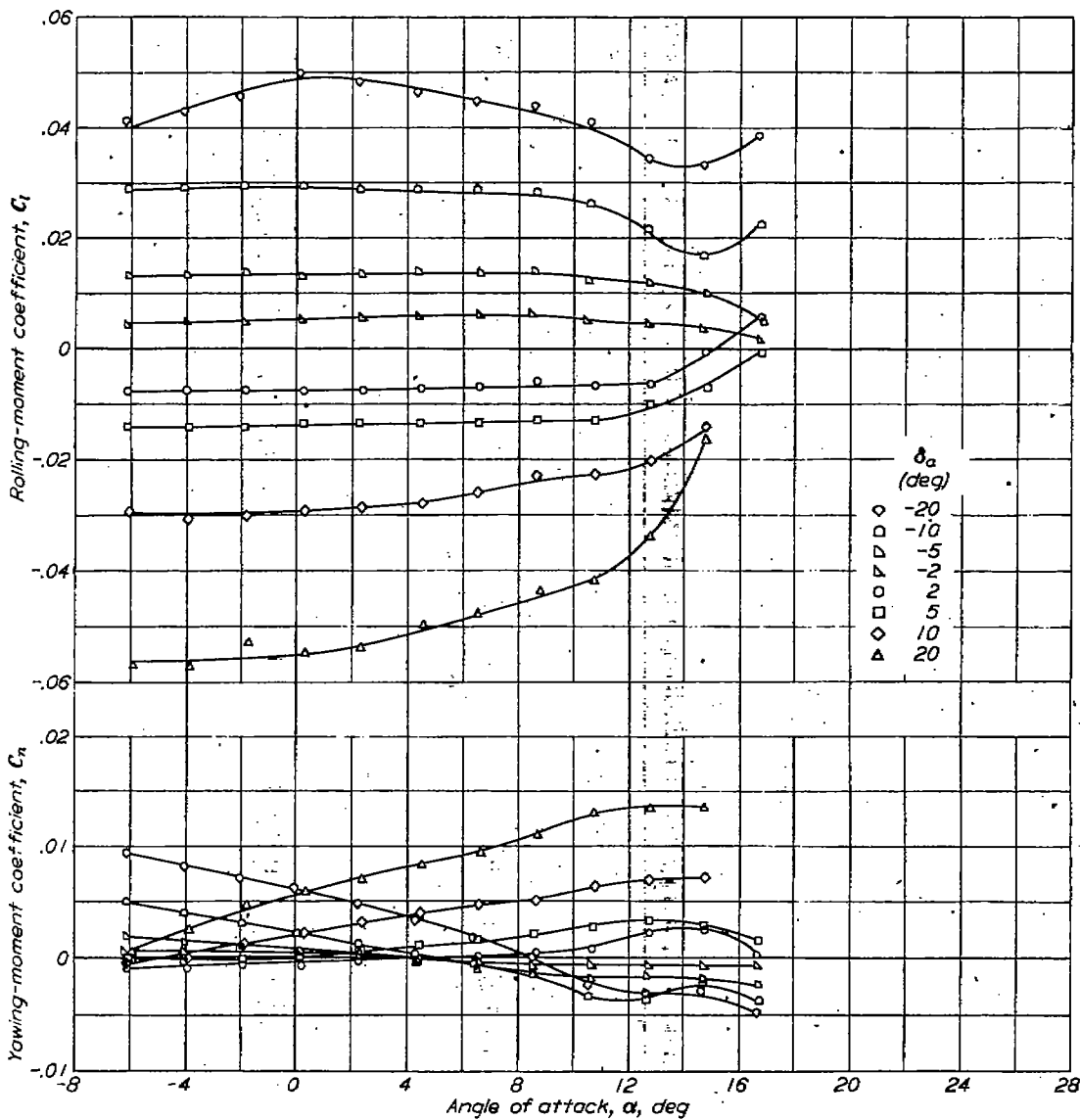


FIGURE 29.—Variation of the lateral control characteristics with angle of attack of the A-6.13 wing equipped with flap ailerons. Outboard ailerons; $\frac{b_2}{b_1} = 0.800$.

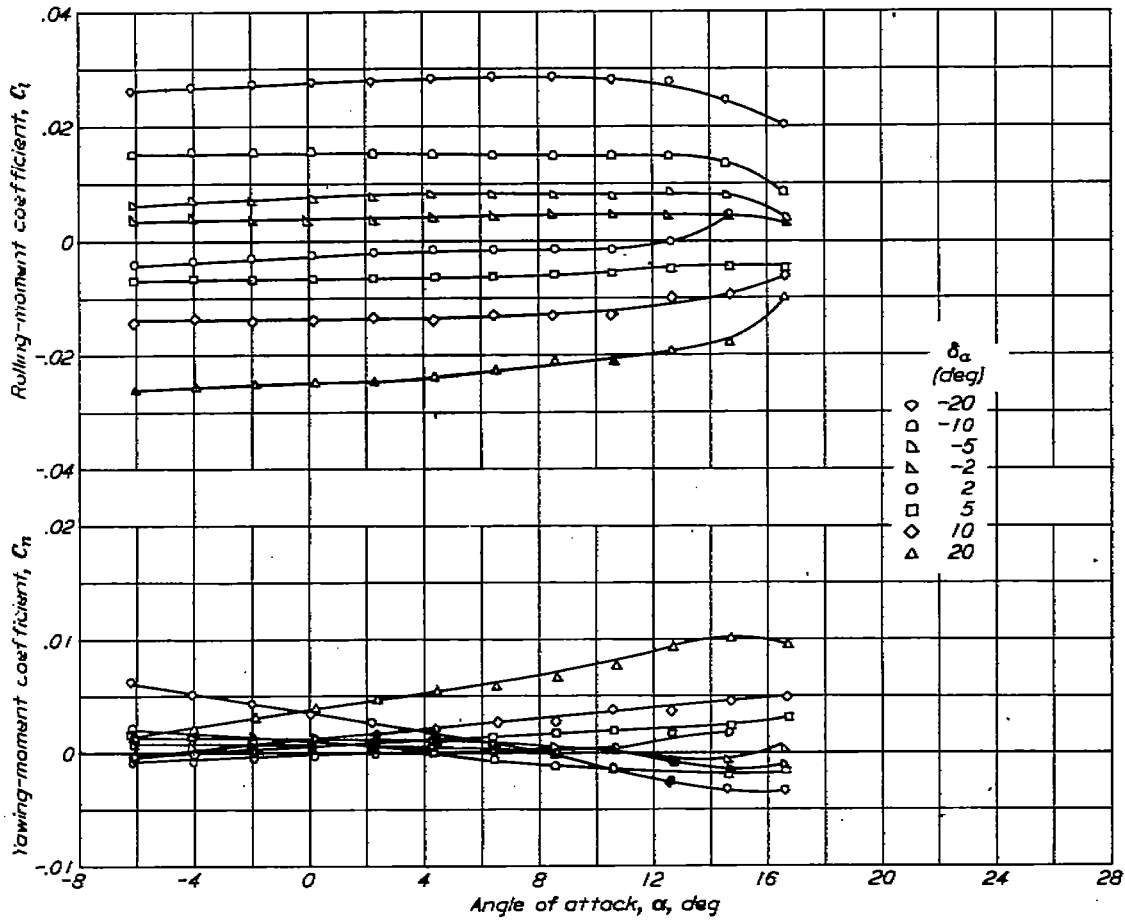


FIGURE 30.—Variation of the lateral control characteristics with angle of attack of the $A=6.13$ wing equipped with flap ailerons. Outboard ailerons; $\frac{b_a}{b} = 0.254$.

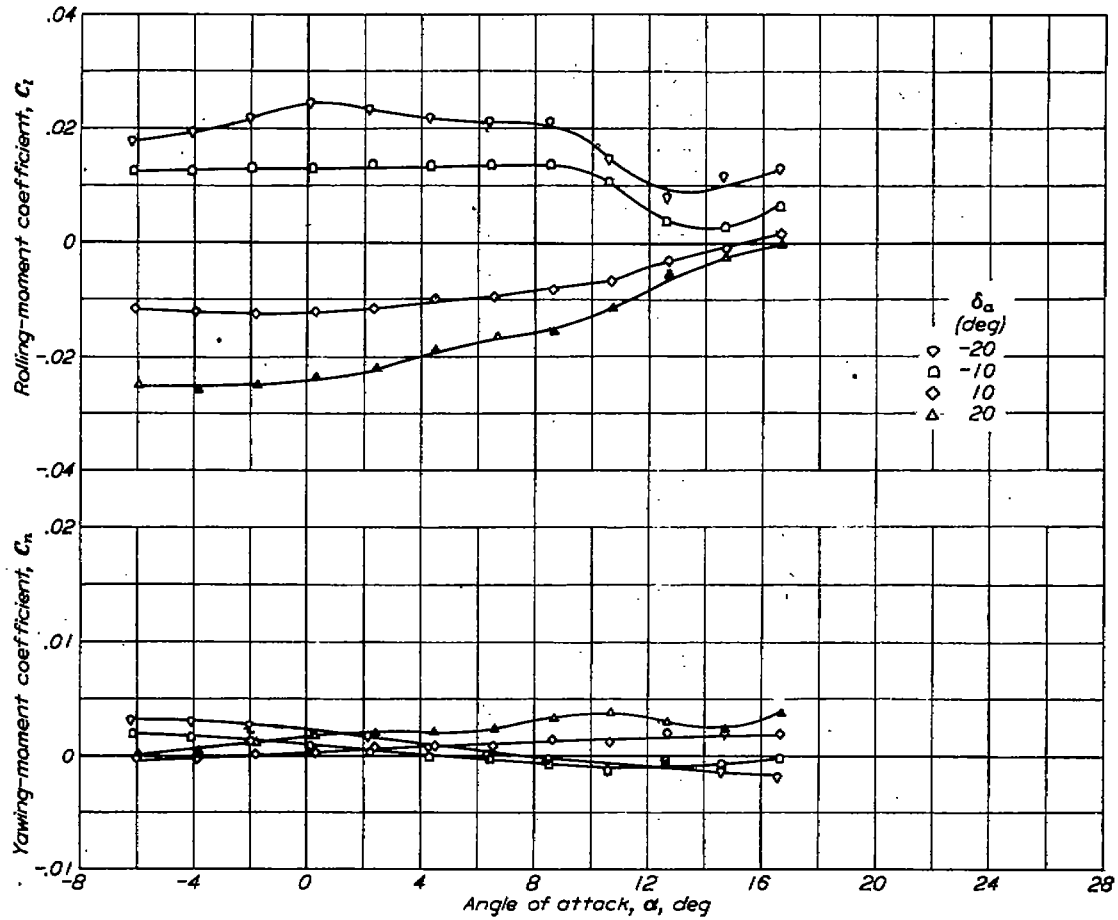


FIGURE 31.—Variation of the lateral control characteristics with angle of attack of the A-6.13 wing equipped with flap ailerons. Inboard ailerons; $\frac{b_a}{b^2} = 0.426$.

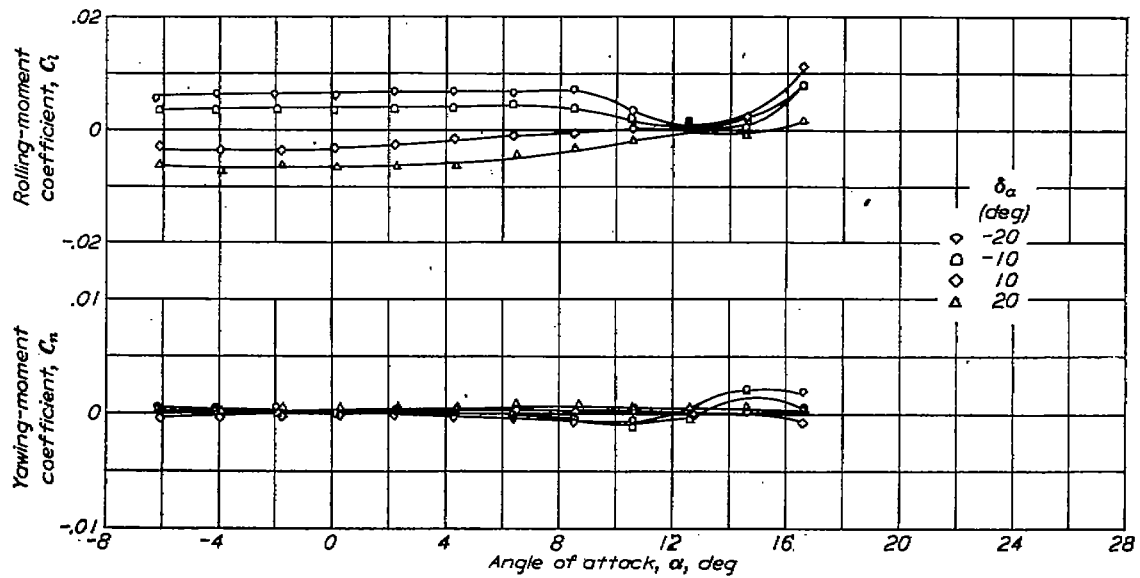
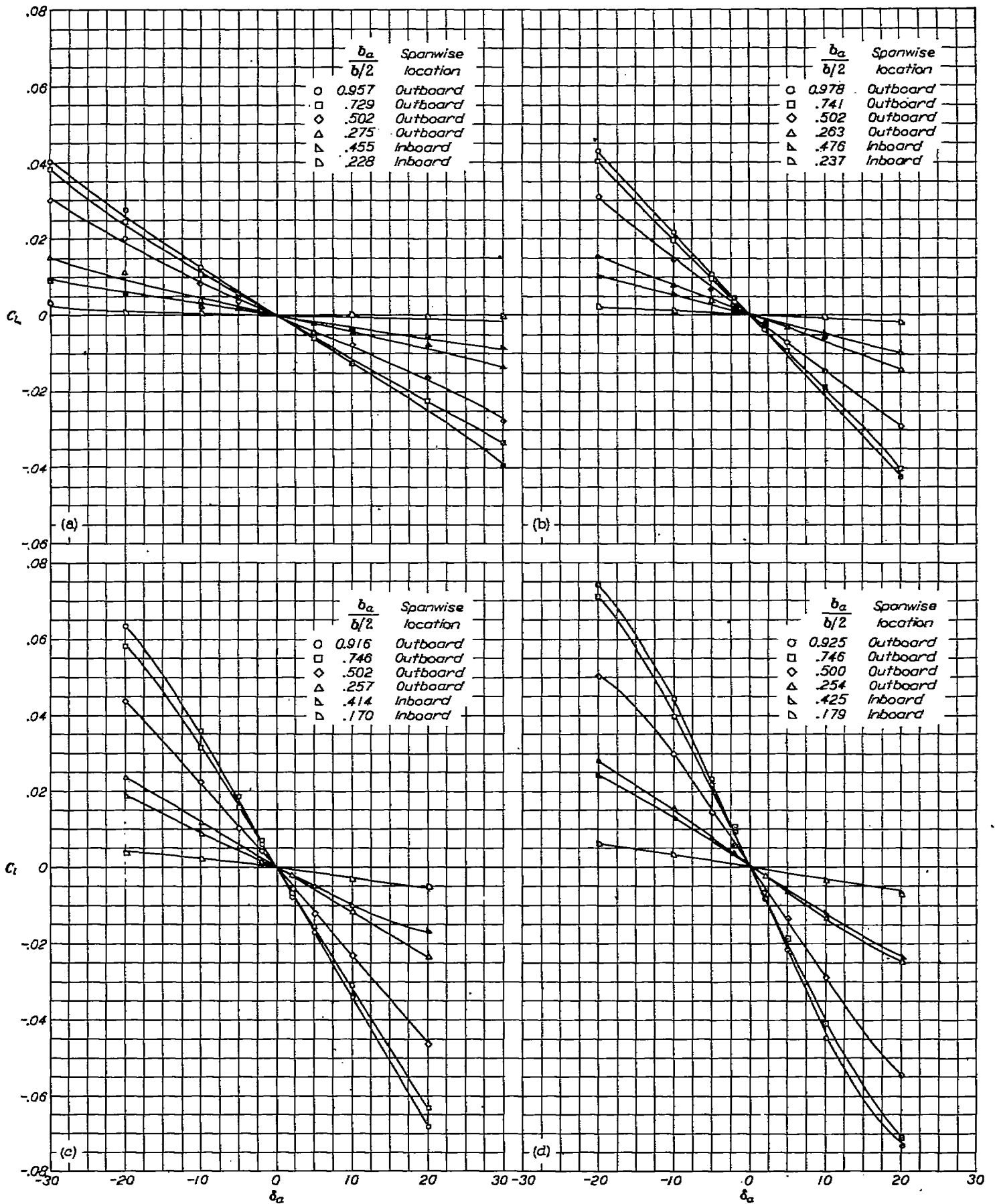


FIGURE 32.—Variation of the lateral control characteristics with angle of attack of the A-6.13 wing equipped with flap ailerons. Inboard ailerons; $\frac{b_a}{b^2} = 0.179$.



(a) $A=1.13$. (b) $A=2.13$.
 (c) $A=4.13$. (d) $A=6.13$.
 FIGURE 33.—Variation of rolling-moment coefficient with flap aileron deflection for various aileron spans. $\alpha \approx 0^\circ$.

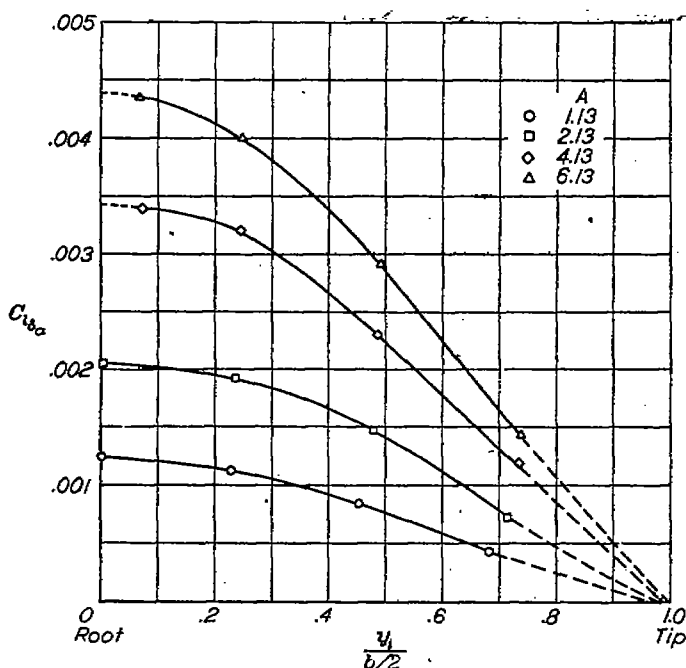


FIGURE 34.—Aileron effectiveness parameter $C_{l_{\delta a}}$, $\alpha \approx 0^\circ$; outboard flap ailerons. The symbols do not represent test points but are used for convenience in plotting the data.

LATERAL CONTROL CHARACTERISTICS OF RETRACTABLE AILERONS FOR UNSWEPT WINGS

The rolling-moment and yawing-moment characteristics over the angle-of-attack range of each of the unswept-wing models equipped with $0.60 \frac{b}{2}$ outboard retractable ailerons at various projections are presented in figures 35 to 37. Cross plots of the rolling-moment data of figures 35 to 37 plotted as a function of retractable-aileron projection and wing aspect ratio are presented in figures 38 and 39, respectively.

Effect of aileron projection.—The values of C_l produced by projection of the retractable ailerons on the unswept wings of aspect ratios 4.13 and 2.13 generally decreased with increase in angle of attack up to the stall angle; however, the values of C_l produced by projection of the retractable ailerons on the unswept wing of aspect ratio 1.13 varied erratically with change in angle of attack and became completely reversed for various projections above angles of attack of 18° to 24° (figs. 35 to 37). This angle-of-attack range of aileron reversal for the wing of aspect ratio 1.13 corresponds to the range of separated flow over the plain wing, where a partial flow recovery probably is caused by the tip vortex on the wing rearward of the aileron. (See fig. 6.)

Each of the unswept wings exhibited a region of zero or reversed aileron effectiveness for small aileron projections, and the aileron-projection range for this phenomenon decreased with increase in wing aspect ratio (figs. 35 to 38). At larger aileron projections, the variation of C_l with retractable-aileron projection was generally fairly linear for each of the wings (fig. 38). Because the data of references 3 and 4

indicate that an increase in aileron effectiveness with increase in Mach number may be expected over the entire projection range for this aileron configuration, particularly for small aileron projections, the aforementioned ineffective region of roll for small aileron projections is believed to be materially alleviated in flight at high-subsonic speeds. For the wing of aspect ratio 1.13, it is rather dubious that this ineffective region of roll would be completely eliminated by increases in Mach number, but on the other wings, rolling-moment coefficient would probably be more linear with retractable-aileron projection. Other means of alleviating the ineffectiveness of the retractable aileron at small projections are also available—such as slotting the wing immediately behind the aileron and thereby making it a plug aileron (reference 5).

The yawing moments produced by projection of the retractable ailerons on the three unswept wings were generally favorable (having the same sign as the rolling moments) and increased linearly except at small projections with increase in aileron projection (figs. 35 to 37). The values of C_n decreased with increase in α on the wings of aspect ratios 4.13 and 2.13 but increased with increase in α up to $\alpha \approx 20^\circ$ on the wing of aspect ratio 1.13.

Effect of wing aspect ratio.—For a given aileron projection, larger values of C_l were produced as the wing aspect ratio increased. This increase in C_l with increase in aspect ratio was larger at low lift coefficients and was almost linear (fig. 39, also figs. 35 to 38). Also, as discussed in the preceding section, increase in wing aspect ratio of the unswept wings reduced the aileron-projection range of zero or reversed aileron effectiveness encountered at small projections (figs. 35 to 38).

At small values of α or C_L , more favorable values of C_n were produced by given aileron projections as the wing aspect ratio was increased, but at large values of α or C_L , an opposite effect occurred (figs. 35 to 37). In addition, the ratio of C_n to C_l tended to decrease with increase in wing aspect ratio, particularly at large values of α or C_L .

LATERAL CONTROL CHARACTERISTICS OF RETRACTABLE AILERONS FOR 45° SWEEPBACK WING

The rolling-moment and yawing-moment characteristics over the angle-of-attack range of the 45° sweptback wing of aspect ratio 2.09 equipped with $0.60 \frac{b}{2}$ plain and stepped retractable ailerons located from $0.20 \frac{b}{2}$ to $0.80 \frac{b}{2}$ and having various projections are presented in figures 40 and 41. The rolling-moment data of figures 40 and 41 are shown cross-plotted against aileron projection in figure 42. The effects of aileron spanwise location and of aileron actuating arms on the lateral control characteristics of the sweptback wing equipped with $0.60 \frac{b}{2}$ plain and stepped retractable ailerons having a projection of $-0.08c$ are shown in figures 43 and 44, respectively.

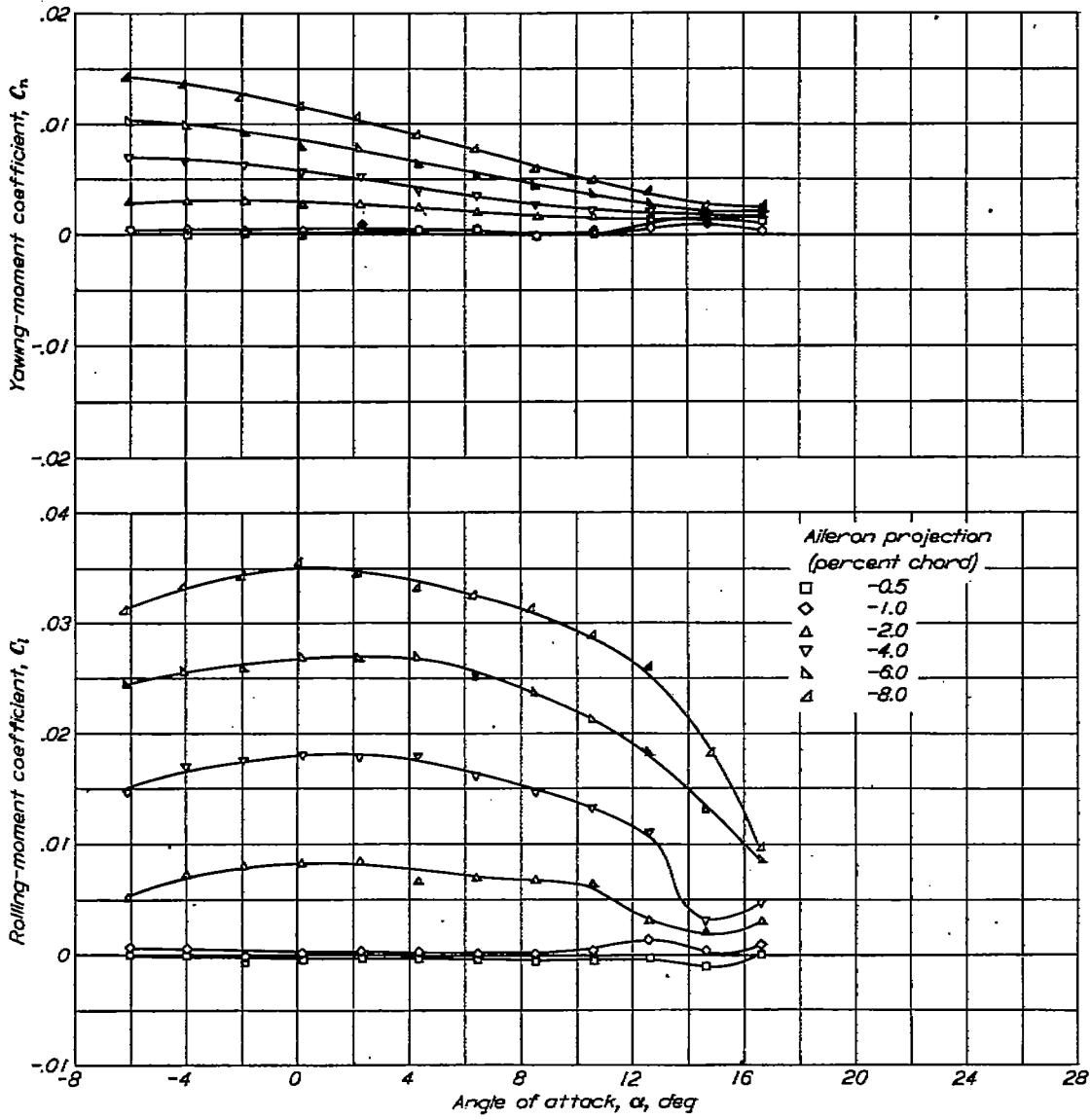


FIGURE 35.—Variation of lateral control characteristics with angle of attack of the unswept untapered wing of aspect ratio 4.13 equipped with retractable ailerons. $\delta_x = 0.60 \frac{b}{2}$

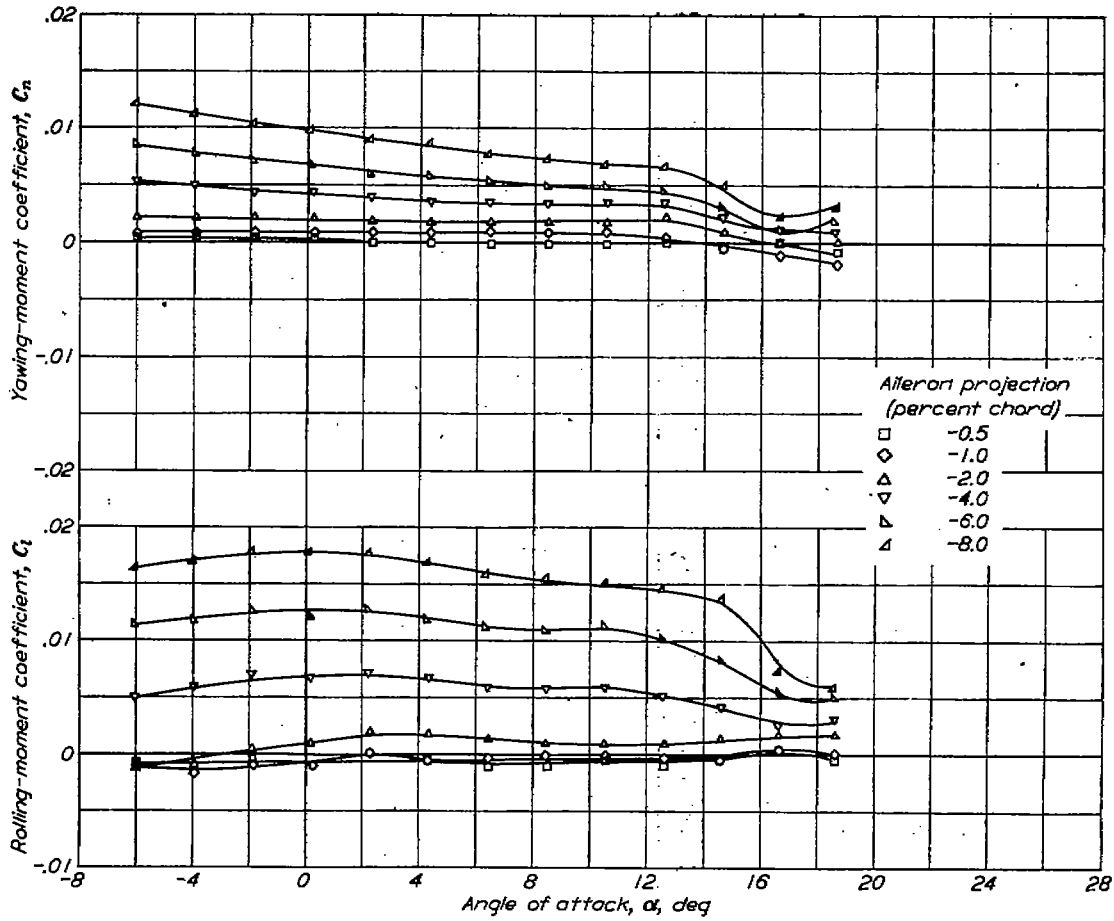


FIGURE 36.—Variation of lateral control characteristics with angle of attack of the unswept untapered wing of aspect ratio 2.18 equipped with retractable ailerons. $b_a=0.60 \frac{b}{2}$.

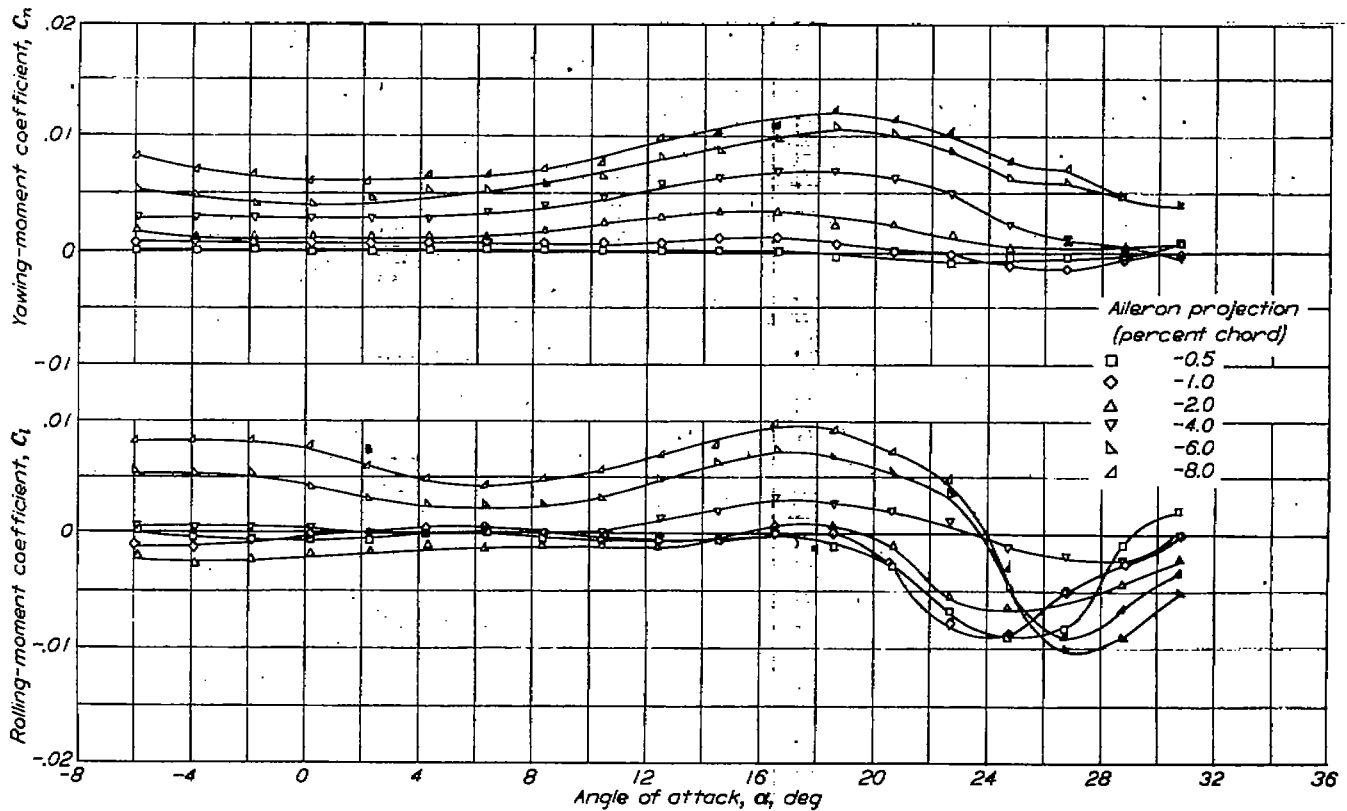


FIGURE 37.—Variation of lateral control characteristics with angle of attack of the unswept untapered wing of aspect ratio 1.13 equipped with retractable ailerons. $b_a=0.60 \frac{b}{2}$.

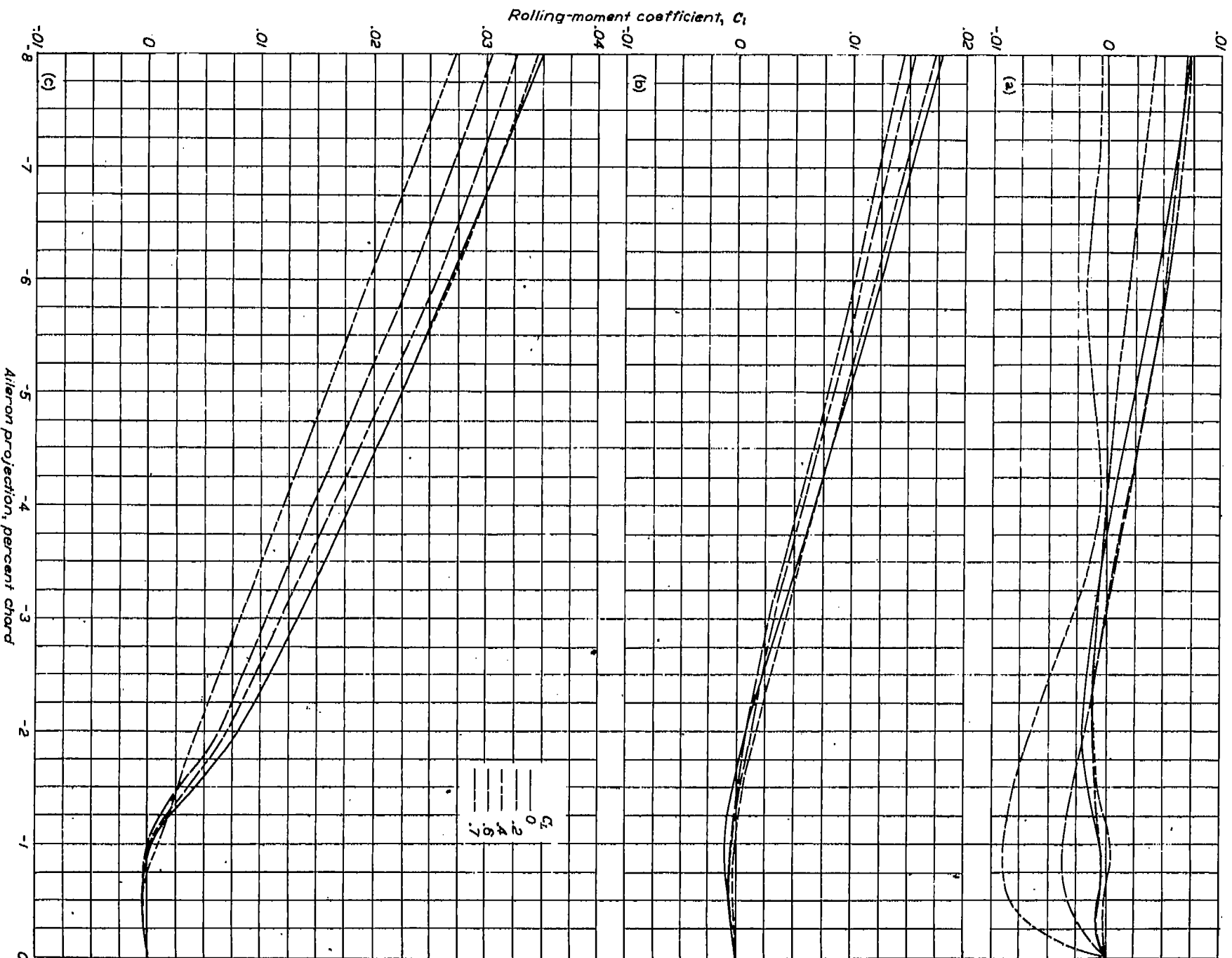


FIGURE 38.—Variation of rolling-moment coefficient with retractable-aileron projection on the unswept untapered wings investigated. $\delta_a=0.60 \frac{b}{c}$

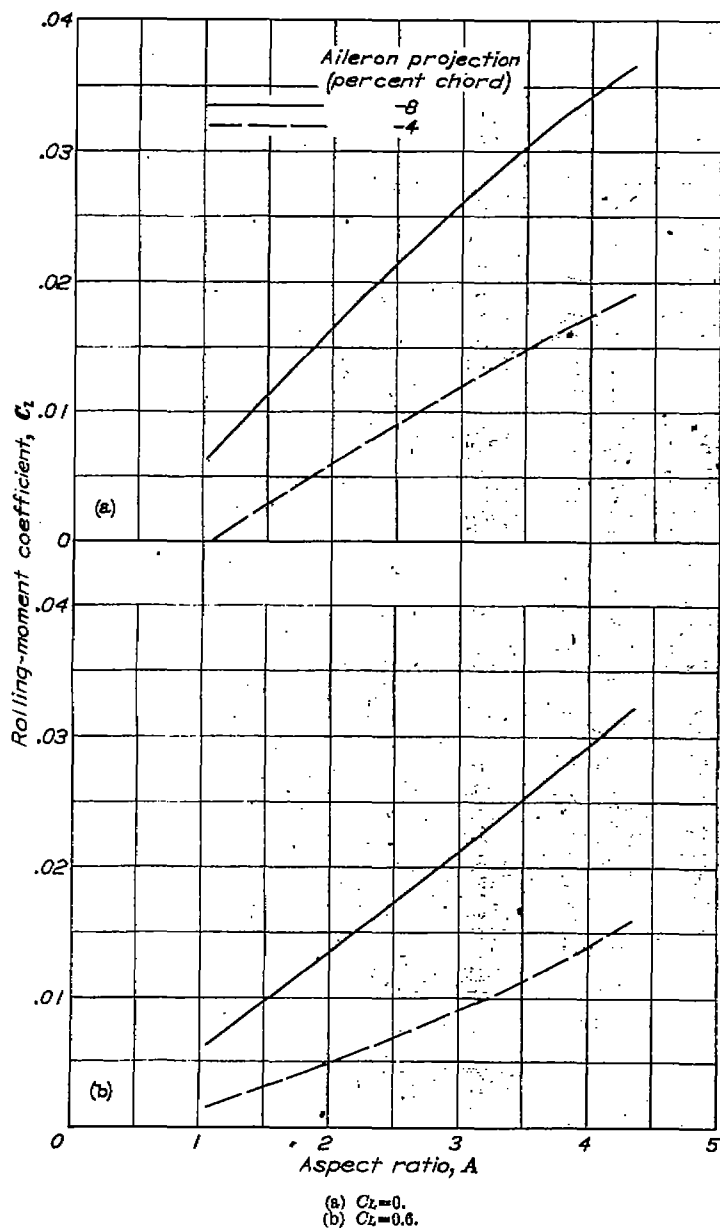


FIGURE 39.—Effect of wing aspect ratio on the rolling-moment characteristics of the unswept untapered wings equipped with retractable ailerons. $b_a = 0.60 \frac{b}{2}$

Effect of aileron projection.—The values of C_l produced by various projections of the plain and stepped retractable ailerons varied nonlinearly over the angle-of-attack range and, with the exception of a range of small projections, varied almost linearly with aileron projection (figs. 40 to 42). The region of aileron ineffectiveness or reversed effectiveness, which occurred to a slight extent as noted in figure 42 for small projections for the plain retractable aileron, was also observed on the unswept wings but, as previously discussed, was found to be a low-speed phenomenon and should be alleviated at high-subsonic speeds (references 3 and 4). This effect of Mach number would thus be expected to provide for an almost linear variation of C_l with aileron projection at high-subsonic speeds, a phenomenon which has been noted in some unpublished data obtained on another sweptback-wing model at high-subsonic speeds.

The yawing moments produced by projection of both plain

and stepped retractable ailerons were generally favorable at values of α below 18° and became less favorable with a further increase in α (figs. 40 and 41). With both retractable-aileron configurations, C_n increased almost linearly with aileron projection except at small projections.

Comparison of plain and stepped retractable ailerons.—Comparison of the data of figures 40 and 41 shows that the $0.60 \frac{b}{2}$ plain retractable aileron located from $0.20 \frac{b}{2}$ to $0.80 \frac{b}{2}$ generally produced larger values of C_l at small values of α and smaller values of C_l at large values of α than the stepped retractable aileron located at the same spanwise stations. Both ailerons had some effectiveness near the wing stall angle. At small aileron projections, the plain retractable aileron generally exhibited zero or reversed effectiveness; whereas the stepped retractable aileron always had positive effectiveness.

The plain retractable aileron generally produced larger (more favorable) values of C_n at various projections than did the stepped retractable aileron over the angle-of-attack range.

Effect of aileron spanwise location.—The values of rolling-moment coefficient produced by a $0.60 \frac{b}{2}$ plain retractable aileron projected $-0.08c$ generally increased appreciably as the aileron was moved inboard on the wing (fig. 43). This trend agrees with unpublished results obtained at low speed for a 51° sweptback wing of aspect ratio 3.1. The values of C_l produced by stepped retractable ailerons generally increased at low and moderate angles of attack when the ailerons were moved outboard on the wing (fig. 44). This trend at low and moderate values of α is opposite to that noted in an investigation of a 42° sweptback wing of aspect ratio 4.01 (reference 6) and in the investigation of the aforementioned 51° sweptback wing of aspect ratio 3.1.

When the ailerons were moved outboard on the wing, however, the values of C_l produced by stepped retractable ailerons decreased at very large angles of attack. This trend is in agreement with the data obtained on the other wings at very large values of α . Reasons for this discrepancy are unknown but it may be attributed to differences in wing geometry—particularly, in the wing aspect ratio.

In general, the inboard, $0.60 \frac{b}{2}$ plain retractable aileron, which was the optimum configuration for the plain retractable aileron on the 45° sweptback wing, produced larger values of C_l over the angle-of-attack range of the wing model than did the optimum configuration for the stepped retractable aileron, which was the outboard stepped retractable aileron.

With either the plain- or stepped-retractable-aileron configuration, C_n generally decreased (became less favorable) as the $0.60 \frac{b}{2}$ aileron was moved inboard on the wing, but C_n was generally larger for all plain retractable ailerons than for comparable stepped retractable ailerons. This decrease in C_n as the aileron moved inboard agrees with results obtained on the aforementioned 42° and 51° sweptback wings (reference 6 and unpublished data, respectively).

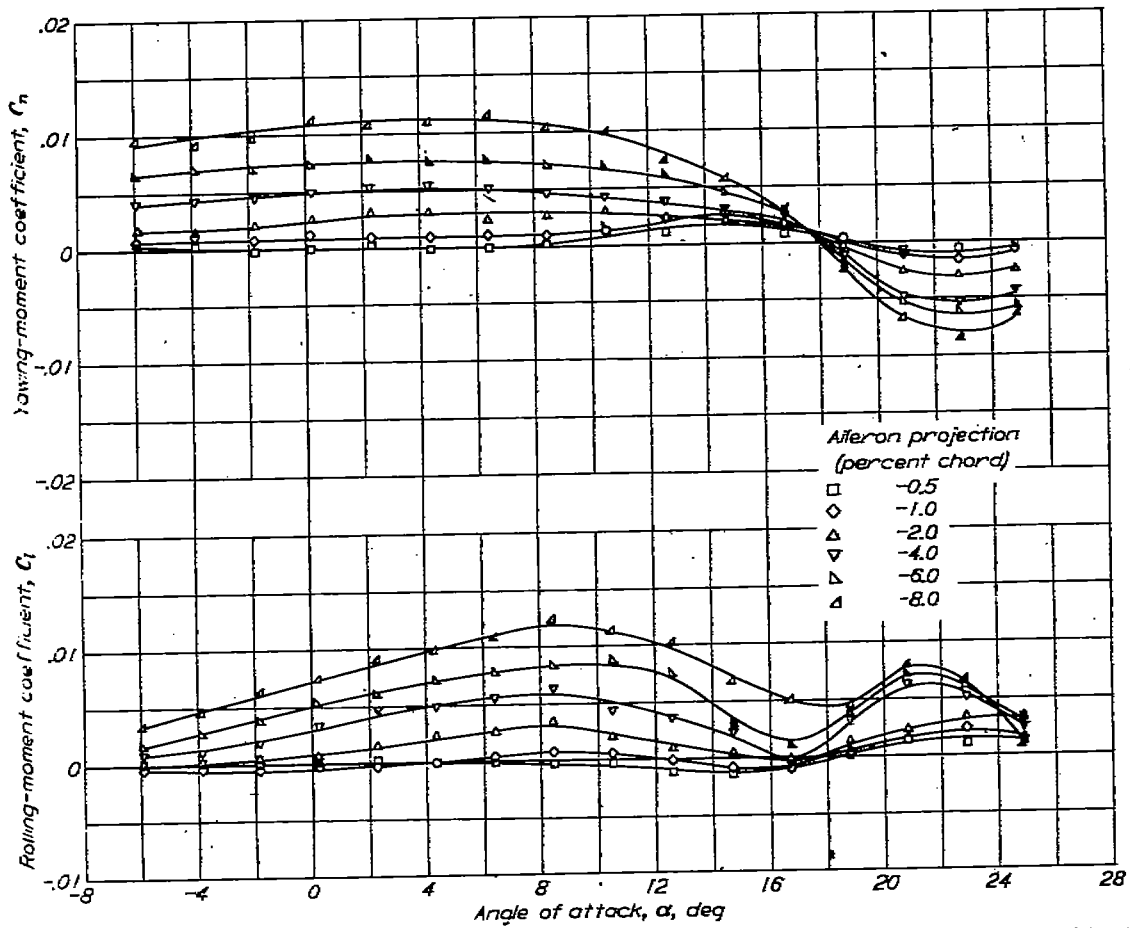


FIGURE 40.—Variation of lateral control characteristics with angle of attack of the 45° sweptback untapered wing of aspect ratio 2.09 equipped with plain retractable ailerons.
 $b_s = 0.60 \frac{b}{c}$; $\eta = 0.20 \frac{b}{c}$

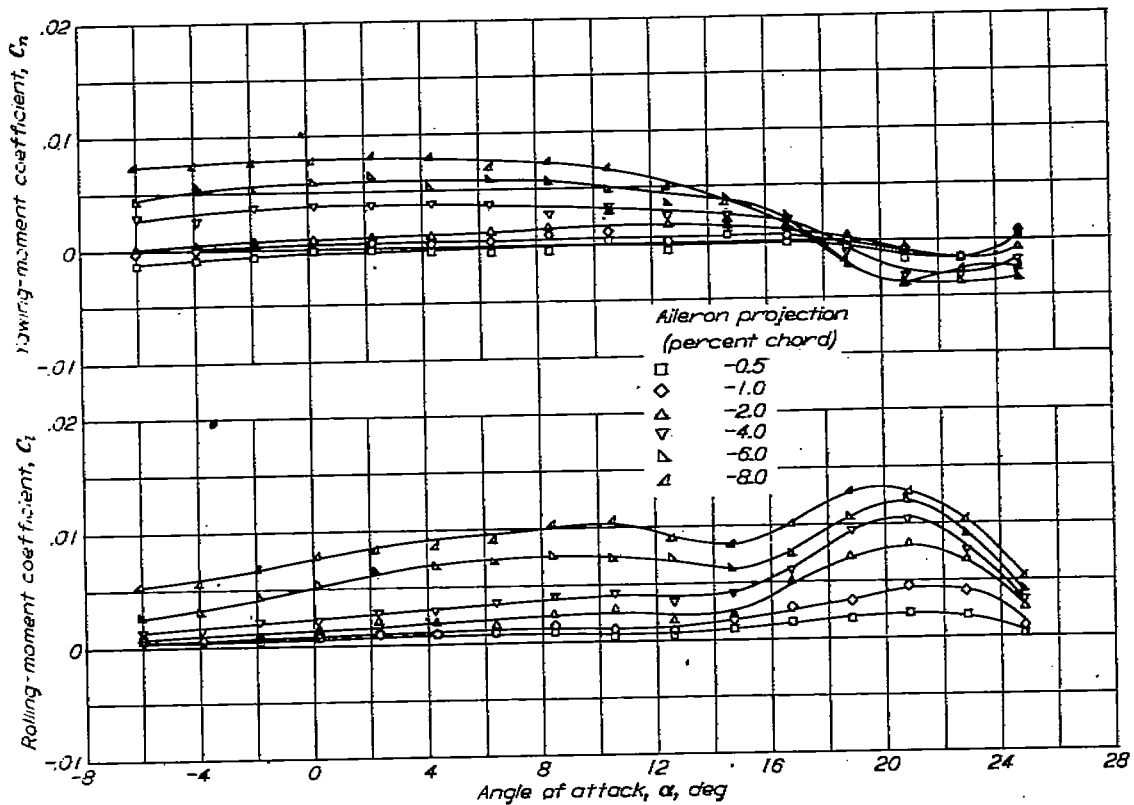
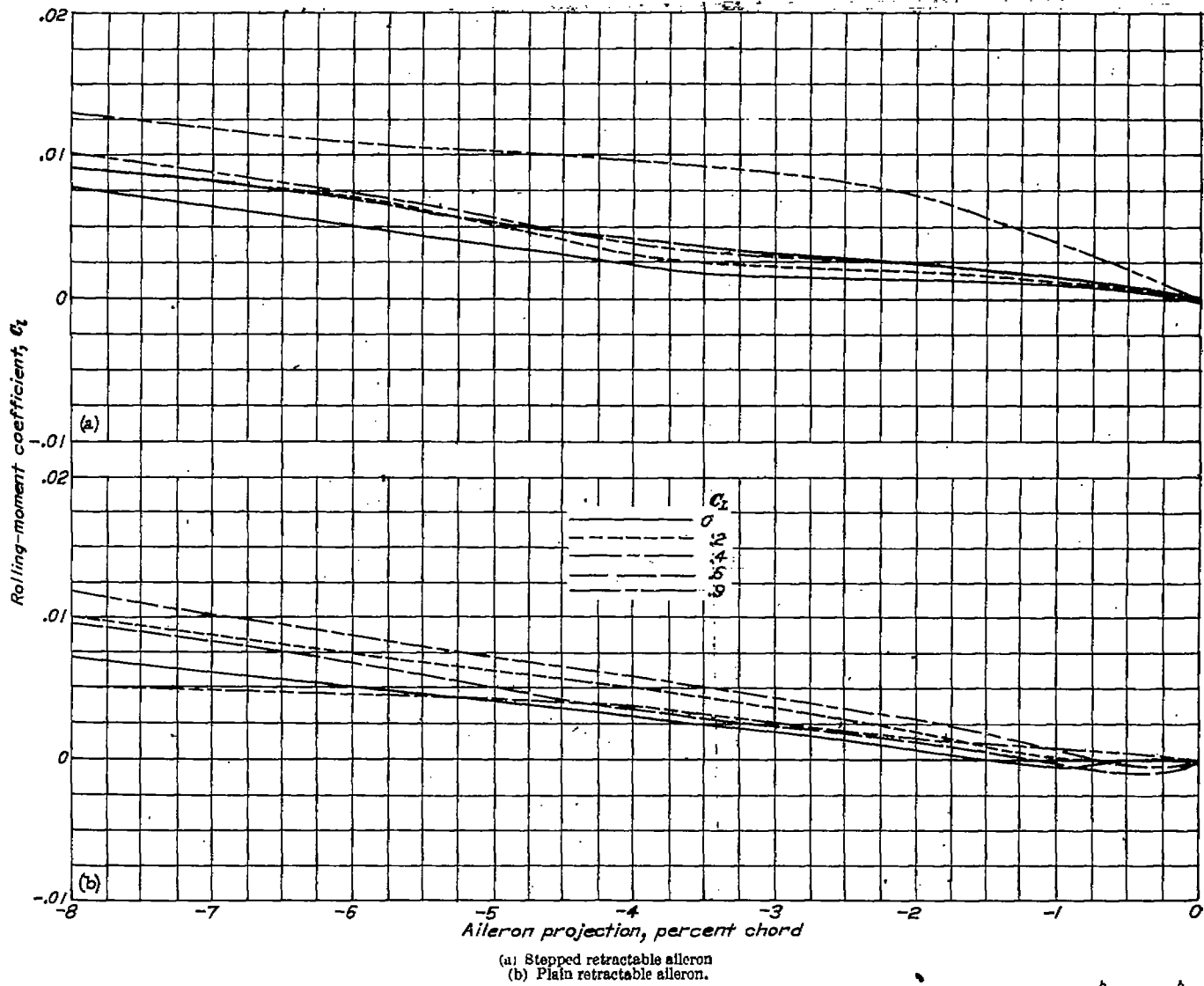


FIGURE 41.—Variation of lateral control characteristics with angle of attack of the 45° sweptback untapered wing of aspect ratio 2.09 equipped with stepped retractable ailerons.
 $b_s = 0.60 \frac{b}{c}$; $\eta = 0.20 \frac{b}{c}$



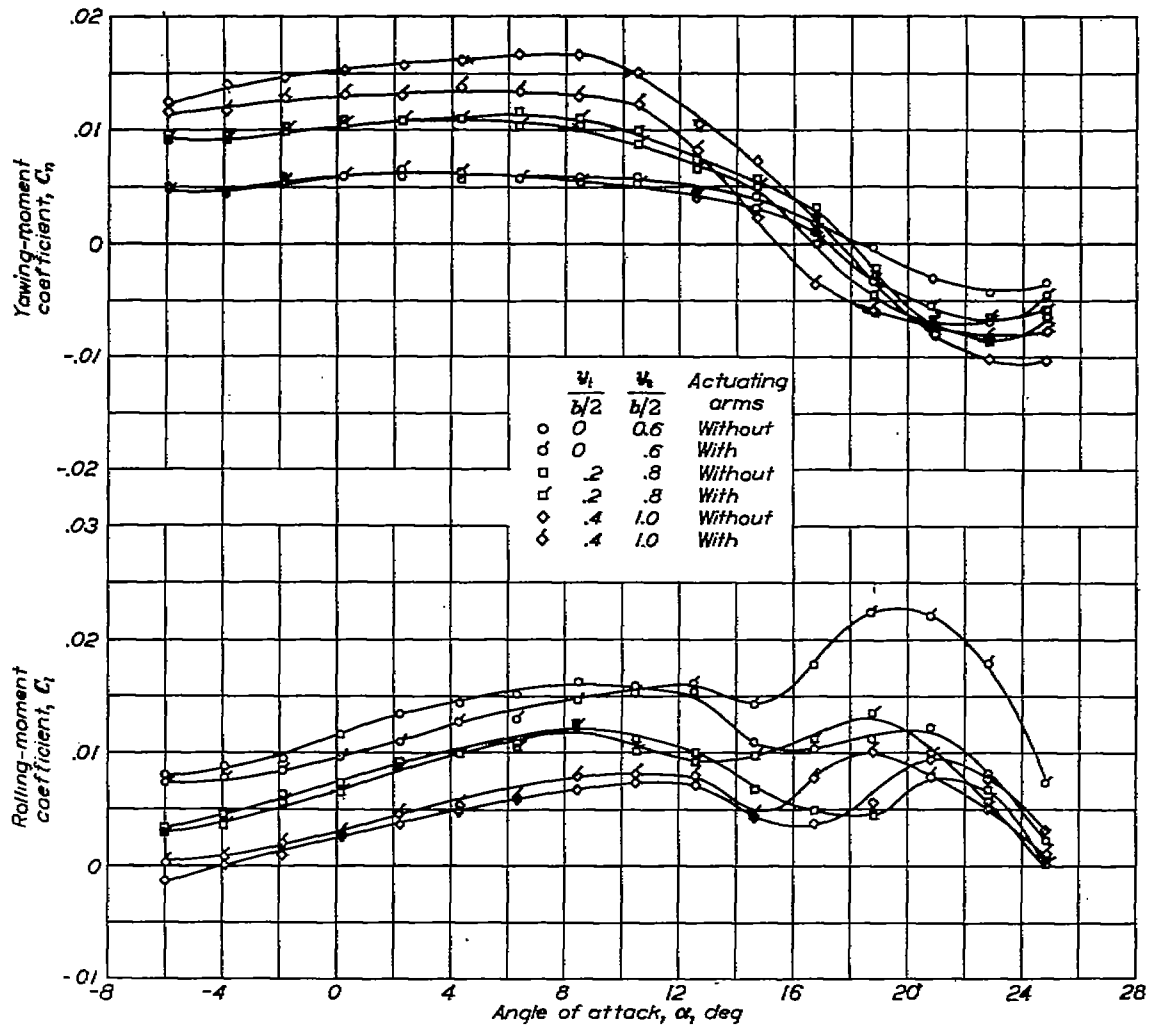


FIGURE 43.—Effect of alleron spanwise location and alleron actuating arms on the lateral control characteristics of the 45° sweptback untapered wing of aspect ratio 2.09 equipped with plain retractable allerons. Alleron projection, $-0.08c$; $\delta_a = 0.00 \frac{b}{2}$

Effect of aileron actuating arms.—The addition of aileron actuating arms (fig. 5) to $0.60\frac{b}{2}$ plain and stepped retractable ailerons having a projection of $-0.08c$ at each of three spanwise locations generally tended to increase the values of C_l produced by the ailerons alone over most of the angle-of-attack range, except at small angles of attack for the plain retractable aileron at the two inboard locations investigated (figs. 43 and 44). In general, the effects on C_l produced by the actuating arms were very small at low angles of attack, except with the stepped ailerons at the inboard location, but were appreciable at large angles of attack.

With the exception of the outboard stepped retractable aileron in the low angle-of-attack range, all aileron configurations exhibited slightly less favorable yawing-moment characteristics with aileron actuating arms on the wing than when the ailerons were tested alone on the wings (figs. 43 and 44).

Effect of wing sweep.—A comparison of the data obtained with outboard, $0.60\frac{b}{2}$ retractable ailerons on the unswept wing of aspect ratio 2.13 (figs. 36 and 38) with comparable data obtained with midsemispan, $0.60\frac{b}{2}$ plain and stepped retractable ailerons on the 45° sweptback wing of aspect ratio 2.09 (figs. 40 to 42) shows that the ailerons on both wings generally produced a linear variation of C_l with aileron

projection over most of the aileron-projection range. At given values of lift coefficient, the retractable ailerons on the unswept wing generally were appreciably more effective than on the sweptback wing; however, because the wing stall occurred at larger values of α and C_L on the sweptback wing (fig. 6), this wing retained more of its aileron effectiveness to larger values of α , particularly with the stepped retractable ailerons, than did the unswept wing. The yawing moments produced by these ailerons on both wings generally exhibited the same trends with increase in angle of attack and aileron projection and, at given values of C_l , were slightly larger for the plain retractable aileron on the 45° sweptback wing than for the retractable aileron on the unswept wing.

The data of references 2 and 16 show that the outboard portions of unswept wings are the most effective spanwise locations for both spoiler and flap controls, respectively; however, the data of reference 6 and unpublished data obtained on a 51° sweptback wing of aspect ratio 3.1, as well as the present data (figs. 43 and 44), show that aileron configuration and wing geometry influence the most effective spanwise location of spoiler controls on swept wings. Therefore, a comparison of the effectiveness of spoiler ailerons on unswept and swept wings should be made for the optimum aileron configuration on each wing. Accordingly, a comparison of the data of figure 36 with the data of figure 44 shows that larger values of C_l were produced by the optimum

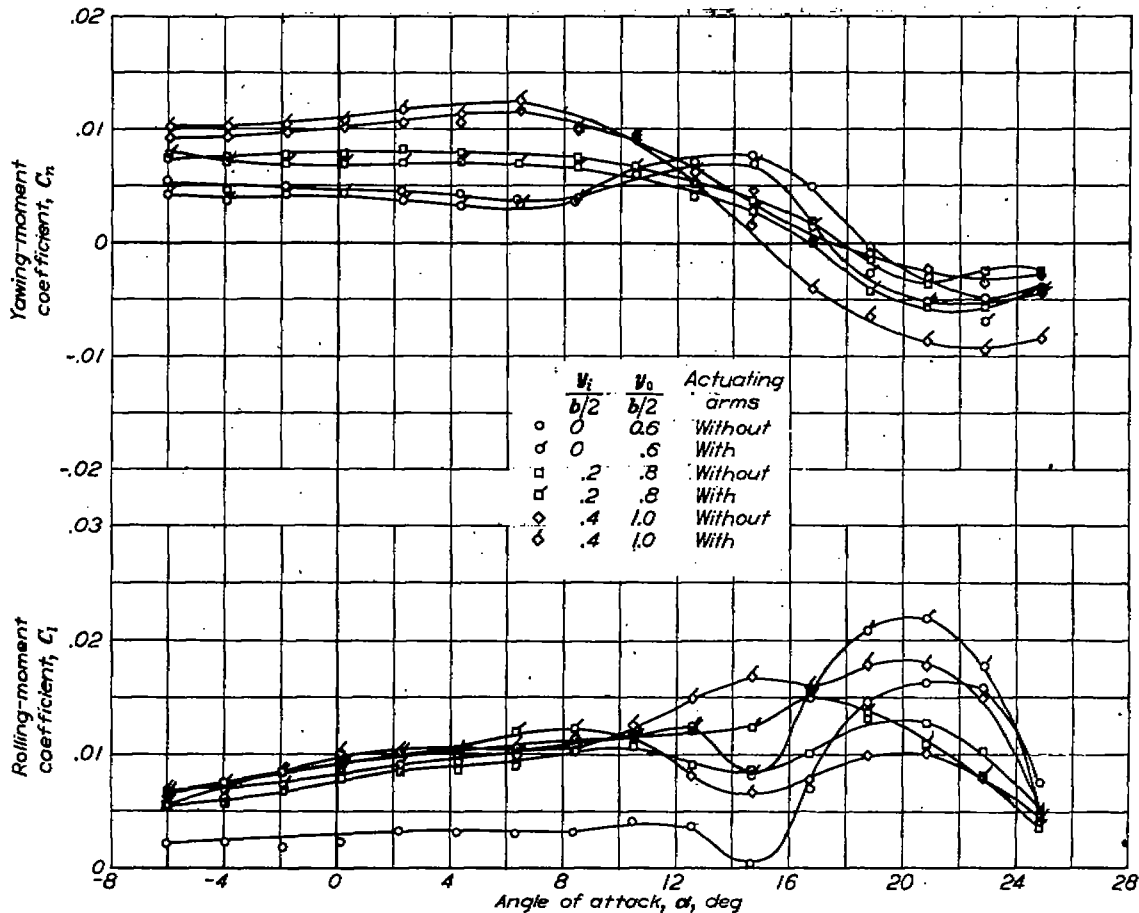


FIGURE 44.—Effect of aileron spanwise location and aileron actuating arms on the lateral control characteristics of the 45° sweptback untapered wing of aspect ratio 2.09 equipped with stepped retractable ailerons. Aileron projection, $-0.08c$; $b_a = 0.60\frac{b}{2}$.

retractable-aileron configuration on the unswept wing than by the optimum stepped-retractable-aileron configuration on the sweptback wing. At low lift coefficients the retractable aileron on the unswept wing produced larger values of C_l than the optimum plain-retractable-aileron configuration on the sweptback wing, but at large lift coefficients (or angles of attack greater than about 7°) an opposite effect was generally obtained. (See figs. 36 and 43.) The yawing moments produced by these retractable-aileron configurations exhibited the same trends with increase in α , but the aileron on the unswept wing generally produced larger (more favorable) values of C_n than the optimum configuration of plain retractable aileron and smaller values of C_n than the optimum configuration of stepped retractable aileron on the sweptback wing at comparable values of lift coefficient.

COMPARISON OF EXPERIMENTAL AND ESTIMATED AILERON EFFECTIVENESS

Flap-aileron effectiveness.—A comparison of the aileron effectiveness computed by three existing methods (references 17 to 19) and the experimental values of $C_{l_{\delta a}}$ are presented in figure 45 for outboard-control spans of $\frac{b_a}{b/2} = 1.00, 0.60,$ and 0.30 . The results presented in reference 17 include the data of reference 16, extrapolated for aspect ratios between 4 and 2. The method of reference 18 is an application of the Weissinger method. A value of α_s of 0.54 was used in the theoretical computations. This value was based on NACA 64A010 section data for $\frac{c_a}{c} = 0.30$ (reference 20) corrected to $\frac{c_a}{c} = 0.25$ by the trends given in reference 17. Throughout the aspect-ratio range of 2 to 6, values of $C_{l_{\delta a}}$ computed by the method of reference 17 were in better quantitative agreement with the experimental results than the values of $C_{l_{\delta a}}$ computed by the method of reference 18; however, the trend

of the experimental data was more accurately predicted by reference 18 than by reference 17. For a wing of $A=6$ with controls of about 30 percent span, it was noted that the experimental values of $C_{l_{\delta a}}$ agreed well with the values estimated by the method of reference 17. The agreement would be similar for an $A=6$ wing with controls of smaller span. However, values of $C_{l_{\delta a}}$ computed by the method of reference 17 are considerably lower than the large experimental values of $C_{l_{\delta a}}$ produced by full-span ailerons on the $A=6$ wing. In an effort to resolve this discrepancy, a survey was made of experimental aileron-effectiveness data for $A=6$ wings equipped with various flap ailerons. The experimental values of aileron effectiveness for these $A=6$ wings were compared with values computed by the method of reference 17. Most of the aileron configurations yielded values of $C_{l_{\delta a}}$ of 0.0020 or less, which agreed fairly well with computed values. The meager data available for aileron configurations which gave values of $C_{l_{\delta a}}$ much greater than 0.0020 indicated that these large values of $C_{l_{\delta a}}$ were consistently higher than computed values for these configurations.

The method of reference 19, which predicts a linear variation of $C_{l_{\delta a}}$ with aspect ratio (fig. 45), is based on lifting-line theory of zero-aspect-ratio wings at low speeds or of moderate aspect-ratio wings at the speed of sound. The theory states that $C_{l_{\delta a}}$ is independent of the chordwise position of the control hinge line, or effectively, $\alpha_s = 1$. The low-speed application of this method appears to be limited to wings of aspect ratios less than 1.

Because the theoretical methods were not entirely satisfactory, the experimental data were reduced to a convenient form (figs. 46 and 47) for predicting aileron effectiveness of low-aspect-ratio, unswept, untapered wings. The method used is similar to that of reference 17. The aileron-effectiveness data of figure 34 were reduced to values of $C_l/\Delta\alpha$ for $A=6$ and to the aspect-ratio factor K_l which is the ratio of

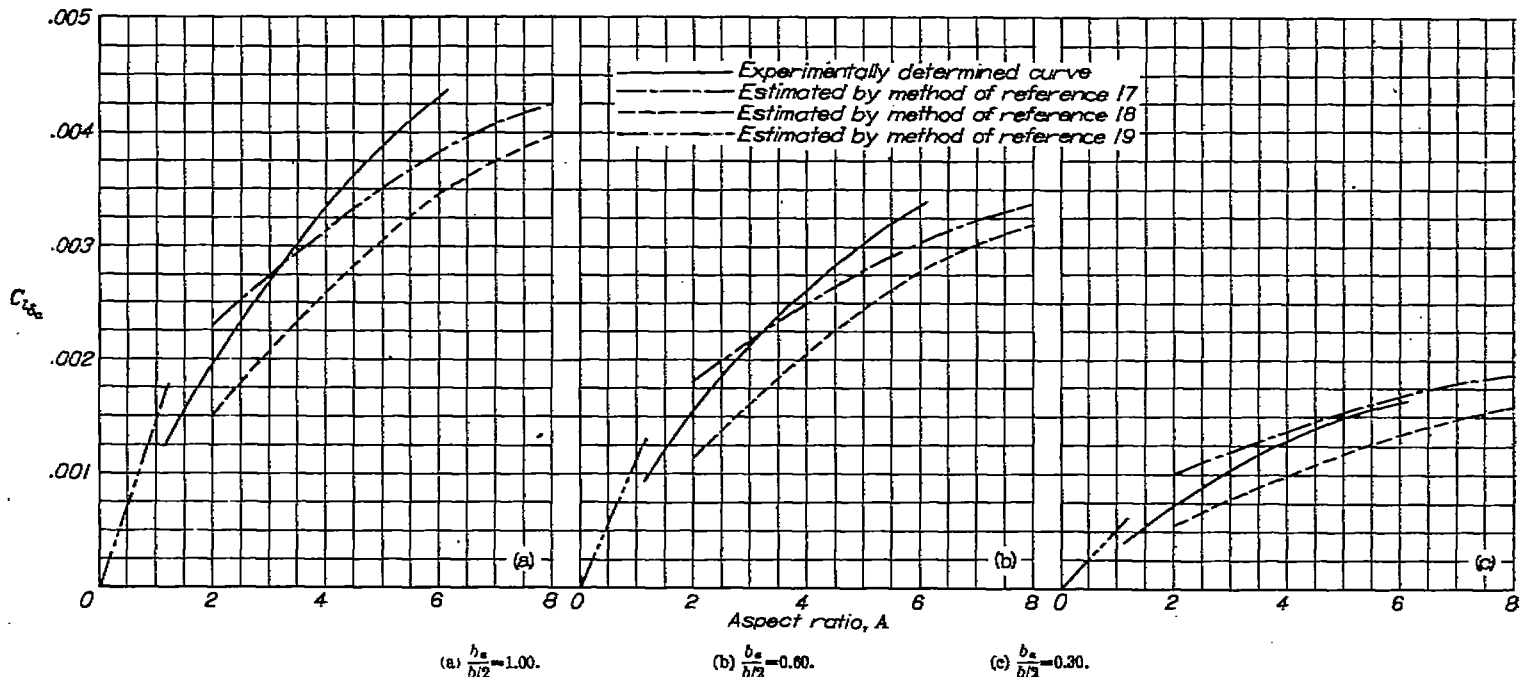


FIGURE 45.—Variation of aileron effectiveness $C_{l_{\delta a}}$ with aspect ratio for various spans of outboard flap ailerons.

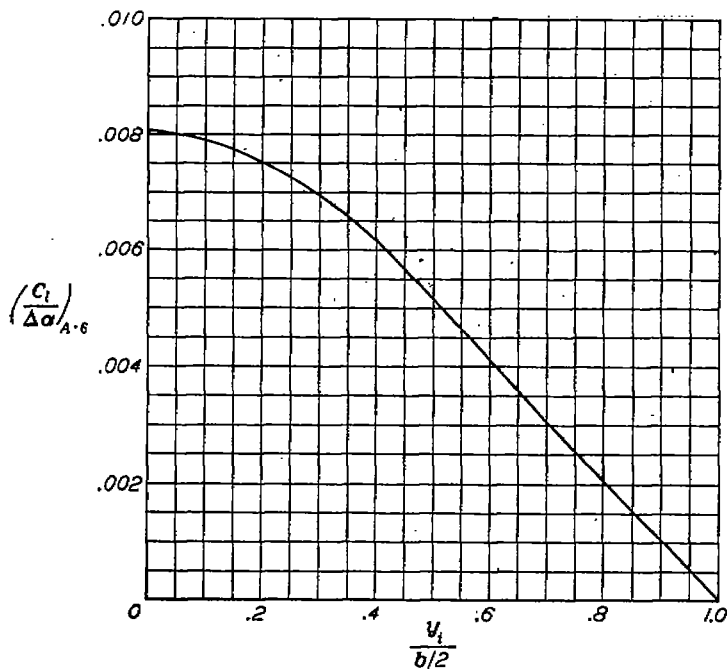


FIGURE 46.—Variation of values of $\left(\frac{C_l}{\Delta\alpha}\right)_{A=6}$ with flap aileron span.

$$C_{l_{a,e}} = \left(\frac{C_l}{\Delta\alpha}\right)_{A=6} \alpha_3 K_1$$

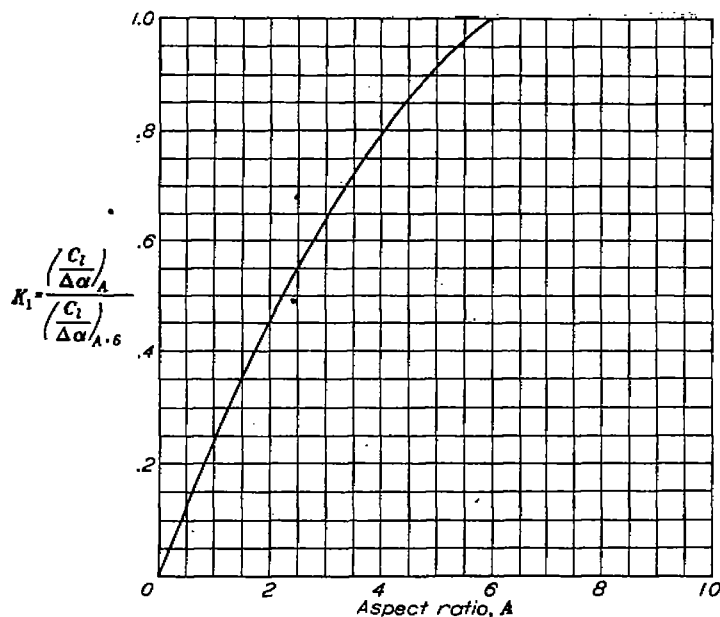


FIGURE 47.—Factor K_1 for computing $C_{l_{a,e}}$.

$C_l/\Delta\alpha$ for any A to $C_l/\Delta\alpha$ for $A=6$. These values and the equation relating them are given in figures 46 and 47. The factor K_1 showed only a slight and inconsistent variation with $\frac{y_l}{b/2}$ and therefore was assumed to be independent of aileron span in these computations. By use of the curves of figures 46 and 47 and appropriate values of α_3 (such as are presented in reference 17), the effectiveness of ailerons on low-aspect-ratio, unswept, untapered wings may be estimated.

Retractable-aileron effectiveness.—In order to determine whether the methods employed for estimating the characteristics of flap controls on unswept and sweptback wings

(references 16 and 17) apply equally as well to spoiler ailerons on low-aspect-ratio wings, values of C_l produced by $0.60\frac{b}{2}$ retractable ailerons at a projection of $-0.08c$ on unswept untapered wings having various aspect ratios and on the 45° sweptback wing of aspect ratio 2.09 for various aileron spanwise locations were estimated and are compared in figure 48 with experimental data obtained in the present investigation for $C_L=0$. The estimated curves of figure 48 were computed by the following equation, which represents a modified version of the method presented in reference 17:

$$C_l = \frac{C_l}{\Delta\alpha} \Delta\alpha K_1 K_2 \cos^2 \Lambda$$

The terms of the foregoing equation are defined as follows:

$C_l/\Delta\alpha$ rolling-moment coefficient produced by 1° difference in angle of attack of various right and left parts of a complete wing

$\Delta\alpha$ change in effective angle of attack caused by retractable-aileron projection, degrees

K_1 aspect-ratio correction factor

K_2 taper-ratio correction factor

Values of $C_l/\Delta\alpha$ and K_2 used in the computations were obtained from reference 17. Experimentally determined values of K_1 (fig. 47) were employed in these computations for all unswept wings having aspect ratios of 4 or less, and values of the aileron-effectiveness parameter $\Delta\alpha$ of 7.6 and 9.5 (obtained from two-dimensional spoiler-control data, references 9, 21, 22) were used in the computations of C_l for the unswept and 45° sweptback wings, respectively.

The data of figure 48 (a) show that the empirical method of reference 17 was reasonably accurate for estimating the effectiveness of the retractable ailerons on the unswept wings, particularly for the larger aspect ratios. The value of aileron effectiveness estimated by the empirical method for the sweptback wing of aspect ratio 2.09 agreed well for the inboard location of the plain-retractable aileron (fig. 48 (b)), but the curves diverged as the aileron location was moved outboard. The estimated curve had the same spanwise trend as the stepped-retractable-aileron experimental results but was considerably higher for all locations of the aileron.

ROLLING PERFORMANCE

In order to illustrate the rolling effectiveness of the aileron configurations investigated, values of the wing-tip helix angle $pb/2V$ were estimated for the unswept wings and also for the 45° sweptback wing. The estimated values of $pb/2V$ were obtained from the relationship $\frac{pb}{2V} = \frac{C_l}{C_{l_p}}$, and the values of C_l used in this equation were for $0.50\frac{b}{2}$ outboard flap ailerons deflected 10° and -10° or a total of 20° and for retractable ailerons having a projection of $-0.08c$. The values of C_{l_p} used for determining the values of $pb/2V$ were obtained from the expression

$$C_{l_p} = (C_{l_p})_{C_L=0} \frac{(C_{L\alpha})_{C_L}}{(C_{L\alpha})_{C_L=0}}$$

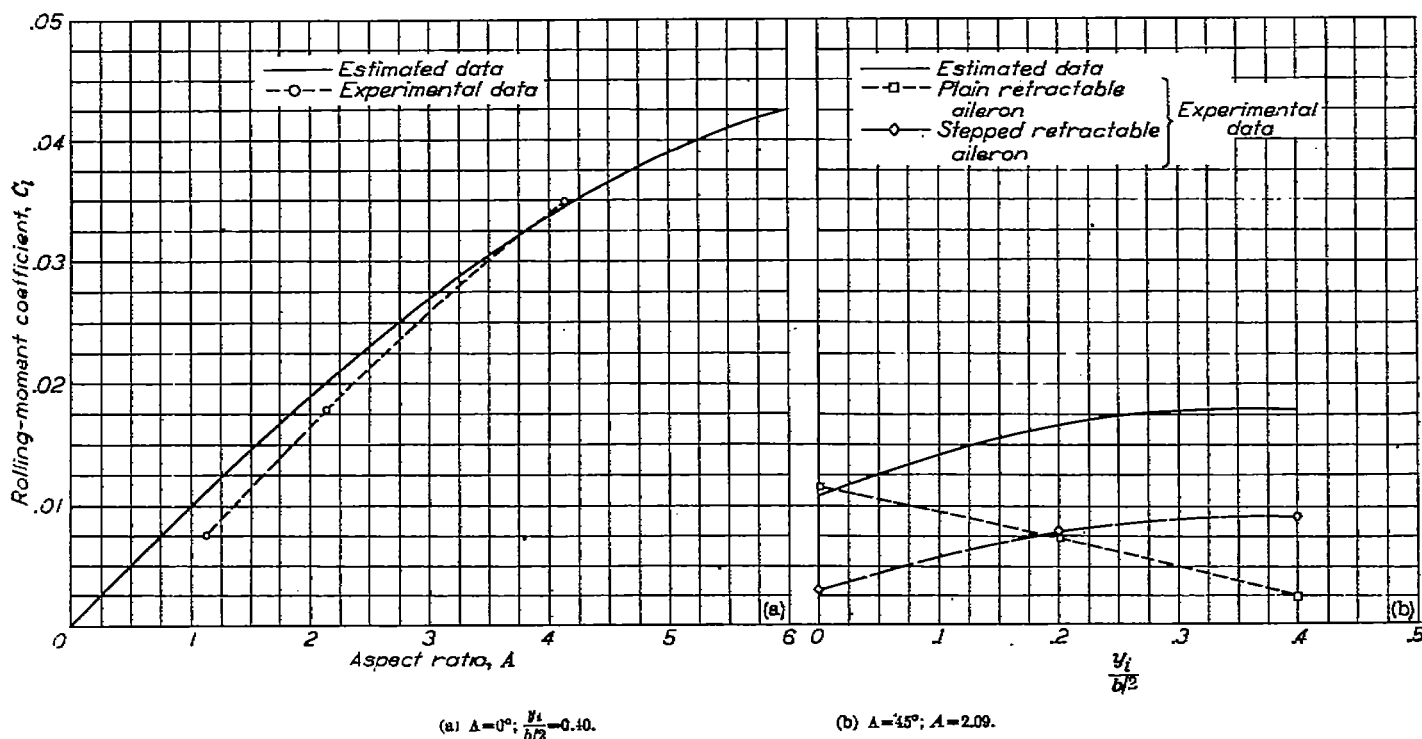


FIGURE 48.—Comparison of experimental and estimated values of C_l for $0.00 \frac{b}{2}$ retractable ailerons at a projection of $-0.08c$ on the untapered wings. $C_L = 0$.

presented as method 1 in reference 15 and are shown in figure 49. The values of $(C_{l_p})_{C_L=0}$ used in the foregoing equation were obtained from reference 15 and were -0.107 , -0.189 , -0.335 , and -0.433 for the unswept wings of aspect ratios 1.13, 2.13, 4.13, and 6.13, respectively, and -0.186 for the 45° sweptback wing of aspect ratio 2.09.

In the following discussion, rolling performance is based on these estimated values of C_{l_p} for wing alone.

The low-aspect-ratio wings with flap ailerons.—The estimated values of $\frac{pb}{2V}$ (fig. 50) show that a wing-tip helix angle of 0.09 radian (an Air Force-Navy requirement) was easily obtained with the $0.50 \frac{b}{2}$ outboard flap ailerons. The rolling effectiveness of the wings of aspect ratios 6.13, 4.13, and 2.13 was fairly regular up to moderate lift coefficients and decreased with increase in aspect ratio. However, the wing of aspect ratio 1.13 showed an erratic variation of rolling effectiveness with lift coefficient and had a greater value of rolling effectiveness than the wing of aspect ratio 2.13 only over the lift-coefficient range of about 0.2 to 0.5.

The low-aspect-ratio wings with retractable ailerons.—At equal aileron projections, the rolling effectiveness of the retractable ailerons (fig. 51) increased with increase in aspect ratio of the unswept wings and decreased with increase in wing sweepback. The required wing-tip helix angle of 0.09 radian (an Air Force-Navy requirement) can usually be met with the retractable ailerons on the wing model of aspect ratio 4.13. The retractable ailerons on the other wings, however, produced much lower values of $pb/2V$. Furthermore, the rolling effectiveness of the retractable ailerons on any of the models was rather erratic over the lift range.

Although the values of $pb/2V$ produced by the retractable

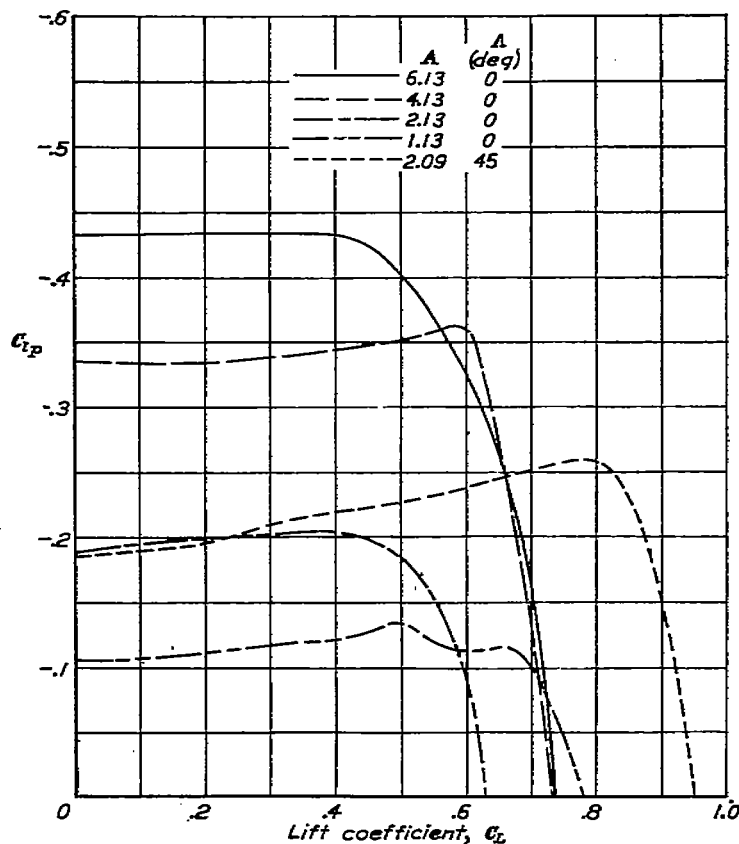


FIGURE 49.—Variation of C_{l_p} (used for determining $\frac{pb}{2V}$) with lift coefficient of the wings investigated.

aileron on some of the wing models were not very large, their magnitude may not be of great importance. For an airplane having a given wing loading (or wing area), values of the rolling velocity p may be more indicative of good control than $pb/2V$ because of the shorter wing span and higher

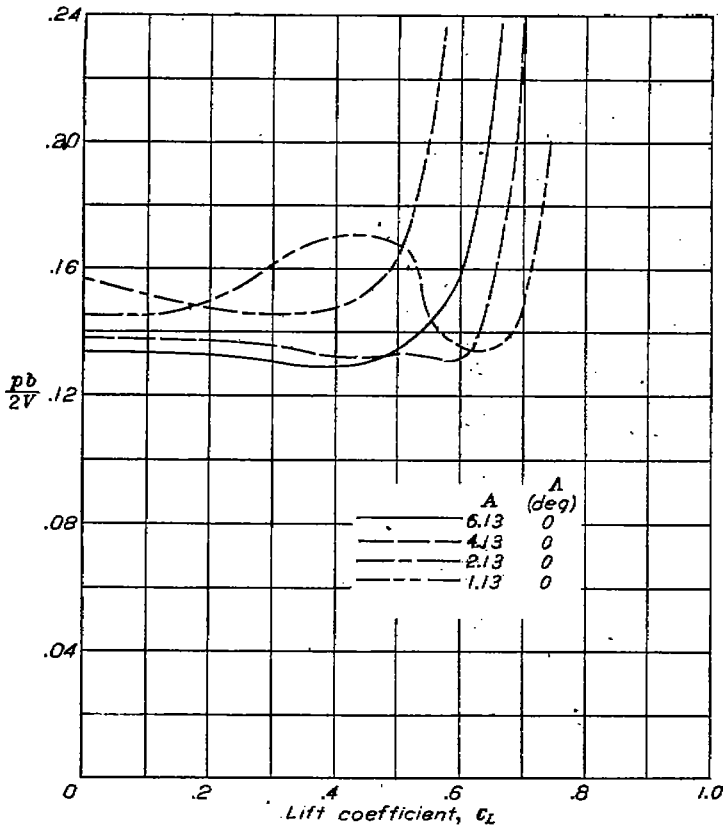


FIGURE 50.—Variation of estimated wing-tip helix angle with lift coefficient for the wing models equipped with half semispan outboard flap ailerons deflected a total of 20°.

rolling velocities experienced by such an airplane at a given value of $pb/2V$ as the wing aspect ratio decreased. On this basis, the rolling velocities of the three unswept wings and the 45° sweptback wing with the optimum plain-retractable-aileron configuration are estimated to be approximately equal for an aileron projection of $-0.08c$ and at the same speed.

Comparison of spoiler and flap ailerons on the low-aspect-ratio wings.—A comparison of the rolling-effectiveness parameter $pb/2V$ of the flap ailerons (obtained from fig. 50 and unpublished data) and that of the retractable ailerons investigated on the same wings (fig. 51) is shown in figure 52.

Both types of ailerons produced similar trends in the variation of $pb/2V$ over the lift range (fig. 52). The half-semispan flap ailerons deflected a total of 20° were more effective than the spoiler ailerons projected $-0.08c$ on the same wings, except for a limited range of lift coefficient on the 45° sweptback-wing model. The following table shows the estimated span of 0.25c flap ailerons deflected a total of 20° that would generally equal the rolling effectiveness of a 0.60 $\frac{b}{2}$ retractable aileron ($\frac{y_1}{b/2} = 0.40$) projected $-0.08c$ on

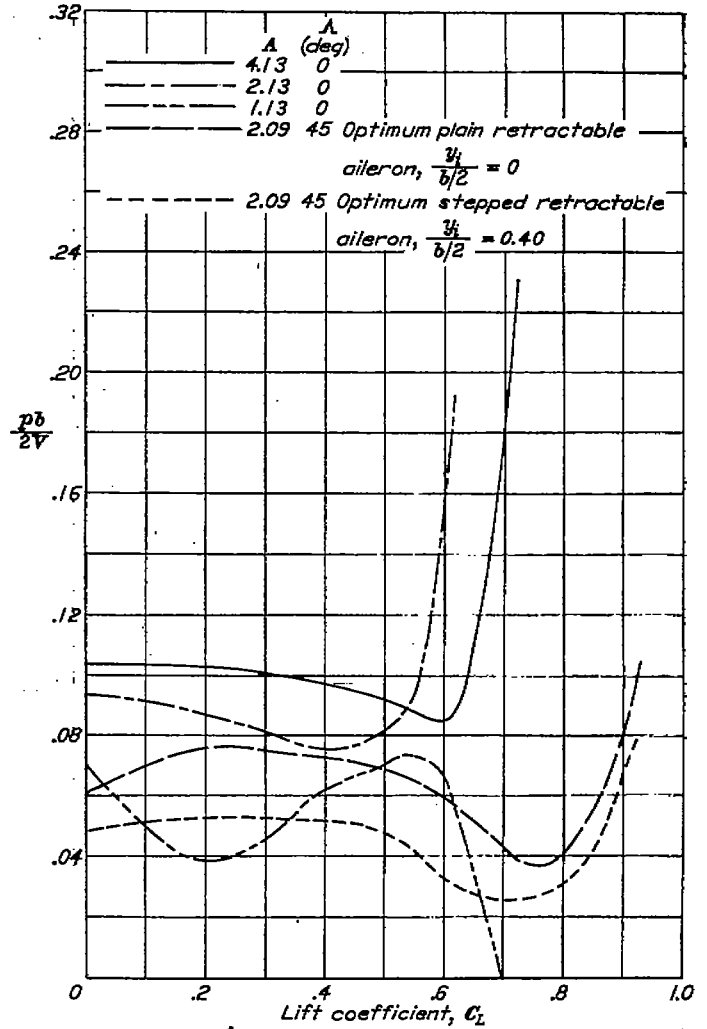
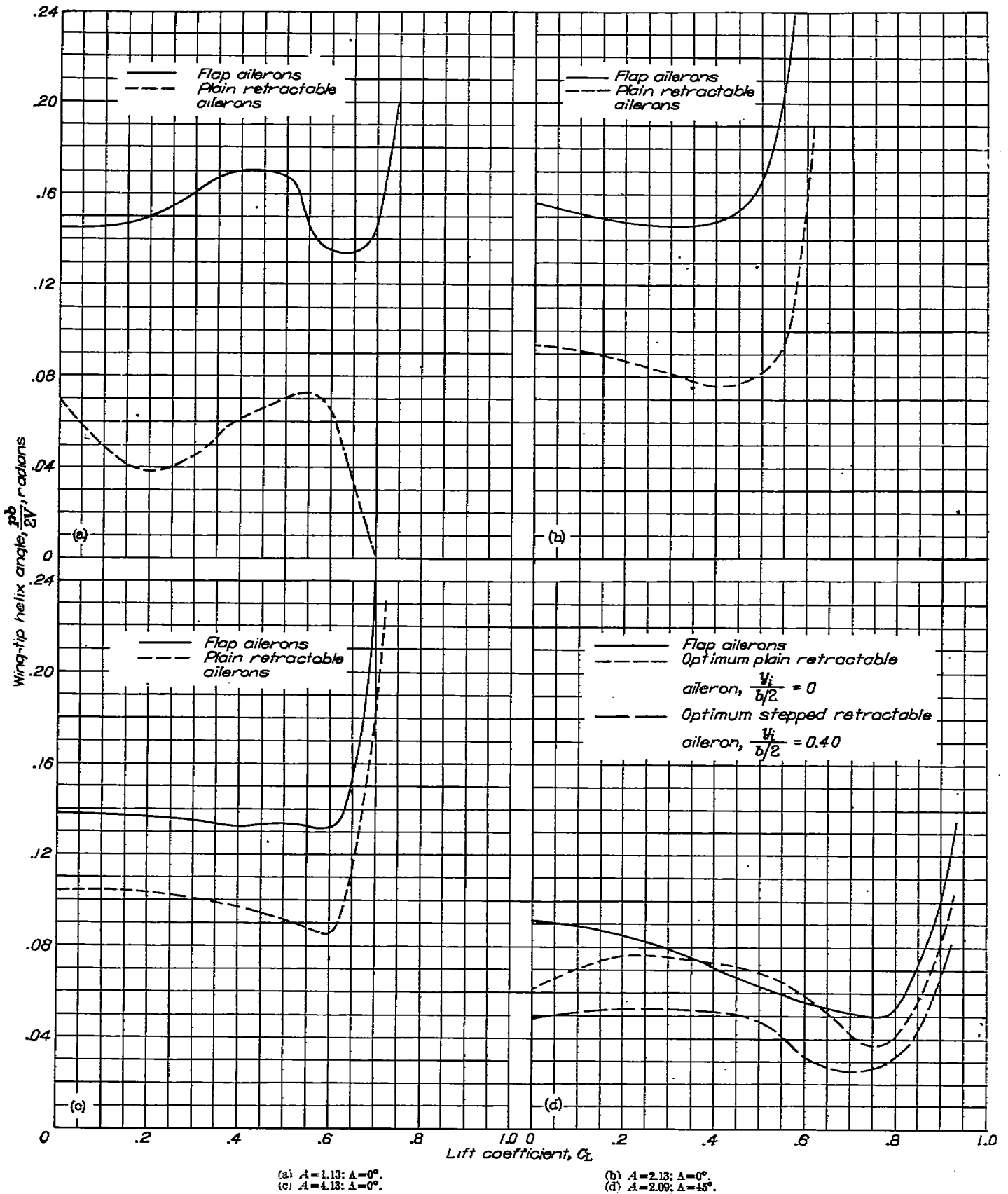


FIGURE 51.—Variation of estimated wing-tip helix angle with lift coefficient for the wing models equipped with retractable ailerons. $b_s = 0.60 \frac{b}{2}$; aileron projection, $-0.08c$. each of the wings:

A	A (deg)	Estimated span of flap ailerons to produce same $pb/2V$ as $0.60 \frac{b}{2}$ retractable ailerons (percent $b/2$)
1.13	0	19
2.13	0	28
4.13	0	37
2.09	45	45

* Comparison made with optimum plain retractable aileron, $\frac{y_1}{b/2} = 0$.

The data given in the previous table, as well as the data of figure 52, show that retractable ailerons on low-aspect-ratio unswept wings are rather ineffective when compared with reasonably normal-size flap ailerons and become progressively worse as the wing aspect ratio is decreased.



(a) $A=1.13; \Lambda=0^\circ$.
 (c) $A=4.13; \Lambda=0^\circ$.

(b) $A=2.13; \Lambda=0^\circ$.
 (d) $A=2.09; \Lambda=45^\circ$.

FIGURE 52.—Comparison of estimated values of $\frac{pb}{2V}$, produced by $0.60 \frac{b}{2}$ retractable ailerons projected $-0.06c$ and by half-span $0.25c$ sealed flap ailerons deflected a total of 20° on each of the untapered low-aspect-ratio wings. (Flap-aileron data were estimated from unpublished data for 45° sweptback wing.)

Such a comparison is rather incomplete, however, when the effects of the aileron yawing moments, of the aileron hinge moments, and of compressibility are not considered. In general, the yawing moments of spoiler ailerons are favorable and would tend to increase the rolling effectiveness of these controls as contrasted to opposite effects exhibited by the flap ailerons at high angles of attack. The data of references 3 and 4 show that the spoiler ailerons were more effective than the flap ailerons when compressibility effects were considered, and, in addition, reference 9 indicates that the twist of the wing with spoiler controls was less than that of the wing with flap controls.

CONCLUSIONS

A low-speed wind-tunnel investigation was made to determine the lateral control characteristics of a series of untapered low-aspect-ratio wings. Sealed flap ailerons of various spans and spanwise locations were investigated on unswept wings of aspect ratios 1.13, 2.13, 4.13, and 6.13; various projections of 0.60-semispan retractable ailerons were investigated on the unswept wings of aspect ratios 1.13, 2.13, and 4.13 and a 45° sweptback wing. The retractable ailerons investigated on the unswept wings spanned the outboard stations of each wing; whereas the plain and stepped retractable ailerons investigated on the sweptback wing were located at various spanwise stations. The results of the investigation led to the following conclusions:

1. The variation of experimental flap-aileron effectiveness with aspect ratio was not accurately predicted for all spans of ailerons by any one of the three theoretical methods with which a comparison was made.

2. Flap-aileron effectiveness increased as aileron span or wing aspect ratio was increased. Rolling effectiveness of the $0.50 \frac{b}{2}$ outboard flap ailerons decreased with increasing aspect ratio except for the low-lift-coefficient range where the aspect-ratio-2.13 wing gave somewhat higher values of rolling effectiveness than the aspect-ratio-1.13 wing produced.

3. At equal aileron projections, the rolling effectiveness of the retractable ailerons increased with increase in aspect ratio of the unswept wings and decreased with increase in wing sweepback; however, the rolling velocities produced on the four wings are estimated to be approximately equal for a given wing area (or wing loading) at the maximum aileron projection investigated.

4. The effectiveness of plain retractable ailerons on the 45° sweptback wing generally increased when the spanwise location of the aileron was moved inboard; whereas the effectiveness of stepped retractable ailerons on the same wing generally increased at low and moderate angles of attack when their spanwise location was moved outboard. The

optimum configuration for the plain retractable aileron (at the inboard location) was usually more effective than the optimum configuration for the stepped retractable aileron (at the outboard location) on the sweptback wing.

5. The addition of simulated actuating arms to the plain and stepped retractable ailerons investigated at various spanwise locations on the sweptback wing generally tended to increase the aileron effectiveness.

6. The effectiveness of the retractable ailerons on the unswept wings could be predicted by an existing empirical method for low angles of attack; however, this empirical method was unsatisfactory for estimating the effectiveness of retractable ailerons on the 45° sweptback wing.

7. The problems associated with adverse yawing moments become serious for flap ailerons well below maximum lift coefficient for unswept wings of moderately low aspect ratio if partial flow separation in the linear lift range is characteristic of the wings.

8. In general, the values of yawing-moment coefficient $C_{y\dot{\alpha}}$ produced by the retractable ailerons on the wings were favorable and increased linearly with aileron projection except at small projections.

LANGLEY AERONAUTICAL LABORATORY,
NATIONAL ADVISORY COMMITTEE FOR AERONAUTICS,
LANGLEY FIELD, VA., February 8, 1952.

REFERENCES

1. Stack, John, and Lindsey, W. F.: Characteristics of Low-Aspect-Ratio Wings at Supercritical Mach Numbers. NACA Rep. 922, 1949. (Supersedes NACA TN 1665.)
2. Fischel, Jack, and Tamburello, Vito: Investigation of Effect of Span, Spanwise Location, and Chordwise Location of Spoilers on Lateral Control Characteristics of a Tapered Wing. NACA TN 1294, 1947.
3. Fischel, Jack, and Schneider, Leslie E.: High-Speed Wind-Tunnel Investigation of an NACA 65-210 Semispan Wing Equipped with Plug and Retractable Ailerons and a Full-Span Slotted Flap. NACA TN 1663, 1948.
4. Laitone, Edmund V., and Summers, James L.: An Additional Investigation of the High-Speed Lateral-Control Characteristics of Spoilers. NACA ACR 5D28, 1945.
5. Fischel, Jack, and Ivey, Margaret F.: Collection of Test Data for Lateral Control with Full-Span Flaps. NACA TN 1404, 1948.
6. Schneider, Leslie E., and Watson, James M.: Low-Speed Wind-Tunnel Investigation of Various Plain-Spoiler Configurations for Lateral Control on a 42° Sweptback Wing. NACA TN 1646, 1948.
7. Lovell, Powell M., Jr., and Stassi, Paul P.: A Comparison of the Lateral Controllability with Flap and Plug Ailerons on a Sweptback-Wing Model. NACA TN 2089, 1950.
8. Lovell, Powell M., Jr.: A Comparison of the Lateral Controllability with Flap and Plug Ailerons on a Sweptback-Wing Model Having Full-Span Flaps. NACA TN 2247, 1950.

9. Purser, Paul E., and McKinney, Elizabeth G.: Comparison of Pitching Moments Produced by Plain Flaps and by Spoilers and Some Aerodynamic Characteristics of an NACA 23012 Airfoil with Various Types of Aileron. NACA ACR L5C24a, 1945.
10. Gillis, Clarence L., Polhamus, Edward C., and Gray, Joseph L., Jr.: Charts for Determining Jet-Boundary Corrections for Complete Models in 7- by 10-Foot Closed Rectangular Wind Tunnels. NACA ARR L5G31, 1945.
11. Herriot, John G.: Blockage Corrections for Three-Dimensional-Flow Closed-Throat Wind Tunnels, with Consideration of the Effect of Compressibility. NACA Rep. 995, 1950. (Supersedes NACA RM A7B28.)
12. Polhamus, Edward C.: A Simple Method of Estimating the Subsonic Lift and Damping in Roll of Sweptback Wings. NACA TN 1862, 1949.
13. Zimmerman, C. H.: Characteristics of Clark Y Airfoils of Small Aspect Ratios. NACA Rep. 431, 1932.
14. Goodman, Alex, and Brewer, Jack D.: Investigation at Low Speeds of the Effect of Aspect Ratio and Sweep on Static and Yawing Stability Derivatives of Untapered Wings. NACA TN 1669, 1948.
15. Goodman, Alex, and Adair, Glenn H.: Estimation of the Damping in Roll of Wings Through the Normal Flight Range of Lift Coefficient. NACA TN 1924, 1949.
16. Weick, Fred E., and Jones, Robert T.: Résumé and Analysis of N.A.C.A. Lateral Control Research. NACA Rep. 605, 1937.
17. Lowry, John G., and Schneiter, Leslie E.: Estimation of Effectiveness of Flap-Type Controls on Sweptback Wings. NACA TN 1674, 1948.
18. DeYoung, John: Theoretical Antisymmetric Span Loading for Wings of Arbitrary Plan Form at Subsonic Speeds. NACA TN 2140, 1950.
19. DeYoung, John: Spanwise Loading for Wings and Control Surfaces of Low Aspect Ratio. NACA TN 2011, 1950.
20. Dods, Jules B., Jr.: Wind-Tunnel Investigation of Horizontal Tails. IV—Unswept Plan Form of Aspect Ratio 2 and a Two-Dimensional Model. NACA RM A8J21, 1948.
21. Ashkenas, I. L.: The Development of a Lateral-Control System for Use with Large-Span Flaps. NACA TN 1015, 1946.
22. Liddell, Robert B.: Wind-Tunnel Tests of Spoilers on Tail Surfaces. NACA ARR L5F28, 1945.